10/7-28-92 OSTI

SANDIA REPORT

SAND91—2607 • UC—253
Unlimited Release
Printed June 1992

Development and Evaluation of a Meter for Measuring Return Line Fluid Flow Rates During Drilling

Glen E. Loeppke, Diane M. Schafer, David A. Glowka,
Douglas D. Scott, Marcus D. Wernig, Elton K. Wright

Prepared by
Sandia National Laboratories
Albuquerque, New Mexico 87185 and Livermore, California 94550
for the United States Department of Energy
under Contract DE-AC04-76DP00789

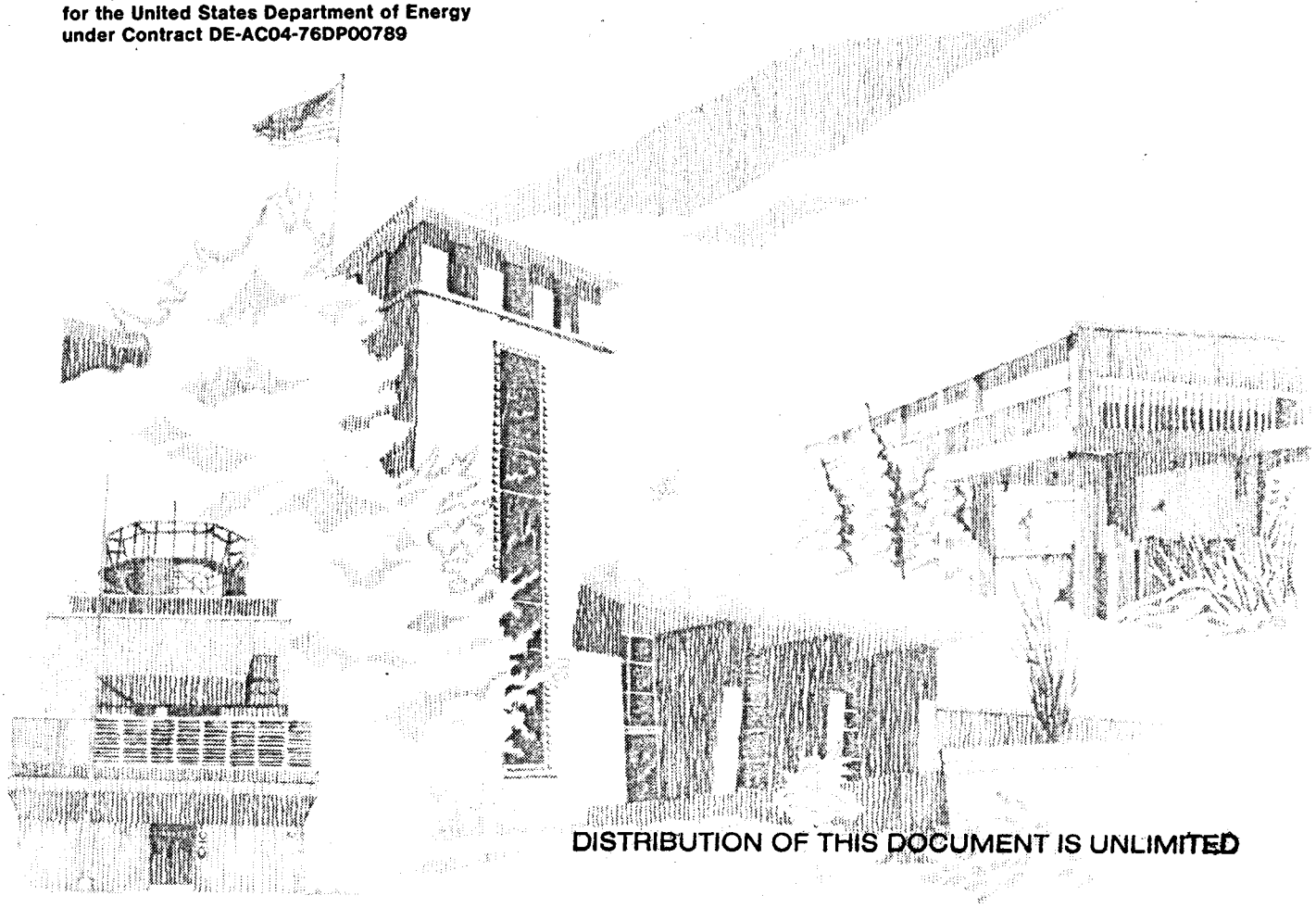

DISCLAIMER

Issued by Sandia National Laboratories, operated for the United States Department of Energy by Sandia Corporation.

Available to DOE and DOE contractors from
Office of Scientific and Technical Information
PO Box 62
Oak Ridge, TN 37831

Prices available from (615) 576-8401, FTS 626-8401

Available to the public from
National Technical Information Service
US Department of Commerce
5285 Port Royal Rd
Springfield, VA 22161

NTIS price codes
Printed copy: A06
Microfiche copy: A01

SAND--91-2607
DE92 017352

SAND 91-2607
Unlimited Distribution
Printed June 1992

DEVELOPMENT AND EVALUATION OF A METER FOR MEASURING RETURN LINE FLUID FLOW RATES DURING DRILLING

Glen E. Loeppke
Diane M. Schafer
David A. Glowka
Douglas D. Scott
Marcus D. Wernig
Sandia National Laboratories

Elton K. Wright
Ktech Corporation

ABSTRACT

The most costly problem routinely encountered in geothermal drilling is lost circulation, which occurs when drilling fluid is lost to the formation rather than circulating back to the surface. The successful and economical treatment of lost circulation requires the accurate measurement of drilling fluid flow rate both into and out of the well. This report documents the development of a meter for measuring drilling fluid outflow rates in the return line of a drilling rig. The meter employs a rolling counterbalanced float that rides on the surface of the fluid in the return line. The angle of the float pivot arm is sensed with a pendulum potentiometer, and the height of the float is calculated from this measurement. The float height is closely related to the fluid height and, therefore, the flow rate in the line. The prototype rolling float meter was extensively tested under laboratory conditions in the Wellbore Hydraulics Flow Facility; results from these tests were used in the design of the field prototype rolling float meter. The field prototype meter was tested under actual drilling conditions in August and September, 1991 at the Long Valley Exploratory Well near Mammoth Lakes, Ca. In addition, the performance of several other commercially available inflow and outflow meters was evaluated in the field. The tested inflow meters included conventional pump stroke counters, rotary pump speed counters, magnetic flowmeters, and an ultrasonic Doppler flowmeter. On the return flow line, a standard paddlemeter, an acoustic level meter, and the prototype rolling float meter were evaluated for measuring drilling fluid outflow rates.

ACKNOWLEDGMENTS

This work was sponsored by the U. S. Department of Energy, Geothermal Division, at Sandia National Laboratories under Contract DE-AC04-76DP00789. The assistance of John Finger and Ron Jacobson during the field testing is gratefully acknowledged.

TABLE OF CONTENTS

TABLE OF CONTENTS (cont.)

LIST OF FIGURES

Figure Number	Title	Page Number

LIST OF TABLES

NOMENCLATURE

Symbol	Definition
A	cross-sectional flow area
α	angle associated with partially-full pipe flow, defined in Figure A2
B	flow width
D	pipe diameter
E	specific energy of the fluid in open channel flow
f	non-dimensional Darcy friction factor in pipe flow
g	acceleration due to gravity
h_l	head loss
L	length of pipe section
n	Manning coefficient, roughness coefficient used in open-channel flow analysis having different values for different types of boundary roughness
P	wetted wall perimeter
Q	volumetric flow rate
θ	slope of the pipe in gravity-driven inclined pipe flow
ρ	fluid density
R_h	hydraulic radius (A/P)
S	local energy loss in accelerating flow
S_b	pipe slope (tan θ)
τ	shear stress at the pipe wall
V	average fluid velocity.
y	height of the fluid in pipe
y_c	critical height, height associated with minimum specific energy of fluid in open channel flow
z	elevation of pipe bottom

INTRODUCTION

Background

The most costly problem routinely encountered in geothermal drilling is lost circulation. This condition occurs when the drilling fluid, pumped downhole to cool the bit, carry rock chips out of the wellbore, and in some cases control the well, is lost to the rock formation rather than circulating back to the surface. Such a loss of circulation is caused by an incompetent or permeable rock formation (characterized by porous matrix, fractures, vugs, or caverns) which does not have adequate physical integrity or pore-fluid pressure to support the hydrostatic pressure inside the wellbore.

Although drilling can often continue under lost circulation conditions, it is generally imperative that the fluid loss be stopped as soon as possible after it is discovered, for several reasons:

- Drilling fluid is expensive (typically $5/bbl), so pumping thousands of barrels into the formation can significantly increase drilling costs;
- Changes in the rock formation being drilled cannot be easily detected if rock chips are not circulated out of the wellbore; rock chips lost to the formation can also flow back into the wellbore when drilling stops, thereby sticking the drillstring in the hole;
- The well may be difficult or impossible to control if a high-pressure zone is encountered with the wellbore only partially filled with drilling fluid;
- Drilling fluid invasion of the surrounding rock formation alters *in-situ* conditions and therefore affects the logging response of the formation;
- Freshwater aquifers associated with loss zones can be contaminated by drilling mud and connate fluids produced at other wellbore intervals; and
- Loss zones not treated during the drilling phase can cause cement to be lost to the open formation during completion operations, resulting in a poor or incomplete bond between the casing and the rock formation and requiring expensive remedial action to prevent inter-interval flow and possible casing collapse when the well is put on production.

Lost circulation problems tend to be more severe in geothermal drilling than in oil and gas drilling because of the highly fractured and underpressured nature of many geothermal formations. Bridging materials used as drilling mud additives for lost circulation control in oil and gas drilling are ineffective in plugging large fracture apertures, particularly under high-temperature conditions. As a result, the standard lost circulation treatment in geothermal drilling is to fill the loss zone surrounding the wellbore with cement. This is an expensive operation in terms of both material costs (typically several hundred cubic feet of cement at $\$15/ft^3$) and rig time spent on the cementing operation, on waiting for the cement to harden, and on drilling through the cemented zone to reach new rock formations (typically 24 hours at $300/hr). Consequently, the costs of lost circulation in a typical geothermal well may range from several thousand to several hundred thousand dollars, depending on the severity and number of loss zones encountered.

Lost circulation costs represent an average of 10% of the total well costs in mature geothermal areas [1], and they often account for over 20% of the costs in exploratory wells and developing fields. Well costs, in turn, represent 35-50% of the total capital costs of a typical

geothermal project [2]. It can thus be concluded that lost circulation accounts for roughly 3-10% of the total costs of a typical geothermal project.

These direct costs, and the unknown costs associated with possible contamination of freshwater aquifers, provide strong incentives for a technology development program to address these problems. DOE sponsors the Lost Circulation Technology Development Program at Sandia National Laboratories for this purpose. The five-year goal of this program is to develop and transfer to industry new technology to reduce lost circulation costs by 30-50%. The Level III programmatic objective adopted by DOE is to reduce the costs associated with lost circulation by 30%. This objective combines with others to produce a Level II objective of reducing the life-cycle cost of hydrothermal electricity by 10-13% through improvements in fluid production technology. Expectations for technology improvements in several areas combine to produce a Level I objective of reducing the life-cycle cost of hydrothermal-produced electricity to 3-7 cents/kWh. This compares with a cost of 4-15 cents/kWh in 1986.

Need for Outflow Meter Development

Various tools and types of treatment for solving lost circulation problems in geothermal drilling are under development in the Lost Circulation Technology Development Laboratory. All of these techniques require the prompt diagnosis of lost circulation during the drilling of a well. In addition, a technique for characterizing lost circulation zones that is currently under development is the use of mathematical wellbore hydraulics models coupled with transient and steady state flow and pressure measurements. Both the timely diagnosis and hydraulic characterization of lost circulation require the accurate measurement of drilling fluid flow rates both into and out of the well.

Lost circulation is not as significant and costly of a problem in the drilling of oil and gas wells. However, unexpected influxes (kicks) of gas or oil can occur which can be dangerous and result in loss of control of the well. If an influx is detected at an early stage, steps can be taken to remedy the influx and drilling operations can continue. An accurate and reliable means for measuring flow rates into and out of the well offers the best approach to reducing the hazard associated with well kicks. This has become particularly important with the increased use of slimhole drilling for exploration. Well control in a smaller diameter hole requires that influxes be detected more rapidly than in a conventional well [3].

It is a challenge to find instrumentation that can be used on a drilling rig and can provide the necessary accuracy and response time for measuring delta flow (inflow minus outflow). Studies by Orban et al. [4] concluded that a delta-flow accuracy of at least 50 gpm is required to successfully detect the influx or loss of fluid during the drilling process. If a pumping rate of 1000 gpm is assumed, the combined accuracy of the inflow and outflow measurements should then be at least 5%. This is much better accuracy than that of present field equipment. Flow meters with the desired accuracy exist, but the problem becomes practical application and acceptance by the industry.

The goal then is to provide a useful system for measuring delta flow that will be widely accepted and eventually found on every drilling rig where kicks and loss circulation must be controlled. Experience shows that this will require a system with the following characteristics: acceptable accuracy, low impact on the drill rig hardware and instrumentation, low cost, easy installation and maintenance by personnel that are normally present at the drill site, and minimum interference with the return flow.

Inflow rate measurements are usually made on drill rigs by counting the mud pump strokes over a period of time and calculating a flow rate using volume per stroke and an assumed pump efficiency. Pump efficiency is typically 85-95%; however, the actual pump efficiency is rarely known, and can change with changes in pump pressure, piston seal wear, temperature, and mud properties. The pump stroke rate method suffers from a lack of absolute accuracy, although changes in flow rate due to pumping speed can be measured. The inflow rate is often displayed on the rig floor in terms of strokes per minute rather than absolute flow rate. Although rarely done, accurate inflow measurements can be made with a variety of commercial flowmeters installed in the mud pump inlet line or in the high pressure line at the inlet to the drillstring.

Outflow rate measurements are more difficult to make because of the partially filled nature of the return line. The viscous and abrasive characteristics of the rock-chip-laden drilling fluid also preclude the use of probes that protrude into the fluid stream. Furthermore, protrusions or bends in the flow line path can cause suspended rock chips to fall out of the flow and plug the return line. Due to these difficulties, the most common method of detecting delta flow is by monitoring changes in mud tank volume as measured by pit level meters. While this system provides a measure of the total pit volume gained or lost over a period of time, it does not permit rapid detection or accurate quantification of wellbore production or loss rates that are essential for rapid response to gas kicks or lost circulation [3].

When outflow rate measurements are made, they are most often made with the industry standard, the paddlemeter. This meter employs a single, spring-mounted vane that protrudes into and is deflected by the flow. The angle of the vane, which is measured with a potentiometer, is thus related to the flow rate. Although not very accurate, the paddlemeter meets all the other criteria listed above for an outflow measuring device. It is often calibrated in terms of percent of full-scale deflection and is used more as an indicator of flow rather than as a quantitative measure of flow rate.

Outflow measurements can also be made with an acoustic level meter, as has been done by another service company [4,5]. Because of the changes in sonic velocity that occur with changes in temperature and gas composition in the air above the fluid in the return line, it is necessary to compensate for these effects with additional measurements and corrections to the flow rate data. This requires the monitoring of additional data channels and complicates the data reduction routine.

Other researchers have measured delta flow in studies using magnetic flowmeters in both the inflow and outflow lines [3,6,7]. Although extremely accurate, magnetic flowmeters are generally very expensive and thus are not often used in drilling practice. These methods also require a completely-filled pipe, which requires a U-tube section to be installed in the return flow line and necessitates special attention to prevent rock chips from accumulating in and plugging the return line.

A return line flow meter that employs a horizontal deflection in the return line has been developed that is based on the measurement of forces generated due to a change in momentum of the fluid in the return line [8]. Although the meter has high accuracy, its use is limited by the need for installation of a turn (J-pipe) in the return line. In addition, it requires the monitoring of two channels of data from the meter, as well as the use of a densimeter in the line to determine the density of the fluid passing through the meter.

Because of the limitations identified above, the need for a simple, reliable flow meter for measuring drilling fluid outflow rates was evident. As a result, the rolling float meter was conceived. The original idea was to measure both fluid level and velocity in the flow line, thereby providing two redundant measures of flow rate that could be used to improve accuracy. Hence, the name "velocity-level" or V-L meter was originally used. It was found as a result of our development program, however, that the velocity is not sensitive enough to flow rate to be of use

in this application. Consequently, the name of the meter was changed to the "rolling float meter" to better characterize its operation.

The purpose of this report is to document the development of the rolling float meter. The laboratory test facility and the design of the prototype meter are described. In addition, theoretical predictions and experimental measurements of the fluid height and velocity in the drilling fluid return flow line are presented. An analysis of laboratory test results of both the prototype meter and conventional paddlemeter is given. Finally, the performance and reliability of several inflow and outflow transducers during field operations in August and September, 1991, at the Long Valley Exploratory well near Mammoth Lakes, Ca. are evaluated.

LABORATORY TEST FACILITY

The Wellbore Hydraulics Flow Facility (WHFF) was constructed to provide full-scale simulation of fluid flow out of a wellbore during drilling. The facility has been used to test and develop the prototype rolling float flowmeter, as well as to evaluate commercial outflow and inflow flowmeters. The WHFF also will be used to develop expert system software for the detection, analysis, and treatment of lost circulation during well drilling. A schematic of the WHFF is shown in Figure 1; a photo of the facility is shown in Figure 2. The loop consists of a storage tank, butterfly shut-off valve, pump primer, centrifugal pump, flow restriction (metering) valve, commercial inflow meter, a simulated wellbore, return line, and outflow meter (commercial or prototype).

The fluid storage tank is open to the atmosphere and is capable of holding approximately 310 gallons of fluid. The storage tank can be isolated from the loop by means of the butterfly type shut-off valve located at the fluid discharge port. The test fluid flows from the storage tank to the pump through approximately 5 ft of 6-inch diameter flexible hose. The pump is a vertically mounted centrifugal pump, coupled to a 25 HP motor, and is capable of pumping 1000 gpm at 50 ft of head. The fluid flow rate is controlled by a diaphragm-type flow restriction valve. From the valve, the fluid flows in 4-inch diameter PVC pipe through a commercial magnetic flowmeter to the top of the simulated wellbore. The simulated wellbore consists of 19-inch diameter steel casing and is covered, but not sealed, so the line pressure at the top of the annular section is atmospheric. The 4-inch PVC pipe is connected to a 5-inch steel pipe that passes through the cover of the casing. The 5-inch pipe, which simulates the drill string in an actual well drilling operation, is held in the center of the casing by a centralizing ring. Fluid flows down the 5-inch pipe and up through the annulus of the simulated wellbore, where it returns to the storage tank through a 12-ft-long return line. Both a 10-inch diameter, transparent plastic tube and a 12-inch steel pipe have been used as the return line during different phases of testing.

The weight of the plastic return line and fluid is supported by a 12-ft length of 6-inch aluminum channel, which is hinged to the simulated wellbore. A support is not needed with the steel return line; instead, tabs have been welded to the line and hinged directly to the simulated wellbore. In both cases, the return line and simulated wellbore are connected by a flexible rubber boot. The height and velocity of the fluid in the return line is directly affected by the angle of the line. As such, the return line can be raised and lowered from 0° - 12.5° with respect to horizontal by a 1-ton hand-operated chain hoist connected on one end to an overhead platform and on the other end either to the aluminum channel or directly to the steel return line. The chain hoist is used only to raise and lower the line; during operation the return line is supported on both sides and bottom by a steel support system.

The tested flowmeters were evaluated against a 4-inch magnetic flowmeter mounted in a section of full pipe between the pump and the simulated wellbore. The magnetic flowmeter was used as the standard measure of flow rate because of its excellent accuracy (within 2% as measured in our facility and ±0.5% as stated by the manufacturer) and its insensitivity to fluid properties. The throttle valve downstream of the pump was used to vary the flow rate over its full range of 0-1000 gpm.

RETURN LINE FLOW CHARACTERISTICS

Theoretical Analysis

To develop a meter for measuring return line fluid flow rates, a prediction of the range of fluid levels and velocities that might be encountered on a drilling rig was necessary. Traditional mathematical equations for open-channel flow [9-12] were used to evaluate flow conditions that would be typical in a drilling rig return line. These mathematical equations, as well as details of the analysis, can be found in Appendix A.

Several assumptions were made in the analysis. It was assumed that the flow in the return line is steady and incompressible, and that the pressure in the fluid is hydrostatic. To simplify the analysis, it was assumed that the velocity profile at each cross-section is uniform, and that the pipe slope is small. Since return line flow is typically in rough pipes at relatively high flow rates it was assumed that the wall shear stress is independent of fluid properties and velocity. This is analogous to flow in the fully rough regime for turbulent pipe flow, where the friction factor is a function of pipe roughness only and is independent of the flow Reynolds number.

The assumptions used to simplify the analysis and the fact that it does not take into account such things as surface waves and rock chips suspended in the flow limit the ability of the model to accurately predict real fluid flow fields. However, the analysis was used only as a design tool in which the effects of changes in location, pipe slope, size, and pipe material on fluid heights and velocities were evaluated.

Theoretical Results

The analysis described above was used to predict the fluid level and average velocity over a range of fluid flow rates (5 - 1000 gpm) for return pipe diameters of 10 and 12 inches, smooth and rough pipe walls, and return line angles, θ, from 5° to 15°.

Results of the analysis show that fluid enters a return line and is accelerated by gravity until the force due to gravity is balanced by shear forces at the pipe wall. During acceleration, the fluid height continuously decreases and the average fluid velocity continuously increases until uniform flow conditions exist. In uniform flow, the fluid height and average velocity remains constant. According to the analysis, at the highest flow rates (1000 gpm) uniform flow conditions do not exist until almost 100 ft from the entrance to the pipe. At moderate flow rates (500 gpm) uniform flow conditions exist approximately 60 ft from the bell nipple, and at 100 gpm uniform flow exists at 20 ft. Any flow metering device on a drill rig will be installed such that at most flow rates, the flow will be in the accelerating flow regime, and the fluid height and velocity will be dependent on the location of the device relative to the bell nipple. Since the fluid height measurements of an outflow meter will be dependent on the installation location on a particular drilling rig, each meter will have to be calibrated against the inflow meter that will be used in the delta-flow measurements.

Average fluid velocity and fluid level at a location 3 ft from the bell nipple are shown as a function of flow rate in Figure 3 for a 10-inch diameter, smooth steel pipe with a 5° angle. At higher flow rates, the level varies almost linearly with flow rate, while the average velocity begins to become asymptotic. As the pipe angle is increased, the fluid level decreases and the velocity increases, as shown in Figures 4 and 5. The effect of pipe roughness on fluid level and velocity is shown in Figures 6 and 7 respectively, where n = 0.017 corresponds to concrete, and n = 0.010 corresponds to plastic. As expected, the fluid velocity is smaller, and, therefore, the level is higher for the rough pipe where friction forces impeding the fluid motion are larger. Finally, the effect of pipe diameter on level and velocity is shown in Figures 8 and 9. Both the fluid velocity and level are smaller in the larger, 12-inch-diameter pipe.

Experimental Fluid Height Measurements

Measurements of the height of fluid in an inclined pipe flow were made in the WHFF. The measurements were conducted for both water and drilling mud flow in a 10-inch-diameter clear plastic pipe at various pipe slopes and at various locations relative to the fluid entrance. The height of the fluid in the channel was determined by measuring the length of the non-wetted portion of the pipe circumference.

Both the theoretical and experimental fluid height profile are shown in Figure 10 for water and drilling mud flowing at 600 gpm. Experimentally, entrance effects at the pipe inlet cause significant waves to occur at the fluid surface. Approximately 2 ft further downstream, surface waves are not as prominent. As expected, therefore, the largest discrepancy between theoretical and experimental fluid heights is closest to the pipe entrance. The experimental results for water are approximately 0.6 inch (14%) higher than theoretical at a location one foot from the pipe entrance, and agree within 0.3 inch (11%) further downstream. The experimental results for drilling mud agree extremely well with the theoretical profile, except at the entrance where the measurements are ±0.5 inch (±11%) from theoretical.

The experimental and theoretical variation of fluid height with flow rate at three different pipe slopes is shown in Figure 11. Again, there is good agreement between the measured and calculated fluid heights. At pipe slopes of 10° and 12.5°, the maximum deviation is less than 0.25 inch. The difference between measured and theoretical heights is somewhat larger for a pipe slope of 5°, with a maximum deviation of approximately 0.5 inch.

Experimental Velocity Profile Measurements

The theoretical analysis presented above predicts the mean fluid velocity at a given flow rate, pipe slope, and position on the pipe. In order to determine the character of the velocity profile at a given location in the pipe, an experimental study was undertaken to measure fluid velocities across the pipe cross-section.

The apparatus shown in Figure 12 was designed and fabricated as a means for traversing a Pitot-tube velocity probe across the pipe. The apparatus allows the Pitot tube to be moved in a controlled manner in a horizontal direction while it is fixed in the vertical direction. After a horizontal sweep, the Pitot tube can be repositioned vertically to allow another horizontal sweep to be performed at a different vertical level. This permits fluid velocities to be measured at fixed grid points over the fluid cross-section. A differential pressure transducer was used together with an absolute-pressure transducer to obtain the data, and Bernoulli's equation was used to convert the pressure readings to fluid velocities.

The level of turbulence in the flow was evaluated by acquiring Pitot-tube data at a high rate and plotting it as shown in Figure 13. These data, acquired 0.1875 inches off bottom, approximately 11 ft downstream of the pipe entrance, and at a flow rate of 800 gpm, indicate that the instantaneous fluid velocity varies about its 9.62-ft/sec mean value by about 4% (average deviation 0.15 ft/sec). The time-averaged value at a point in the flow therefore appears to be representative of the fluid velocity at that point. Consequently, time-averaged values were acquired in all remaining tests by averaging the instantaneous data for each grid point over a 30-second period.

A typical velocity contour plot is shown in Figure 14. This plot shows lines of constant velocity over the fluid cross-section for a pipe slope of 10° and a flow rate of 800 gpm. Note that steep velocity gradients exist near the pipe wall, while the vast majority of the flow cross-section is near the maximum speed. This is the conventional signature of turbulent flow and was found to exist down to the 100-gpm minimum level tested.

Velocity profiles along the centerline of the pipe at various flow rates are shown in Figure 15. The characteristic turbulent profile shape is again seen for all flow rates tested. The maximum velocity measured for each flow rate is plotted in Figure 16. Note that the maximum velocity increases rapidly from 0 to 100 gpm and immediately begins to become asymptotic. This is similar to the behavior of the mean fluid velocity predicted by the theoretical analysis; at high flow rates, an increase in flow rate is accompanied by an increase in fluid height (flow area) while the velocity increases only slightly. The fluid velocity is, therefore, seen to be a relatively insensitive indicator of flow rate. In other words, there is a significant uncertainty in estimating the flow rate based on fluid velocity measurements.

Both experimental and theoretical results show that the fluid height is a more sensitive indicator of flow than the fluid velocity. Although the prototype rolling float meter included a float speed transducer, it was quickly determined that the float velocity would not be a necessary or useful measurement for correlation to fluid flow rate in partially-filled, inclined-pipe flow.

ROLLING FLOAT METER

Rolling Float Meter Concept

The abrasive, viscous mud environment requires that an outflow meter have inherent wear resistance and be self-cleaning. It must not cause rock chips to fall out of the mud stream and possibly plug the return flow line. It must be accurate at all flow rates and capable of being installed on many different sizes of pipe. It must have a simple design, be rugged, and require little maintenance. In addition, it must be insensitive to changes in fluid properties, temperature, and the existence of solids in the flow.

The rolling float meter, shown schematically in Figure 17, was developed to satisfy all of these requirements. It employs a rolling, counterbalanced plastic float that rides the surface of the fluid in the return flow line. The vertical location or height of the float is closely related to fluid height and thus the flow rate. The float height is determined by measuring the angle of the pivot arm with a pendulum potentiometer. Prototype models of this transducer were also built with: a magnetic rotary sensor incorporated into the float in order to measure the spin rate of the float, which is a function of the fluid velocity in the flow line; and an adjustable dashpot to provide inertial damping of the pivot arm. A photograph of the first prototype rolling float flowmeter is shown in Figure 18 without its brass counterbalance. A reduced copy of the final design drawings for the rolling float meter can be found in Appendix B.

Design Considerations

The rolling float meter design variables investigated included the following:

Float Shape - The shape and size of the float cross-section affects the buoyancy of the float and its interaction with the fluid surface. Cross-sections tested during development of the meter include a 4-inch-wide oval, a 3-inch oval, a 2-inch "V", and a 2-inch flat section. These cross-sectional shapes are shown in Figure 19.

Float Traction - The nature of the traction between the float and the fluid affects the manner in which the float spin rate is related to the fluid velocity. Floats both with and without lugs were evaluated in the laboratory prototype testing.

Float Weight - The float weight affects the buoyancy of the float and, therefore, its interaction with the fluid surface. Float weight was varied in the laboratory prototype testing by adjusting the position of a counterweight mounted on the pivot arm. Increasing the float weight simulates the accumulation of drilling mud on the float. Excess float weight (effective float weight minus effective counterbalance weight) was measured by placing a scale directly beneath the float at different counterbalance locations. The scale used in the evaluation of excess float weight had an output in grams; although grams is a unit of mass, measurements have not been converted to equivalent units for weight. The readings have been left in grams to aid in the practical application of setting the counterbalance weight on a rolling float meter in which a scale with an output in grams will likely be used. The hollow float used in the laboratory tests was approximately 500 g, including the magnetic rotary speed transducer. Excess float weight was varied between 5 and 500 g during the laboratory tests.

Pivot Arm Length - The length of the pivot arm affects its angular response as the float moves vertically due to changing flow conditions. The pivot arm length was varied between 7.7 and 9.5 inches in the laboratory testing.

Inertial Damping - Inertial damping affects the dynamic behavior of the pivot arm as the float responds to turbulent flow fluctuations. An adjustable air dashpot was used in the laboratory tests to provide this damping. The dashpot setting was varied so that the time required for the float to drop in air from a 70° to a 45° angle with respect to vertical varied from 0.3 to 18 seconds.

LABORATORY TEST RESULTS

The flowmeters tested in the WHFF included a 4-inch magnetic flowmeter, an ultrasonic Doppler meter, a conventional paddlemeter, and the prototype rolling float meter. The magnetic flowmeter was tested first by diverting the flow to a calibrated flow tank for a prescribed period of time and measuring the volume of fluid pumped into the tank. Once confirmed accurate, the magnetic flowmeter was used to test the other flowmeters. Testing of these flowmeters consisted of measuring the response of each flowmeter as the flow rate was increased from 0 to 1000 gpm in 50-gpm increments. The flow rate was then decreased back to zero in 100-gpm increments to test the repeatability of the flowmeter response. Data were recorded at 1-second intervals for approximately 30 seconds at each flow rate. These data were then averaged to determine the time-averaged response of each flowmeter at each flow rate.

In addition to the flow rate, the test parameters included the circulating fluid (water, water-based bentonite drilling mud, weighted drilling mud, and drilling mud with drill cuttings) and the return flow line slope (0-12.5 °). The design configuration of the laboratory prototype rolling float

meter was also varied to determine the optimal wheel cross-section, excess wheel weight, pivot arm length, and inertial damping. Testing of the laboratory prototype flowmeter was conducted using the 10-inch transparent plastic return line. The optimal configuration determined from this testing was then used in the design of the field prototype rolling float meter.

Magnetic Flowmeter

The magnetic flowmeter was tested with both water and drilling mud. A 310-gallon calibrated tank was used together with a flexible tube attached to the end of the return flow line. At the beginning of a test, a flow rate through the facility was established, then the flexible tube was diverted to fill the calibrated tank. After fluid was collected, the tube was removed from the calibrated tank, and the volume of fluid in the tank was measured. In addition, a totalizer was placed on the magnetic flowmeter output to measure the total amount of fluid pumped into the tank. The two fluid volume measurements were then compared. This process was repeated for several flow rates.

The results are shown in Table 1. Note that the flowmeter demonstrated an accuracy exceeding ±2.2% in both water and drilling mud. This was within the accuracy of the testing technique. The specifications stated by the manufacturer include an accuracy of ±0.5% In any case, the magnetic flowmeter demonstrated sufficient accuracy to use its output as the reference flow rate in testing the other flowmeters.

Table 1 - Magnetic flowmeter calibration results.

	Flow rate (gpm)	Total volume from meter reading (gallons)	Total volume measured in tank (gallons)	% Difference
Water	300	163	165	+1.2%
	300	154	157	+1.9%
	600	148	147	-0.7%
	600	142	143	+0.7%
	850	144	147	+2.1%
Drilling Mud	100	53	52	-1.9%
	200	96	96	0.0%
	400	145	145	0.0%
	500	176	180	+2.2%
	600	158	161	+1.9%

Laboratory Prototype Rolling Float Meter

The float in the rolling float meter spins and rides on the surface of the water. The spin rate is affected by the profile and traction of the float. Each tested float shape was constructed of a shell of plastic approximately 9 inches in diameter. The traction of each float consisted of raised rectangular tread areas or "bumps", as seen in the photograph in Figure 18. This tread was approximately the same for each float shape.

The height and spin rate response of the meter with a 4-inch and 3-inch wide oval profile is shown in Figures 20 and 21. These two wheels had the same basic profile consisting of a flat area and rounded corners; however, one was 4 inches wide while the other was three inches wide. The measured height of the flowmeter is only slightly affected by the change in wheel shape. However, the repeatability error at low flow rates was slightly smaller with the 3-inch wide wheel than with the 4-inch wide wheel. The float perimeter velocity measurements show a larger discrepancy between the two wheel shapes. The data for the 4-inch wide wheel reach a maximum at approximately 400 gpm and then begin to decline at higher flow rates, while the data for the 3-inch-wide wheel approach an asymptotic value. The asymptotic behavior displayed by the 3-inch wide wheel is more representative of the actual centerline fluid velocity expected in the return line, and is, therefore, considered a better measurement.

A comparison of responses from wheels with a 3-inch-wide oval, a 2-inch-wide "V", and a 2-inch-wide flat profile shape are shown in Figures 22 and 23. The different profile shapes of these wheels made a larger difference in float height measurements. The hydrodynamics of a spinning float can be such that the fluid accelerates under the float. This causes a lower pressure which provides a force that holds the float to the surface of the fluid and prevents it from bouncing free when it encounters surface waves moving down the return line. This is a necessary feature of the meter as it causes the rolling float to produce a relatively stable reading without significantly disturbing the flow. During testing, the 2-inch-wide flat profile wheel was not strongly held to the fluid surface, and continuously bounced free; this is manifested in a larger float height and a smaller float velocity measurement. For this reason, further testing of that profile was not conducted. Finally, the 3-inch-wide oval wheel displayed slightly lower repeatability errors than the 2-inch "V" profile wheel. For this reason, the 3-inch-wide oval wheel was chosen as the optimal wheel shape.

The two-inch-wide flat wheel was tested both with and without surface roughness. The smooth wheel, achieved by fitting the wheel with a smooth rubber sleeve, did not spin at all. It is the spinning of the wheel which causes the adhesion to the fluid surface. As the ability of the rolling float meter to closely track the fluid surface is an important function of the meter, it was determined that surface roughness was a necessary feature of the rolling float meter.

The effect of the pivot arm length on the float height and velocity measurements is shown for the 3-inch-wide oval wheel in Figures 24 and 25. The length of the arm had very little effect on the float height measurements. The pivot arm length had a more significant effect on the float perimeter velocity; however, as the measured velocity is not a good indication of fluid flow rate, the difference was not considered when choosing the optimal parameters.

The instantaneous response of the rolling float meter height and velocity measurements is shown in Figures 26 and 27 for a configuration that included air dashpot damping. Even with damping, the surface waves inherent in the return line flow cause the float to fluctuate vertically, which causes an apparent scatter of almost 0.5 inch in the float height and 0.5 ft/sec in the velocity measurements. A series of tests were conducted to determine the effects of damping on the fluctuations in float height. The level of damping was adjusted by controlling the size of the air escape orifice on the dashpot. The level of damping was characterized by measuring the length of time required for the float and pivot arm to fall from 70° to 45° with respect to vertical. For the

damping study, the fluid flow rate was set, and data were sampled at a frequency of 30 Hz for approximately 30 seconds. The instantaneous data at flow rates of 300 and 900 gpm were taken for dashpot settings of 0.3 (no damping), 6, and 18 second fall times. The fluctuations in float height caused a scatter in the pendulum reading of approximately 0.15 V at 300 gpm and 0.4 V at 900 gpm. Both the level of scatter and the frequency of the readings were independent of the level of damping provided by the dashpot. It was determined that filtering or averaging the signal from the rolling float meter is more practical for achieving a stable reading than mechanically damping the float.

The rolling float meter is counterbalanced to make the float light enough to ride on the surface of the fluid. The counterbalance is set by adjusting the location of the counterweight with respect to the pivot axis (see Figure 17). During operation it is possible for drilling fluid to accumulate on either the float or the counterweight, changing the counterbalance on the system. Therefore, the effects of the amount of counterbalance or excess wheel weight was studied. The effects of excess wheel weights from 5-60 g are shown in Figures 28 and 29 for tests in water. Excess wheel weight in this range has very little effect on the average height measurements, but affects the average perimeter velocity measurements by approximately 0.3 ft/sec. Again, as the float velocity was determined to be unnecessary in the measurement of flow rate, the effects on velocity are unimportant.

The effects of excess wheel weight in the range of 20-517 g in drilling mud are shown in Figures 30 and 31. Excess weights in the range 20-100 g had little effect on the height or velocity measurements. However, an excess wheel weight of 517 g (no counterbalance) caused the float to ride up to 0.3 inch lower in the fluid and caused the spin rate to drop considerably. Since only large changes in excess wheel weight affect the rolling float meter measurements, it was determined that the meter should be produced with a simple splash guard to prevent large amounts of mud build-up, but that small amounts of buildup would not have a measurable effect on meter performance.

The repeatability of the float measurements at each counterbalance setting was analyzed to determine the optimal setting. The error in repeatability for the 3-inch-wide, oval wheel was smallest for the 20 g excess wheel weight setting, with a maximum error of 0.04 inch at a flow rate of 600 gpm. The repeatability error at other counterbalance positions was as high as 0.1 inch Therefore, an excess wheel weight of 20 g was chosen as optimum.

The effects of pipe slope on the rolling float meter height and velocity measurements are shown in Figures 32 and 33. As the pipe slope increases, the fluid height decreases and the fluid velocity increases. This is consistent with the theoretical results, as larger pipe slopes subject the fluid in the return line to greater acceleration.

Field Prototype Rolling Float Meter

The field prototype rolling float meter was constructed after testing was complete on the laboratory prototype. The field prototype meter used a 3-inch-wide, oval-shaped wheel with no dashpot, and the counterbalance was set to an excess wheel weight of 20 g. To match field conditions at the Long Valley Exploratory Well, a 12-inch steel pipe was installed as the return line in the WHFF. The pivot arm length on the field prototype was increased to approximately 11 inches to account for the larger pipe diameter. Several other design changes were made for the field, including the design of a more rugged cover box, relocation of the counterweight inside the box, and installation of a splash guard to minimize mud splash on the float counterweight and the top of the box. The field prototype was tested in the WHFF to determine the effects of drilling fluid properties and solids concentration on the float measurements.

The field prototype rolling float meter was tested in water and in drilling muds with viscosities of 17.5 and 28.5 cP. The results of the height and velocity measurements are shown in Figures 34 and 35. The height measurement of the rolling float meter was not significantly affected by changes in fluid viscosity. However, Figure 35 illustrates a dramatic increase in float perimeter velocity when the circulating fluid was changed from water to drilling mud. This could be due to fluid hydrodynamics as an increase in fluid viscosity will decrease the flow Reynolds number, causing the flow to have a more gentle velocity profile and, therefore, a higher velocity at the surface. These results provide further proof that the float spin rate is not an accurate measure of flow rate.

Drill cuttings from a well site were collected and added to the drilling mud to determine the effects of solids on the rolling float measurements. The results are shown in Figures 36 and 37. The rock chips had little effect on the height measurements. It had more effect on the velocity measurements, where rock chips apparently caused a higher float perimeter velocity. Barite weighting material was added to the drilling mud and used to test the effects of both drilling fluid density and viscosity on the meter response. These results are shown in Figure 38. Again, the change in mud properties was found to have little effect on the meter height measurements. As discussed previously, the rolling float meter will have to be calibrated against an inflow meter when it is installed on a drilling rig. Since both fluid properties and rock chip concentration have little effect on the rolling float meter height measurement, a single calibration of the meter should be sufficient to ensure accurate flow measurements over a range of drilling conditions.

The effects of excess wheel weight were also tested with the field prototype. The results, shown in Figures 39 and 40, are similar to those of the laboratory prototype. The excess wheel weight has little effect on the float height up to a weight of approximately 100 g; at an excess wheel weight of 507 g (no counterbalance), the wheel rides slightly ($\approx$ 0.3 inch) lower in the return line flow. The float velocity results show the same trends as those reported previously for the laboratory prototype meter.

Finally, the repeatability of the field prototype meter was tested at a 10° pipe slope in 21.5-cP drilling mud. The results are shown in Figures 41 and 42. The maximum difference in float height readings between the two runs is 0.02 inch. This corresponds to an error of less than 0.2% of the full scale (12 inches) or 0.6% of the maximum measured height (3.2 inches at 950 gpm). As discussed previously, the float perimeter velocity measurements are not repeatable.

The height measurements of the field prototype rolling float meter proved to be not greatly affected by changes in fluid properties, fluid solids content, and excess wheel weight. In addition, height measurements from the meter were repeatable within 0.02 inch. Based on this performance, it was concluded that field testing of the rolling float meter was justified.

Paddlemeter

A conventional paddlemeter was tested in the WHFF in both water and drilling mud. The paddlemeter voltage readings are shown as a function of water flow rate for 5° sloped pipe in Figure 43. The system configuration was such that the paddle hit the top of the pipe at flow rates above 600 gpm. The paddlemeter showed significant hysteresis effects at low flow rates, in that the data obtained with increasing flow rate differed from the data obtained with decreasing flow rate. The difference in readings at no flow conditions was as much as 1 V. The response of the paddlemeter with weighted drilling mud and rock chips in a 10° inclined pipe is shown in Figure 44. The return line pipe used during this test was a 12-inch steel pipe, and the paddle did not touch the pipe at high flow rates as seen previously. Again, the response shows hysteresis effects at flow rates less than 200 gpm. The scatter in the readings at high flow rates was as much as 0.15

V. In general, however, the response of the paddlemeter to a range of flow rates in the laboratory test facility did not shown the scatter and repeatability errors that are often experienced in the field. This may be due to the location of the meter in the return line or the difference in inflow pumps.

Because the water testing of the flowmeters was conducted in a clear acrylic pipe, the effect of the flowmeter on both the upstream and downstream flow was evident. Photographs of the rolling float meter and the paddlemeter during laboratory testing are shown in Figures 45 and 46. At high flow rates the paddlemeter affected the flow in the pipe such that the pipe was completely filled with water upstream of the meter, while the rolling float meter had very little effect on the return line flow.

Laboratory testing of the paddlemeter showed hysteresis effects at low flow rates, significant disturbance in the return line flow, and a limited flow rate range in smaller pipes. Prior field experience with the paddlemeter has shown both scatter and repeatability problems. It was determined, therefore, that further and more detailed field testing of the paddlemeter was warranted.

Doppler Ultrasonic Flowmeter

A Doppler ultrasonic flowmeter was installed just downstream of the magnetic flowmeter in the WHFF. Tests of the performance of the ultrasonic flowmeter were conducted with both water and drilling mud. Results were better for drilling mud than water, as the fluid contains more particles; however, it still did not accurately measure the fluid flow rate. A comparison of the magnetic flowmeter and Doppler ultrasonic inflow rate measurements with drilling mud is shown in Figure 47.

The Doppler ultrasonic meter accurately measured inflow rates up to approximately 400 gpm. Above 400 gpm, however, the Doppler meter measured flow rates lower than actual. In fact, the Doppler ultrasonic meter indicated flow rates that were as much as 40% lower than those measured by the magnetic flowmeter. Because the Doppler ultrasonic flowmeter is sensitive to noise in the environment, it is possible that the pump speed and pipe vibrations at higher flow rates caused too much noise for the ultrasonic meter to reject. Although the Doppler ultrasonic flowmeter did not accurately measure fluid flow rates in the laboratory, the actual drilling environment could not be fully simulated, so it was deemed necessary to test the meter in the field.

FIELD TESTING

The laboratory test results indicated that field testing of both the rolling float meter and a conventional paddlemeter was warranted. In addition, it was determined that simultaneous testing of various standard and non-standard inflow and outflow measurement techniques would permit a thorough evaluation of the relative accuracy and reliability of the various measurement techniques currently available to the industry. This field testing was conducted during phase-2 drilling of the Long Valley Exploratory Well, a joint U.S. Dept. of Energy-State of California exploratory well being drilled by Sandia National Laboratories in the Long Valley volcanic caldera near Mammoth Lakes, California, to investigate hydrothermal and advanced geothermal systems. The drill rig and surrounding site are seen in Figure 48. Mud flow measurements were made and recorded every one to five minutes during most of the 1½-month drilling period for this phase of the well.

Description of the Tested Flowmeters

Several types of flowmeters were tested in the field. The inflow meters tested included a conventional mud pump stroke counter, a pump rotary speed transducer, a magnetic flowmeter, and a Doppler ultrasonic flowmeter. The outflow meters tested included a conventional paddlemeter, a commercial acoustic level meter, and a rolling float meter. The model and manufacturer of each of the tested flowmeters can be found in Appendix C.

The mud pump stroke counter employs a limit switch that opens and closes with each stroke of the mud pump piston. The number of strokes detected in a given time period is then multiplied by the volume of fluid pumped during each stroke and the pump efficiency to determine the total output rate of the pump. Shortcomings of this type of flowmeter include: slow response due to the relatively long time period (typically 1-2 seconds) between strokes; and inaccuracies due to uncertainties in pump efficiency, which changes with pump pressure, mud temperature and properties, and piston seal wear.

The pump rotary speed transducer uses an optical encoder that provides pulses at a rate proportional to the rotary speed of the mud pump drive shaft. By multiplying this rotary speed by the pump efficiency and the volume of fluid pumped during each rotation of the drive shaft, the total output rate of the pump is determined. The encoder used in the field test produced sixty pulses per revolution of the shaft, and there were 4.79 revolutions per pump stroke; therefore, the encoder output frequency was 287 times the stroke frequency. This method does not suffer from the slow response of the pump stroke counter because the optical pickup senses partial rotations; however, it does share the same uncertainty as the stroke counter with respect to pump efficiency.

The magnetic flowmeter establishes a magnetic field in the fluid flowing through it. Perturbations in the magnetic field are correlated with fluid velocity and multiplied by the flow area to determine the flow rate through the meter. This type of flowmeter is calibrated to flow rate by the manufacturer, provides exceptional accuracy, and the output signal is not affected by changes in fluid properties as long as the fluid is electrically conductive. Disadvantages include high cost and pressure limitations, which generally require the magnetic flowmeter to be installed on the pump inlet. Its use is limited to water-based drilling mud.

The Doppler ultrasonic flowmeter employs a non-intrusive transducer that clamps to the outside surface of the pipe. The transducer emits ultrasonic pulses and detects the Doppler shift of the returning pulses as they are reflected off particles in the fluid. The Doppler shift is a quantified function of the mean fluid velocity, which is multiplied by the flow area to determine the total flow rate through the pipe. Shortcomings include inaccuracies caused by mechanical and electrical noise in the drilling environment and the requirement that solid or gaseous particles be present in the flow.

The paddlemeter commonly used to measure outflow rates in drilling operations employs a single, spring-mounted vane or paddle that extends down into the flow and is deflected upward by fluid impinging upon it. The amount of deflection is a function of the impact force of the fluid on the paddle, which in turn is a function of the fluid height and velocity and, thus, the flow rate. The paddle deflection is calibrated to provide a measure of the flow rate. Limitations experienced with this meter are poor accuracy and repeatability. Consequently, this meter is often used in the field in a qualitative manner, with the output presented in terms of a fraction of full paddle deflection rather than absolute flow rate.

The acoustic level meter uses a transducer mounted above the fluid surface that emits acoustic pulses and detects the return pulses echoed off the fluid surface. The echo time is proportional to the distance between the transducer and the fluid surface, which in turn is a function of the flow rate through the pipe. The primary disadvantage of this type of meter is that the temperature and

composition of the air in the return flow line significantly affect the acoustic velocity and, therefore, the echo time. As a result, the data must be corrected to account for these effects.

The rolling float meter is the developmental flowmeter which is the subject of this report.

Test Hardware Installation

A conventional stroke counter was installed on each of the two mud pumps used at the rig. In addition, the drive shaft of each pump was fitted with an optical encoder to sense rotary speed. This was accomplished by simply securing the rotary shaft of each encoder to a tapered rubber stopper that was pressed into a threaded hole on the end of each drive shaft. The rubber stopper was then squeezed in the axial direction with the shaft-mounting hardware to radially expand the stopper and secure it within the hole. Both the stroke-counter limit switch and the rotary speed transducer on one of the mud pumps can be seen in Figure 49.

A 10-inch magnetic flowmeter was installed on the inlet to each mud pump, as seen in Figure 50. The magnetic flowmeters were installed with approximately 8 feet of straight pipe upstream of the meters. The flowmeter manufacturer recommends the installation of a 10-pipe-diameter length of straight pipe upstream of the meter to ensure highly accurate flow measurements [13]. The installation at the Long Valley Exploratory Well was within 4 inches of the manufacturer's recommendation.

A Doppler ultrasonic flowmeter, shown in Figure 51, was attached externally to a vertical section of the standpipe at a location approximately ten feet above the mud pump level. An RTD temperature probe was externally attached to the standpipe and wrapped with fiberglass insulation. A pressure transducer was also installed in the standpipe to read mud pump pressure.

The acoustic level meter, the prototype rolling float meter, and a conventional paddlemeter were mounted on the return flow line between the wellbore and the shale shakers as shown in Figure 52. Because it does not interfere with the flow, the acoustic level meter was mounted first in line, approximately 15 feet from the wellbore. The paddlemeter, which disturbs the flow for several feet upstream and downstream of the paddle, was mounted 28 feet from the wellbore. The rolling float meter was mounted 20 feet from the wellbore, 5 feet downstream of the acoustic level meter and 8 feet upstream of the paddlemeter. An RTD temperature probe was also installed on the flow line, with the probe protruding directly into the mud flow. A catwalk was built parallel to the flow line to allow easy access to the various instruments. Photographs of the flow line and transducers are shown in Figures 53 - 56.

Description of Data Acquisition System

The data acquisition system included field-hardy hardware for gathering the data and a remote IBM®-class PC for both data processing and storage. The hardware used to gather the raw input signals in the field included Schlumberger Instruments Isolated Measurement Pods (IMPs). The IMPs are sealed in a NEMA-4X enclosure and are typically used for data acquisition in harsh industrial environments. They were installed on the shale shaker platform near the return line flowmeters. The IMPs were powered and computer-controlled and data were transmitted over a simple 2-wire serial link that allowed the computer to be housed in a trailer situated in an area away from the drilling rig. The IMPs transmitted digital readings of the current, voltage, and frequency data they gathered from the various transducers.

RTM 3500® from Micro Specialty Systems, Inc., a real-time multitasking data acquisition software package, was used for communicating with the IMPs through an interface board on the PC. With this package, measured data (raw, conditioned, and averaged signals) were displayed in a spreadsheet as they occurred. Data were recorded on disk at set intervals or at the activation of user-defined alarms. In addition, the software had background/foreground capabilities that allowed continuous, uninterrupted data acquisition while performing other tasks with the computer.

Data Acquisition Strategy

During data acquisition, the data were read and displayed once every second; however, data storage intervals were much longer. Initially, data were stored at five-minute intervals during normal operations and at one-minute intervals during periods of measured lost circulation or production. During the field work, it was determined that a data storage interval of one minute would best capture transducer operation during all drilling conditions. Both instantaneous and average data were displayed on the screen and stored to disk. The average data were tied to data storage such that the averages were reset every time data storage occurred.

Even during steady drilling operations, transducer signals in the field were not steady. A standard RC filter with a 22-μF capacitor and a 100- to 200-kΩ variable resistor (resulting in a 2.2- to 4.4-second time constant) was installed on the rolling float meter to smooth out inherent unsteadiness. The signals from the magnetic flowmeters, acoustic level outflow meter, and paddlemeter were conditioned with the data acquisition software using a first-order digital filter formula with an equivalent time constant of approximately 27 seconds.

Flowmeter Calibration and Testing Procedures

Since the three outflow meters did not directly measure fluid flow rate, a calibration was necessary. Meter calibrations were conducted at the beginning of phase-2 drilling, when the pre-existing phase-1 hole was cased and no lost circulation or production was occurring. Calibrations were again conducted during the field tests when meter settings or parameters were changed. These calibrations were conducted when pit level indicators measured no loss or gain of fluid.

Each flowmeter was calibrated against the magnetic flowmeter inflow measurements. Measurements were taken in increments of approximately 10 strokes/min, from no-flow conditions to the maximum output of the pumps (approximately 40-50 strokes/min on each of two inlet pumps). When the desired flow rate was attained, it was maintained as meter outputs were read once per second for approximately 20-30 seconds, resulting in 20-30 data points at each of ten measured flow rates. The calibration data from each meter were fit with a third-order polynomial using a least-squares curve fit. The resulting equations were then used to convert raw signals to flow rates during drilling.

The calibration procedure described above required less than 15 minutes and resulted in ten measured flow rates. However, subsequent data analysis has shown that as few as four measured flow rates can result in an accurate calibration curve, with two points at low flow rates (e.g., at 0 gpm and 100 gpm) and two points at high flow rates (e.g., 800 gpm and 900 gpm). In addition, five or more equally-spaced measured flow rates that include both zero flow and high flow rates will result in an accurate calibration. Thus, the time necessary for outflow meter calibration could feasibly be reduced from 15 minutes to 5-10 minutes.

The outflow meter calibration procedure was also used to evaluate the various inflow meters under the full range of flow rates. Both the pump stroke counters and pump speed counters were calibrated during the procedure. This resulted in a linear calibration curve based on the pump efficiency during the procedure. The calibration was not expected to remain accurate as the pump efficiency changed with drilling parameters such as temperature, pressure, mud properties, and seal wear. The performance of the pre-calibrated Doppler ultrasonic flowmeter was also evaluated during the outflow meter calibration procedure.

FIELD TEST RESULTS

Flowmeter Calibration and Normal Drilling Conditions

The two magnetic flowmeters measuring drilling fluid inflow were used as standards for evaluating the remaining transducers. The magnetic flowmeters have a rated accuracy of at least 1% of the total span, and their performance during the field test generally confirmed this. For approximately two days during the drilling operation, however, the magnetic flowmeters measured a flow rate consistently 0-5% lower than the other inflow and outflow meters in the system. During this time period, the magnetic flowmeters also read flow rates of up to 40 gpm when the pumps were shut off. Because the drilling crew was having problems with the mud cleaning system at that point, it is possible that fines were settling out in the magnetic flowmeter flow lines, thereby disturbing the magnetic fields and reducing the accuracy of the meters. When the mud cleaning system was repaired, the magnetic flowmeters again measured accurately. Since the magnetic flowmeters were by necessity installed in a horizontal line, they were susceptible to silting. Certainly it would have been preferable to install the meters in a vertical position; however, the flowmeters' pressure limitations required installation on the pump inlet line.

During normal drilling operations, the efficiency of the pumps (calculated by comparison with the magnetic flowmeter inflow measurements) varied by as much as 10%, from 86% to 96%. The efficiency varied by as much as 5% on any given day. In addition, factors such as the presence of air in the drilling mud reduced the pump efficiency to values as low as 65% for periods of up to three hours.

The Doppler ultrasonic flowmeter calibration showed significant scatter and error in readings obtained throughout the flow rate range, as shown in Figure 57. The meter measured rates as much as 50 gpm high at low flow rates, and 200 gpm or 35 % high at higher flow rates. The meter used in this study was designed with a sensitive pick-up for use with clean fluids, making it extremely susceptible to electrical noise and vibrations. As a drilling site is an extremely "noisy" environment, the Doppler meter never operated in a range in which it was not affected by electrical and vibrational noise.

Shown in Figure 58 are typical field calibration data obtained with the paddlemeter. At any given flow rate, the readings from the paddlemeter had significant scatter, sometimes as high as 35% of the average readings. Due to this scatter, there was significant overlap of voltage readings at various flow rates, making accurate calibration of the meter impossible. In addition, the paddlemeter displays very little sensitivity at flow rates above 700 gpm. The paddlemeter, therefore, often produced flow rate errors of ±15% of the actual flow rate, even when readings were averaged over periods of 1-5 minutes.

The acoustic level meter's field calibration data, shown in Figure 59, resulted in a curve similar to that of the paddlemeter; however, during calibration, the meter readings had a scatter of approximately 4%, resulting in a fairly accurate calibration curve. Calibration of the meters was

generally done after an extended period of non-drilling operations, such as tripping, when wellbore circulation was less constant than during drilling. As a result, the temperature of the air in the return flow line was significantly lower during calibration than during normal drilling operations. As drilling resumed, the temperature in the return flow line would increase, thereby increasing the acoustic velocity of the air inside the pipe. The increased velocity would cause the meter to sense a higher fluid level and, therefore, a flow rate higher than actual. Just after calibration the acoustic meter would provide accurate readings, but as drilling proceeded, the meter would read as much as 8% high.

The field calibration data obtained with the rolling float meter also resulted in a third-order polynomial calibration curve. Results of the field calibration that was conducted on August 30, 1991 are shown in Figure 60. During calibration, the meter readings had a scatter less than 2% of the average readings, resulting in an excellent calibration. As predicted by laboratory testing, the transducer readings were unaffected by temperature or changes in mud properties during drilling. Typically, the meter read within an apparent accuracy of ±2% and was often as accurate as ±0.5%. There were often periods when the rolling float meter reading would match the magnetic flowmeter reading within ± 5 gpm out of a total flow rate of approximately 900 gpm.

Problems with the prototype flowmeter were encountered and corrected during the field test. When the return mud temperature reached approximately 145°F, the sidewalls of the polyethylene float softened sufficiently to warp and become disengaged from the hubs and bearings. This problem was corrected by filling the hollow float with polyurethane foam to provide structural rigidity at higher temperatures. One of the float's bearings also experienced periodic sticking toward the end of the test period, causing erroneous readings. Since the problem lasted for only brief periods of time, it was not deemed serious enough in the short remaining test time to warrant repair.

A comparison of typical performance of the three outflow meters is provided in Figure 61. Shown here are the magnetic flowmeter inflow rates for a typical day, along with outflow rates as measured by the acoustic level meter, paddlemeter, and rolling float meter. The drilling report for that day indicates a stable pit level, so no measurable fluid loss or gain was occurring. The rolling float meter measured outflow within -1% to +2% of the magnetic flowmeter inflow rate. The acoustic meter read consistently 2% to 8% high, while the paddlemeter read consistently 2% to 9% low. Although the rolling float meter experienced some problems due to its developmental status, once those problems were resolved, it proved to be the most accurate of the three outflow meters tested.

Detection of Abnormal Hydraulic Conditions

The opportunity to test the outflow meters under abnormal hydraulic conditions such as lost circulation and wellbore fluid production presented itself when both these conditions occurred in the same wellbore within a few days of each other. The drilling report for August 30, 1991, noted a pit loss of 200 bbl of drilling fluid. The measured magnetic flowmeter inflow rates are shown plotted with the results from the rolling float meter, acoustic meter, and paddlemeter, respectively, in Figures 62-64. Both the rolling float meter and the acoustic level flowmeter measured a drop in flow rate relative to the magnetic flowmeter inflow readings. According to these meters, the loss began at approximately 6:30 pm on August 30 and ended just after 4:00 am on August 31, after the addition of lost circulation material (LCM) to the drilling mud. Loss rates up to 56 gpm, or 6% of the inflow, were detected. The drilling crew noted a drop in pit level at a drilling depth of 6140 ft. This was approximately 9:00 pm, 2½ hours after the outflow meters first detected a loss. The paddlemeter measured a lower flow rate than the magnetic flowmeter throughout the entire time

period. The actual loss and subsequent recovery of circulation was not detected by the paddlemeter.

The abnormally high rolling float measurement (Figure 62) between 4:00 am and 6:00 am on August 31 was due to a bearing sticking on the float. If the float is not free to spin, it rides higher in the water resulting in a significantly higher flow rate reading.

Wellbore fluid production during drilling was detected on September 6 and 7, when the mud logger's pit level report indicated an increase of 200 bbl. The flowmeter responses are shown in Figures 65-67. Measurements from the rolling float meter indicated about 5-6% greater outflow than inflow starting at approximately 2:00 pm and ending near midnight on September 6. Since the acoustic level meter read as much as 7% high throughout the day, the wellbore production of fluid was not distinctly detected with this meter. The same is true for the paddlemeter, which read approximately 5-7% low during the entire time period.

DISCUSSION OF FIELD TEST RESULTS

Based on the experience of the field test described above, it would appear that the magnetic flowmeter is nearly ideal for measuring drilling fluid inflow rates of water-based drilling mud. The relatively high cost of magnetic flowmeters, however, may make them impractical for routine use. For instance, the 10-inch magnetic flowmeters used in this field test cost $8700 each. In addition, the magnetic flowmeters are limited to use only with water-based drilling mud.

On the basis of ease of installation, minimum interference, and applicability to all drill rigs, the Doppler ultrasonic flowmeter would be the best option for inflow rate measurement. These meters are non-invasive and theoretically are not affected by fluid properties; however, we were unable to obtain accurate measurements with the flowmeter that was tested. This agrees with our experience in the laboratory and at other field sites. Although we have obtained accurate readings with this type flowmeter under carefully controlled laboratory conditions, we have not found it reliable enough to use by itself in the rig environment.

Although the stroke counter and rotary speed transducer are both reliable in measuring the pump speed, only an accurate knowledge of pump efficiency allows the pump speed to be accurately converted to flow rate. Because pump efficiency cannot be determined without some independent means for measuring the flow rate, and because of the effects of fluid properties and pump speed, pressure, and seal wear on pump efficiency, it is difficult to obtain highly accurate flow rate measurements with these meters. This problem can be overcome by an analysis of the rate of change of the delta-flow measurement [4,5]. Since most significant changes in pump efficiency occur relatively slowly, these meters can be used with an accurate outflow transducer and frequent calibration procedure to detect rapid changes in delta flow. Although slow losses or gains of fluid cannot be measured in this manner, mud pump speed transducers still remain the most practical flowmeters to use for inflow measurements on the rig simply because of their reliability and ease of use.

The pump rotary speed transducers used in this field test were found to be preferable to the conventional pump stroke counters. The rotary transducers used provided a pulse output with a frequency 287 times the pump stroke frequency. Consequently, the response of the rotary transducers to changes in pump speed is much faster than that of the pump stroke counters. Although not all pumps can be easily fitted with rotary transducers, we recommend their use whenever possible.

Of the three outflow meters tested, the rolling float meter was by far the most accurate. This meter was found to measure the outflow rate within an apparent accuracy of at least 2%, and often within 1/2%. It was found capable of detecting very small gains and losses in drilling fluid relative to inflow rates. Some reliability problems were encountered with this meter, but those were due primarily to its developmental status and were temporarily solved in the field. Final solutions to these problems are discussed in a following section.

The acoustic level meter was found to be a fairly reliable meter for outflow measurements, detecting some, but not all, the fluid gains and losses detected by the rolling float. In order to attain the accuracy provided by the rolling float, however, it would be necessary to correct the acoustic level meter readings for the effects of air temperature. In fact, at least one service company currently uses an acoustic level meter in this manner, taking multiple temperature measurements in the air space between the fluid surface and the acoustic transducer and using the data to correct the transducer readings [4,5]. Our field test demonstrates that if the acoustic data are not corrected, accuracies better than 2-8% are not likely, particularly with hot wells. It is therefore necessary to monitor and analyze several channels of data to properly utilize the acoustic level meter.

Although extremely reliable, the paddlemeter evaluated in this field test did not demonstrate sufficient accuracy to be used for delta flow measurement. Oscillations of the paddle due to transient surface waves in the return flow line caused scatter in the paddlemeter signal that did not permit accurate calibration. Measurement accuracy was rarely better than 5%, and often ranged from 10 to 15%. The meter did not detect any of the fluid gains or losses detected with the other outflow meters. Although the paddlemeter provides a highly reliable *qualitative* measure of flow rate (i.e., high-flow, low-flow, or no-flow), it was not found to have the sensitivity needed to determine *quantitative* levels accurately.

Because of the outstanding accuracy demonstrated by the rolling float meter and the simplicity of its design and operation, this flowmeter has undergone further development since the field test.

FURTHER ROLLING FLOAT METER DEVELOPMENT

Foam Float Development

It was recognized early in the development program that the plastic float used in the laboratory and field tests did not have the structural or thermal stability required for a field-hardy instrument. The float failure experienced during the field test confirmed this conclusion. Consequently, development and testing of a field-hardy float was initiated after the field test.

The structural and thermal properties of closed-cell polyurethane foam were determined to be suitable for such a float. By eliminating the magnetic rotary speed transducer from the meter, it became possible to use a solid foam float that could be cast as a single piece. It was desired to maintain the same wheel shape and size as had been used in the laboratory development and field test. Accordingly, the plastic float used in the field was used to cast a silicone rubber mold, which was then used to cast solid polyurethane floats. Figure 68 is a schematic of the aluminum mold box used to contain the silicone rubber mold.

A photograph of a solid foam float cast from this mold is shown in Figure 69. The foam used in this and the other tested floats consisted of a two-part, closed-cell polyurethane foam with an expanded density of 6 lb/ft^3. A machined steel tube was cast into the float as a means for fitting

the float with bearings. A stainless steel bearing assembly is pressed into each end of this tube. The inner races of the bearing assemblies fit the shaft of the pivot arm, which is the rotational axis of the float.

To test the thermal integrity and abrasive wear resistance of the float, the float durability tester shown in Figure 70 was fabricated. It consists of a 55-gallon drum fitted with a drive shaft that is powered by a variable-speed electric motor. The test float is mounted on this shaft and is rotated at speeds of approximately 130 rpm. The drum is filled with drilling mud to a level such that the lower portion of the float is below the mud surface when the float spins. Electric band heaters are attached to the outer surface of the drum to heat it to temperatures up to 200 °F. An air-powered mixer is used to stir the mud and maintain consistent properties throughout the drum. A lid is placed on the top of the drum during operation to minimize evaporation of the water from the drilling mud.

The first float tested in the drum was cured in the silicone rubber mold at 165 °F for 4 hours. It was initially tested at room temperature for 6 days with no apparent degradation. The temperature of the drilling mud was then raised to 180 °F. After running at this temperature for 3 days, the float developed severe cracking at multiple locations on its surface, as shown in Figure 71. Although the cracking did not significantly affect the structural integrity of the float, this cracking was considered unacceptable for long-term use of the float.

To solve the cracking problem, a second float was fabricated and cured at 250 °F for 16 hours. The float was then tested at room temperature and temperatures up to 195 °F for over 28 days. The temperature history of the test is shown in Figure 72. In addition to elevated temperatures, the float was subjected to multiple cooling cycles to simulate down-time on the rig. Despite the rigorous thermal environment, the float developed only two superficial cracks (less than 1/8 inch deep) on its sidewall. These cracks developed soon after the mud temperature was raised to 180 °F but did not grow in length or depth with further testing. This cracking was considered insignificant and should not affect the long-term performance of the float.

The closed-cell structure of the polyurethane foam float was found to absorb very little water during testing. The initial weight of the float, including the integral steel tube, was 380 g. Immediately after 28 days of testing, the float weighed 420 g, indicating an absorption of 40 g. After 18 hours of drying in air, the float weighed 406 g; thus the permanent weight gain due to water absorption was only 26 g, or 6.8% of the initial float weight.

These tests indicate that the polyurethane foam float developed during this program should be structurally and thermally stable to temperatures of at least 195 °F. Furthermore, no abrasive wear of the foam surface was detected, even after 28 days of testing. The goal of developing a low-cost, rugged float for use in the rolling float meter has, therefore, been accomplished.

Bearing Assembly Development

During field testing of the rolling float meter, a bearing on the float periodically bound up, causing erroneously high readings. Because of this, a simple, lightweight splash guard was designed to prevent drilling mud from splashing into the bearing regions. By preventing mud from accumulating on the bearings, the bearings should last indefinitely, since they are subjected to very little load. To determine the utility of the splash guard, it was deemed necessary to test the entire bearing assembly in drilling mud at elevated temperatures in the laboratory.

Initially, a rolling float meter was assembled with new bearings and tested with water over a range of flow rates (0-900 gpm) in the WHFF. As the friction in the bearings will have an effect

on the float height measurement, the initial testing was used as a calibration test for the bearing assembly. After the initial test, the meter was reassembled with a different set of new bearings. The meter was again tested in the WHFF to determine the effects of variations between bearings on the meter height measurements.

After initial calibrations, the float and bearing assembly were then installed in the float durability tester. The axle of the float was rotated at approximately 225 rpm, with the float allowed to drag in the drilling mud and remain stationary. The bearing assembly was rotated in this manner for 18 days at temperatures ranging from room temperature to 183 °F. The temperature history of this test is shown in Figure 73.

After testing, the rolling float meter was reassembled and tested in the WHFF over the same range of flow rates. The rolling float readings both before and after bearing testing are shown as a function of flow rate in Figure 74. Differences in the angle measurement before and after high temperature testing are no greater than the measurement differences between meters with different sets of new bearings. Although the angle measurement is not repeatable between different meters, each meter has to be calibrated in place, so differences between individual meters are not important. The repeatability of a single meter, however, is important; the rolling float meter was shown to be repeatable within 0.02 inch in laboratory tests (Figures 41 and 42). The measurements indicate no significant change in meter performance after high-temperature testing for 21 days. These results indicate that the splash guard assembly is preventing mud accumulation on the bearings, and the bearing assembly should last for an extended period.

ROLLING FLOAT METER FABRICATION COSTS

The goal of this work has been to develop an accurate and reliable meter for measuring fluid outflow rates on a drilling rig. To be widely used, the meter must also be inexpensive and easily fabricated for a user by a local machine shop. An estimate of the total costs for the rolling float meter is provided in Table 1. With the exception of the polyurethane foam float, materials used in the fabrication of the meter are commercially available or can be easily machined. Estimates of fabrication times shown in Table 1 are for the fabrication of a single meter. If multiple meters were fabricated simultaneously, the fabrication times and, therefore, the total cost of the meters would go down accordingly.

The cost for fabrication of the polyurethane foam float has been estimated at $50. Although the fabrication costs of the foam float are low, the casting does require special equipment and persons trained in plastic molding procedures. Consequently, as part of the technology transfer effort for the rolling float meter, an attempt will be made to identify a plastic parts manufacturer that would be willing to supply foam floats as a commercially available item to users interested in fabricating their own rolling float meter.

Table 2 - An estimate of costs associated with the fabrication of the rolling float meter.

Item		Cost
Materials		
Bearings	2 @ $22 and 2 @ $13	$70
Stainless steel sheet for cover box		≈ $20
Float (estimated cost)		≈ $50
Remaining Materials	(brass counterbalance weight, threaded rod, SS tubing, SS collars, miscellaneous screws, etc.)	< $50
Instrumentation		
Pendulum potentiometer		$420
Fabrication		
Machine set-up time	est. 10.5 hrs @ $40/hr	$420
Machining time	est. 15 hrs @ $40/hr	$600
Assembly time	est. 4 hrs @ $40/hr	$160
Total Estimated Cost		**$1790**

CONCLUSIONS

A meter has been developed for measuring fluid flow rates in the return line of a drilling rig. The meter employs a rolling float that rides on the surface and tracks the height of the fluid in the line, which can be calibrated to fluid flow rate. The meter was extensively tested in a laboratory facility simulating a full-scale drilling fluid return line. Several design parameters were optimized during laboratory testing to develop a field prototype of the meter. In addition, a conventional paddlemeter was tested in the laboratory facility. Results from the laboratory testing indicated the need for field testing of both meters.

The prototype rolling float meter, as well as several other commercial inflow and outflow meters, were tested during actual drilling operations at the Long Valley Exploratory Well near Mammoth Lakes, Ca. The rolling float meter measured drilling fluid outflow rates within 1/2-1%, compared with accuracies of 2-8% for an acoustic level meter, and 5-15% for the conventional paddlemeter. The rolling float meter distinctly captured periods of minor lost circulation as well as wellbore fluid production. Rolling float meter design problems apparent during field testing were addressed during further laboratory development and testing after field testing was complete.

The rolling float meter has proven to be an accurate and reliable meter for measuring drilling fluid outflow rates. It is simple, requiring only one channel of data, and can be easily installed on any drilling return line with minimum interference. With the exception of the polyurethane foam float, all parts used in the construction of the meter are commercially available or can be easily machined at a local machine shop. Fabrication costs for a rolling float meter have been estimated at less than $1800.

REFERENCES

1. Carson, C. C. and Lin, Y. T., 1982, "The Impact of Common Problems in Geothermal Drilling and Completion," Geothermal Resources Council, TRANS., Vol. 6, pp. 195-198.

2. DOE (U. S. Dept. of Energy), 1989, "Programmatic Objectives of the Geothermal Technology Division, Volume I," May, 1989.

3 Bode, D.J., Noffke, R.B., and Nickens, H.V.: "Well-Control Methods and Practices in Small Diameter Wellbores," *Journal of Petroleum Technology* (November 1991), pp. 1380-1386.

4. Orban, J.J., Zanker, K.J., and Orban: A.E., "New Flowmeters for Kick and Loss Detection During Drilling," SPE 16665, Presented at the 62nd Annual Technical Conference and Exhibition of the Society of Petroleum Engineers, Dallas, TX, September, 1987.

5. Orban, J.J., and Zanker, K.J.: "Accurate Flow-Out Measurements for Kick Detection, Actual Response to Controlled Gas Influxes," IADC/SPE 17229, Presented at the IADC/SPE Drilling Conference, Dallas, TX, February-March, 1988.

6. Speers, J.M., and Gehrig, G.F.: "Delta Flow: An Accurate, Reliable System for Detecting Kicks and Loss of Circulation During Drilling," SPE/IADC 13496, Presented at the SPE/IADC Drilling Conference, New Orleans, LA, March, 1985.

7. Maus, L.D., Peters, B.A., and Meador, D.J.: "Sensitive Delta-Flow Method Detects Kicks or Lost Returns," *Oil and Gas Journal*, August 20, 1979, pp. 125-132.

8. Johnsen, H.K., Skalle, P., Podio, A.L., Sirevaag, G., and Vigen, A.: "Development and Field Testing of a High-Accuracy Full-Bore Return Flow Meter," IADC/SPE 17228, Presented at the 1988 IADC/SPE Drilling Conference, Dallas, TX, February 28 - March 2, 1988.

9. Daily, J. W. and Harleman, D. R. F., *Fluid Dynamics*, Addison-Weslew Co., Massachusetts, 1966, pp.293-302, 349-359.

10. Daugherty, R. L., and Franzini, J. B., *Fluid Mechanics with Engineering Applications*, McGraw-Hill Book Co., New York, 1965, pp.276-326.

11. Fox, R. W., and McDonald, A.T., *Introduction to Fluid Mechanics*, J. Wiley and Sons, New York, 1985, pp. 501-560.

12. Plapp, J.E., *Engineering Fluid Mechanics*, Prentice-Hall, New Jersey, pp.340-371.

13. "Instruction Manual - Yewmag Models YM100, YM200, YM300, YM400, and YM500 Magnetic Flowmeters," IM 1E4C2-01E, Yokogawa Electric Corporation, Tokyo, Japan, February, 1991.

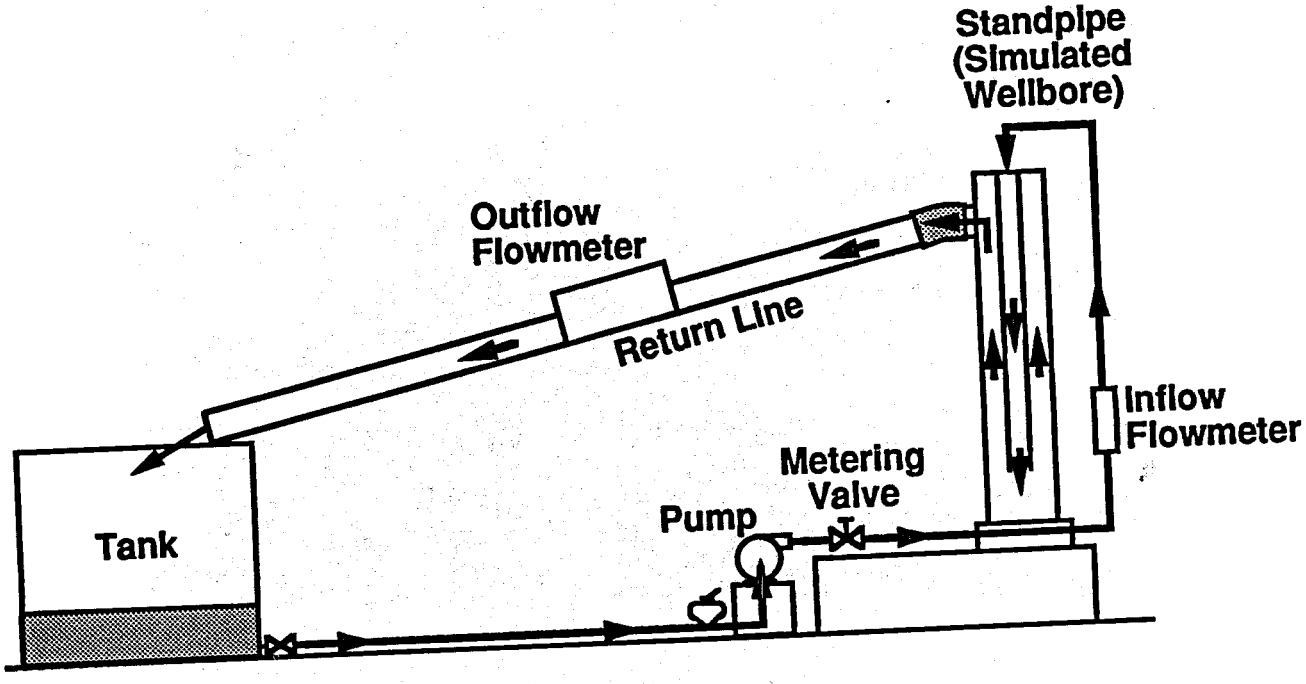

Figure 1 - Schematic of the Wellbore Hydraulics Flow Facility (WHFF).

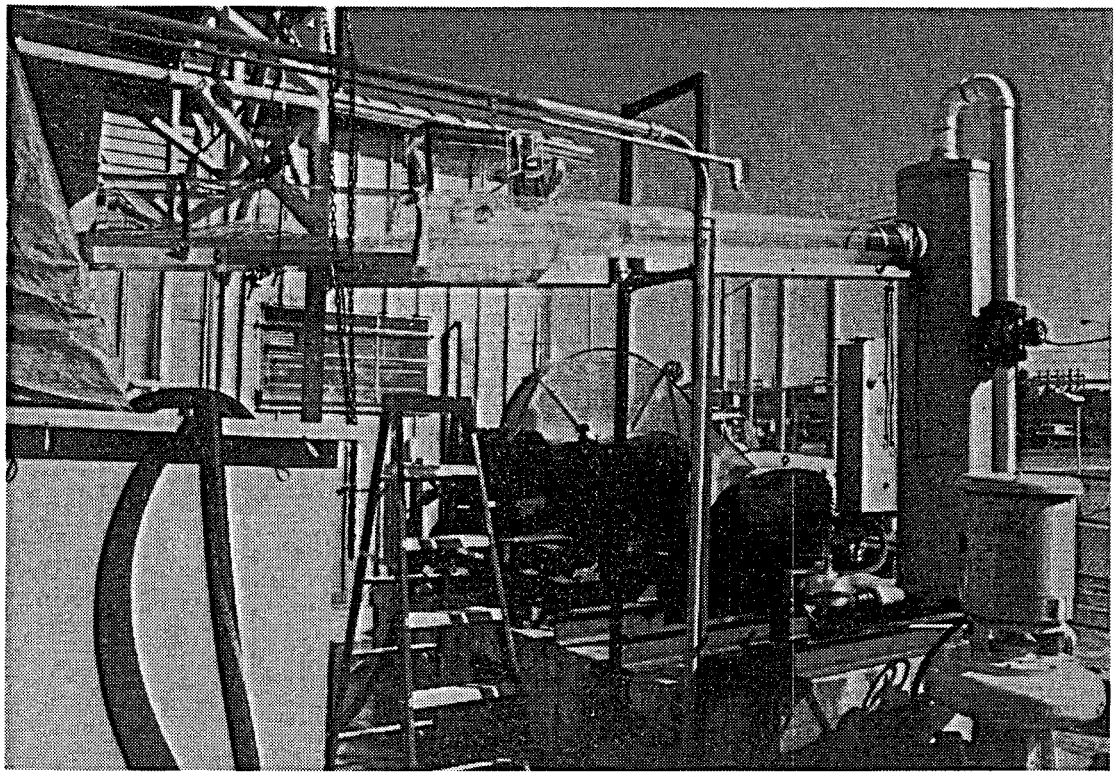

Figure 2 - Photograph of the Wellbore Hydraulics Flow Facility (WHFF).

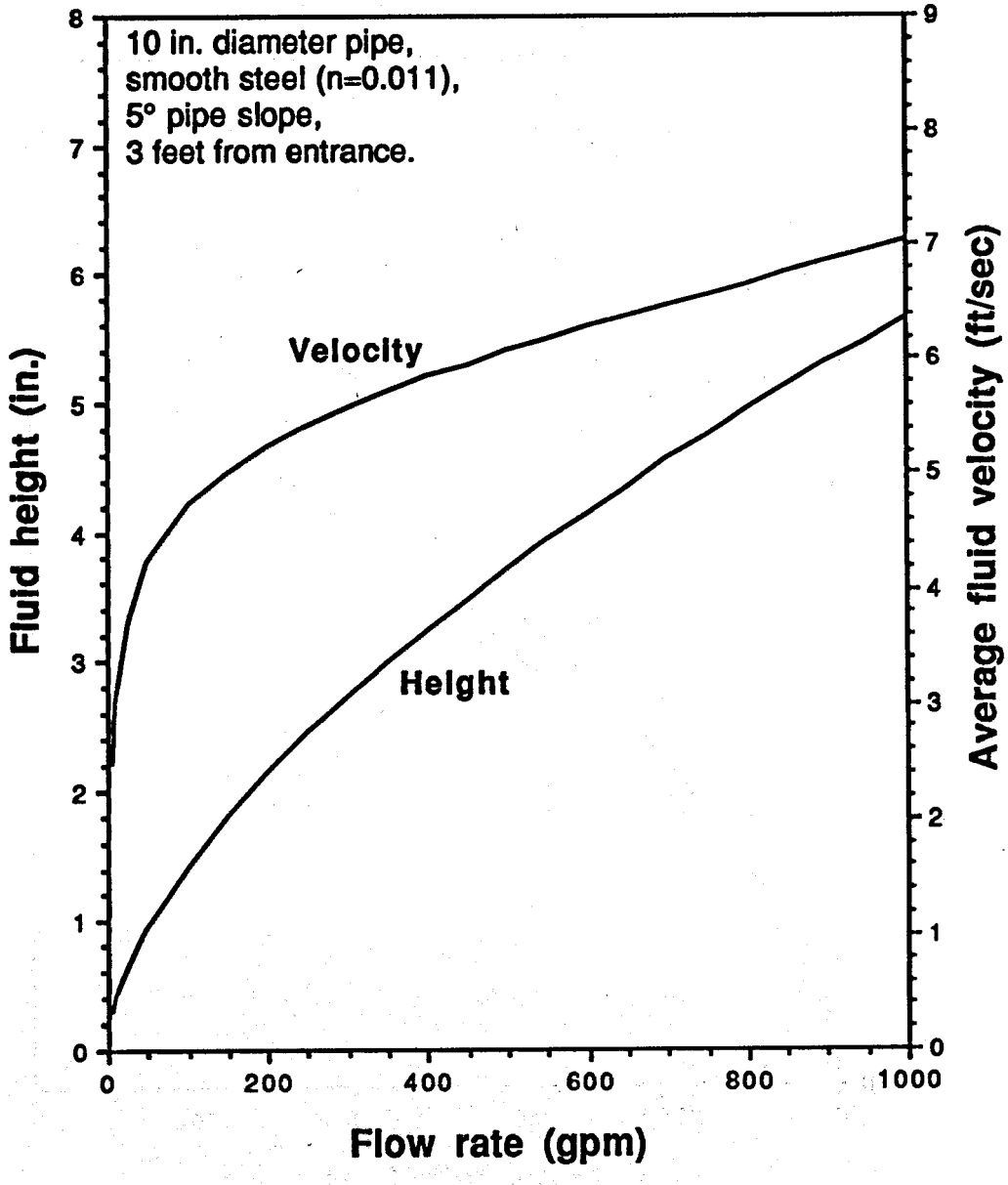

Figure 3 - Theoretical fluid height and average velocity as a function of fluid flow rate in a 10-inch diameter smooth steel pipe with a 5° slope at a location three feet from the fluid entrance.

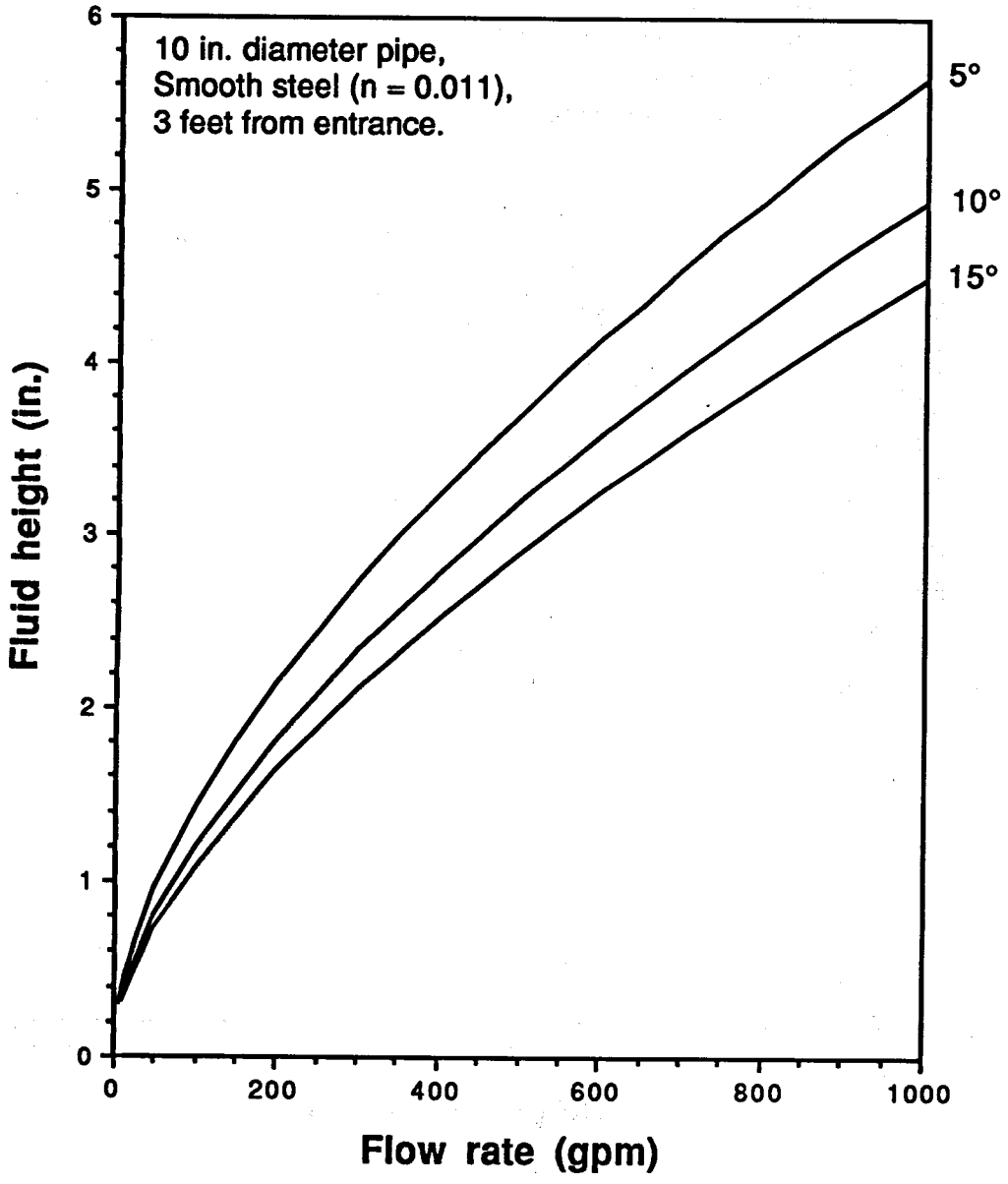

Figure 4 - Theoretical fluid height as a function of flow rate for various pipe slopes in a 10-inch diameter smooth steel pipe at a location three feet from the fluid entrance.

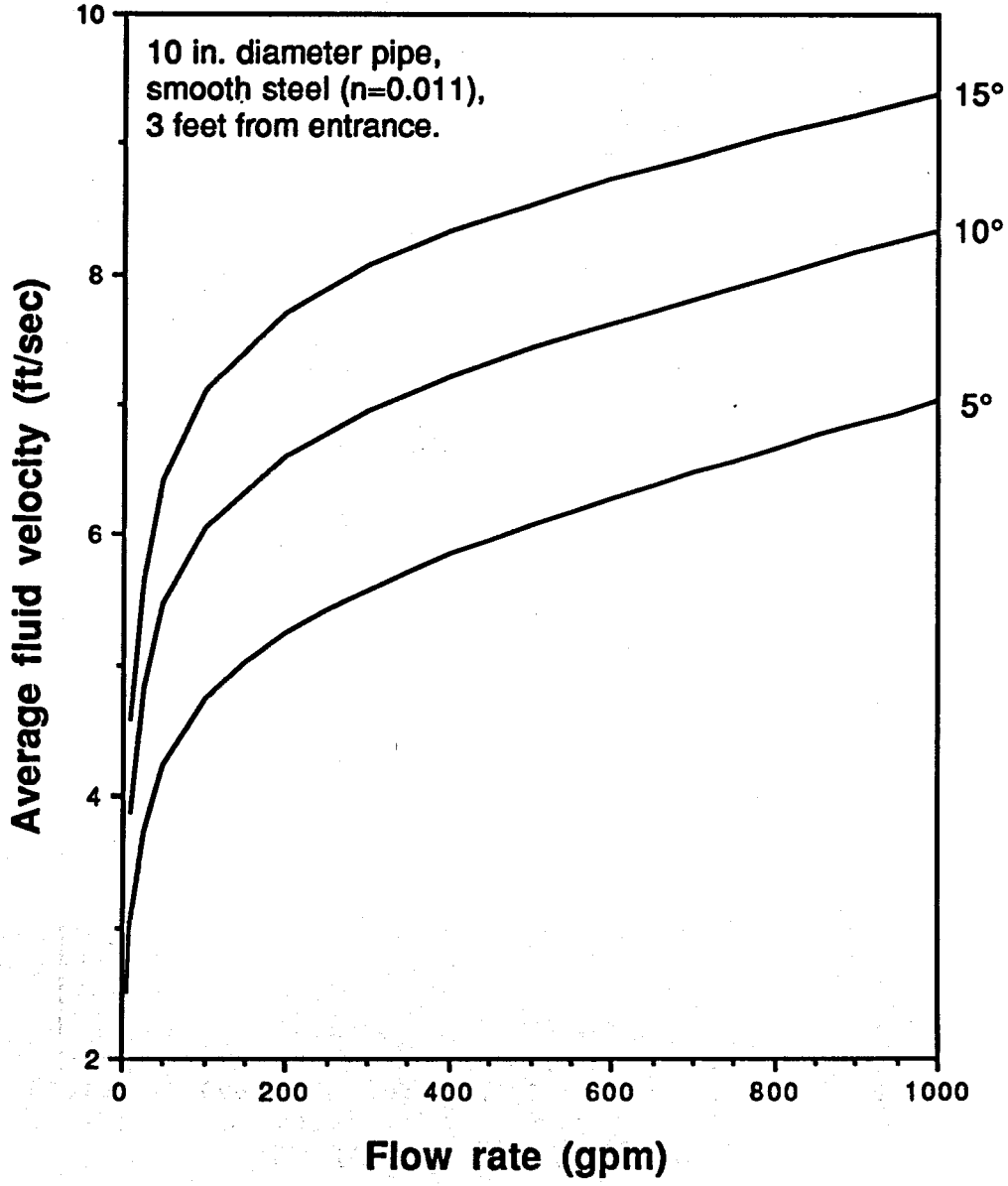

Figure 5 - Theoretical average fluid velocity as a function of flow rate for various pipe slopes in a 10-inch diameter smooth steel pipe at a location three feet from the fluid entrance.

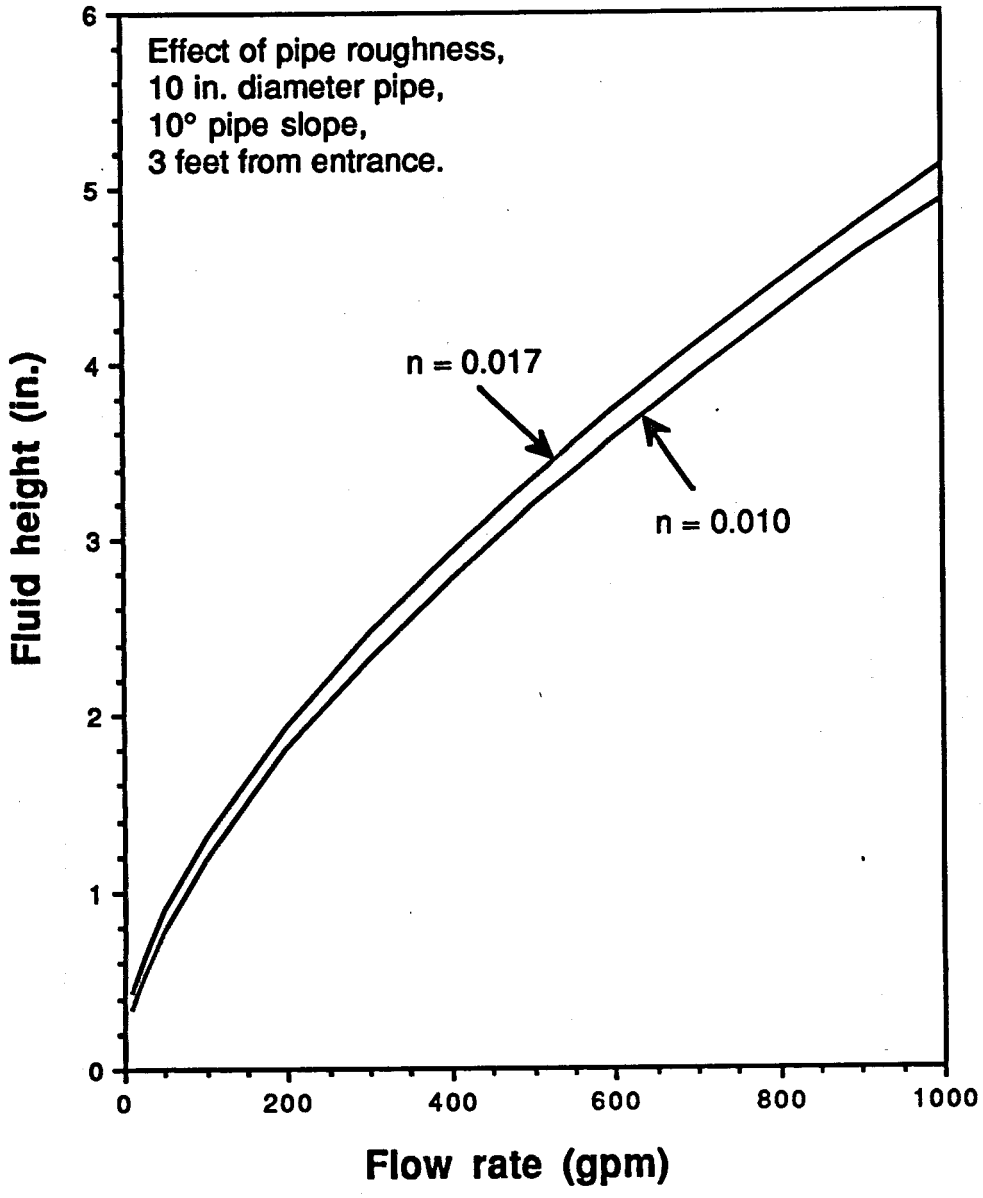

Figure 6 - Theoretical fluid height as a function of flow rate for pipes of various roughness in a 10-inch diameter pipe with a 10° slope at a location three feet from the fluid entrance.

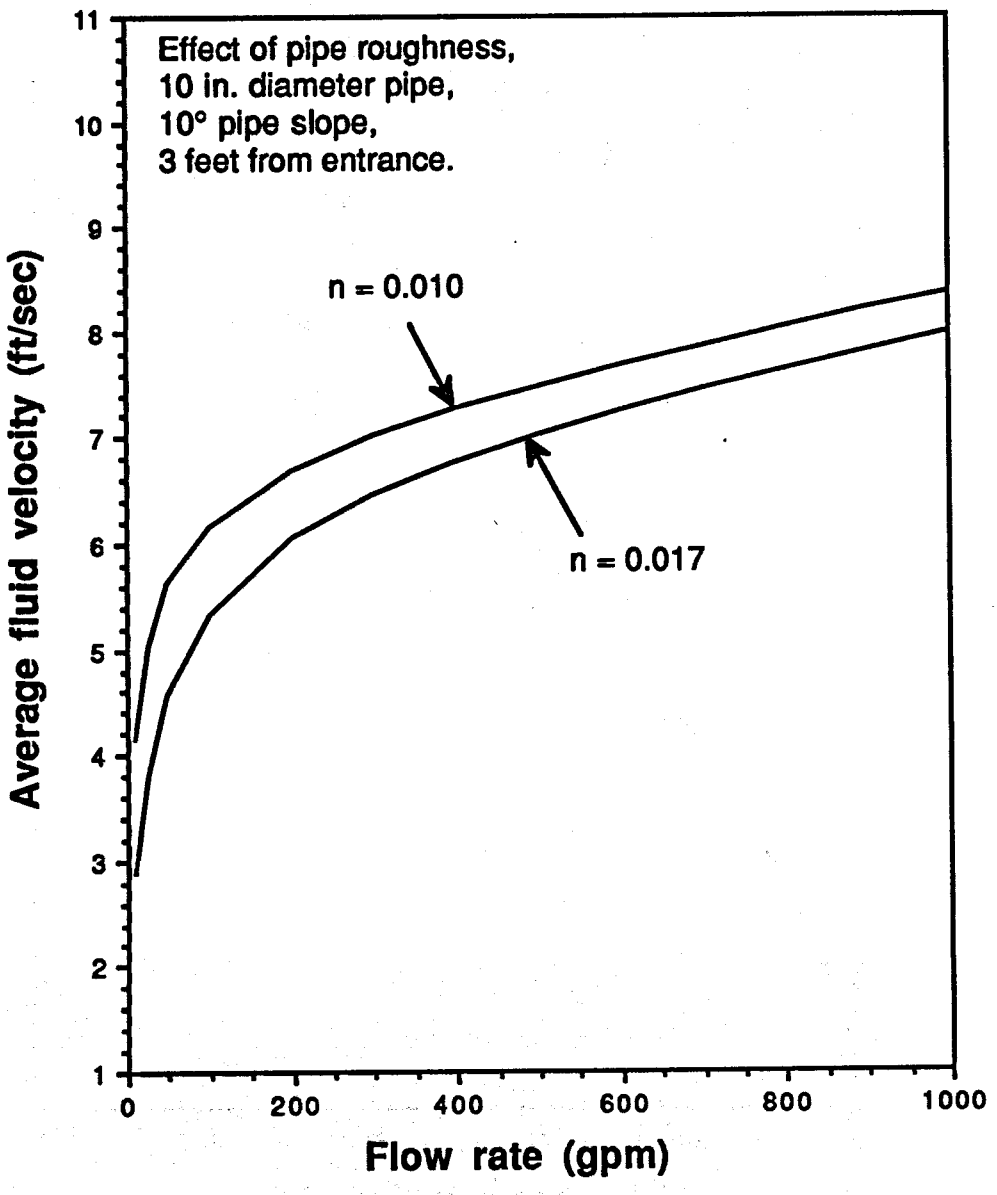

Figure 7 - Theoretical average fluid velocity as a function of flow rate for pipes of various roughness in a 10-inch diameter pipe with a 10° slope at a location three feet from the fluid entrance.

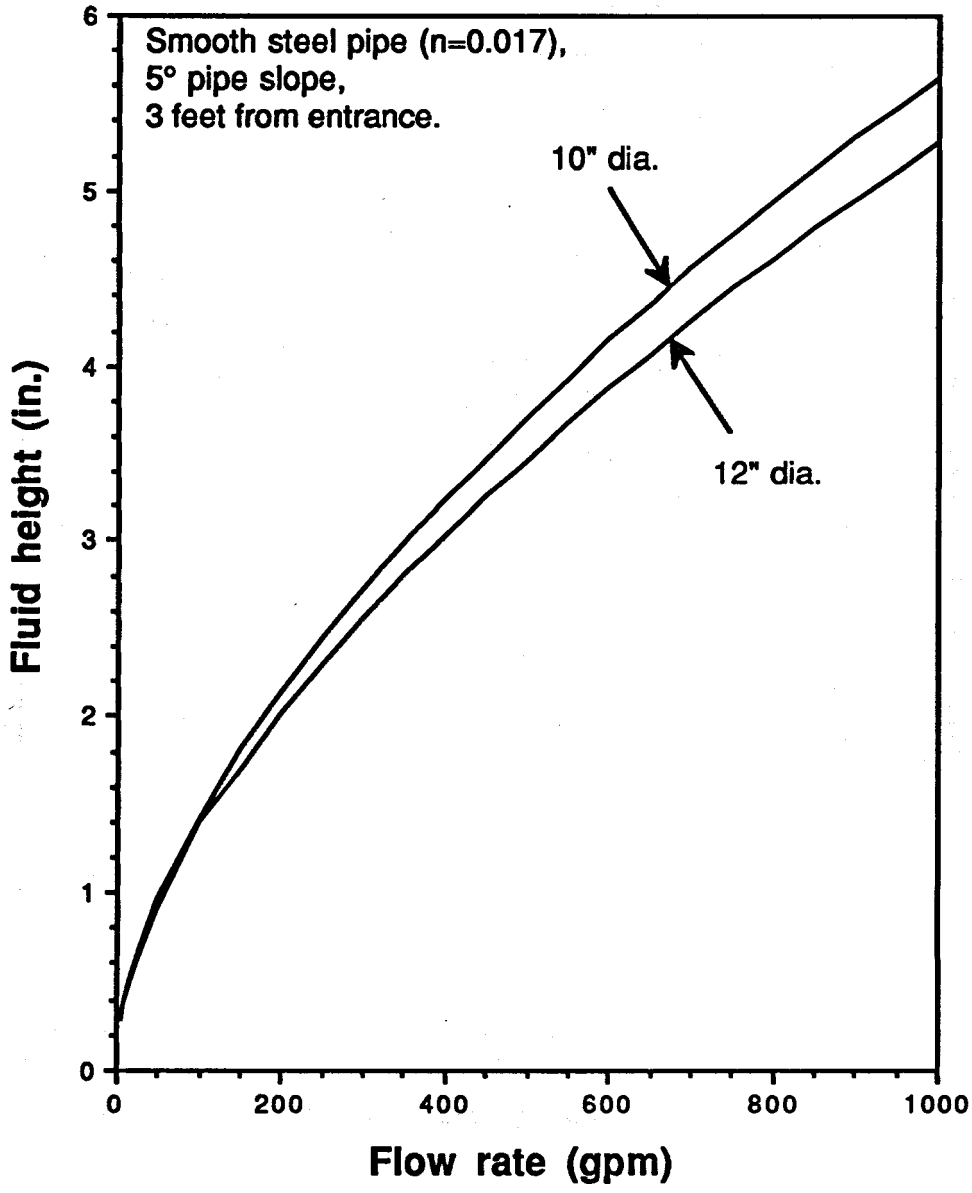

Figure 8 - Theoretical fluid height as a function of flow rate for various diameter smooth steel pipes with a 5° slope at a location three feet from the fluid entrance.

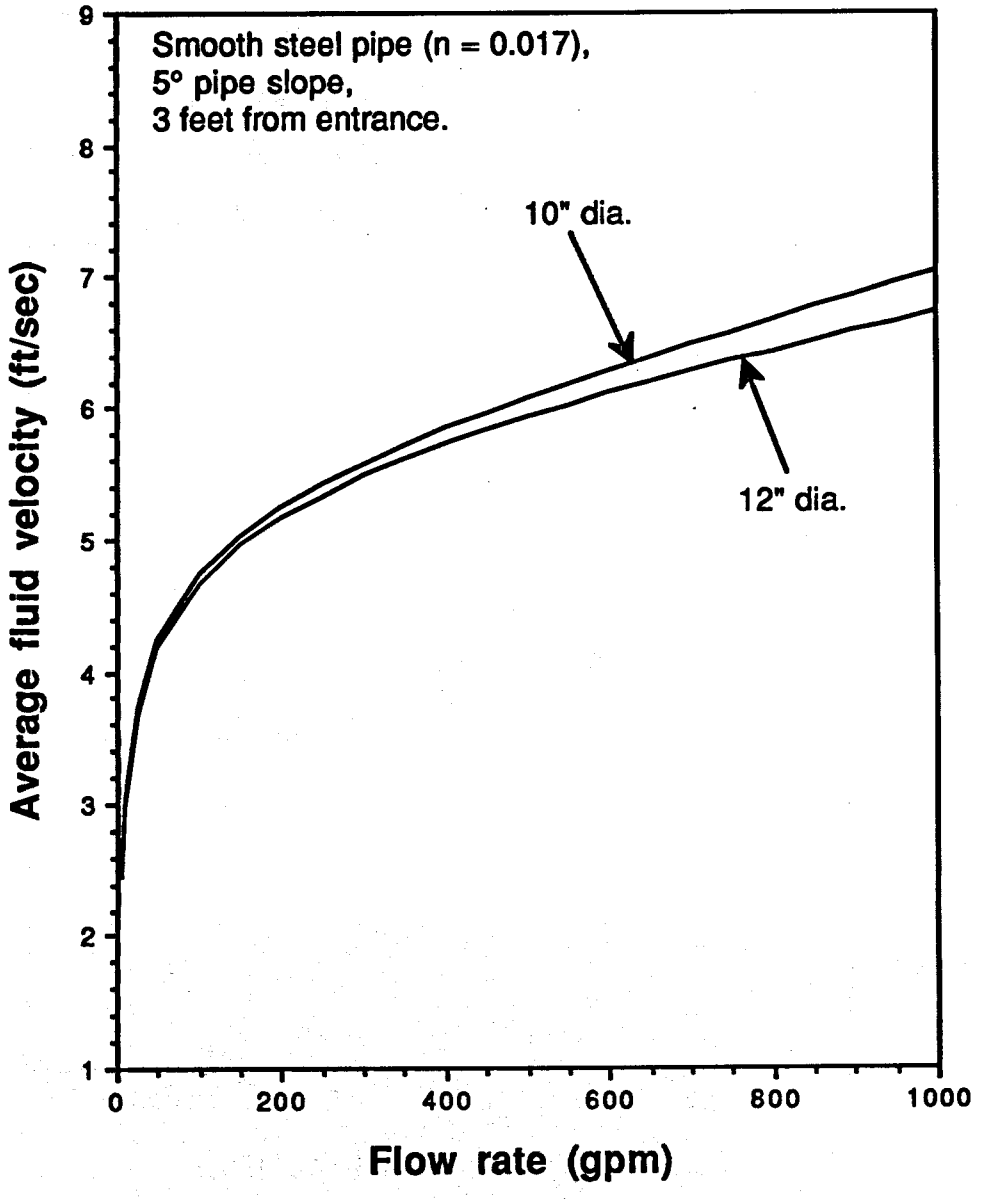

Figure 9 - Theoretical average fluid velocity as a function of flow rate for various diameter smooth steel pipes with a 5° slope at a location three feet from the fluid entrance.

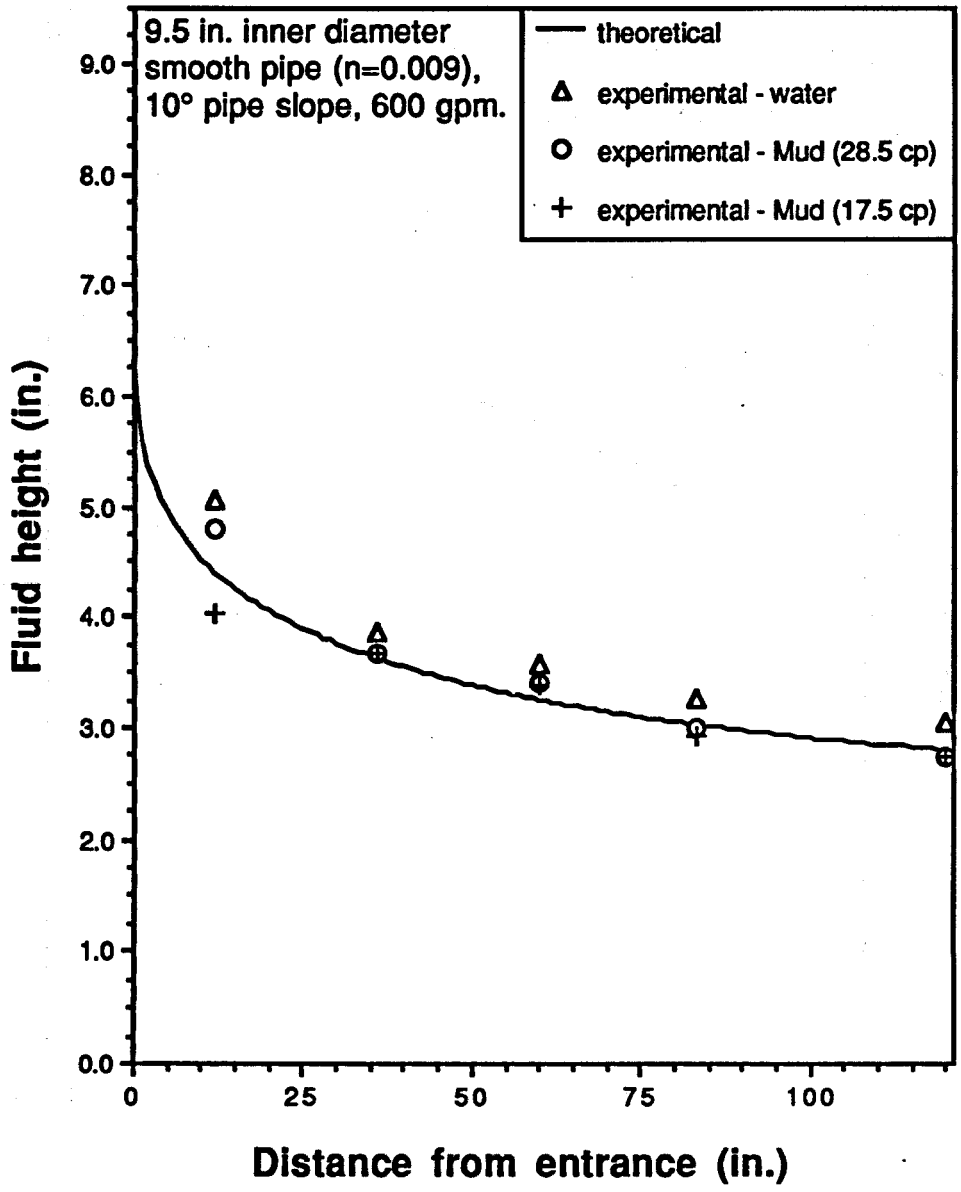

Figure 10 - Comparison of experimental and theoretical fluid height profiles in a 9.5-inch inner diameter acrylic pipe with a 10° slope at a flow rate of 600 gpm.

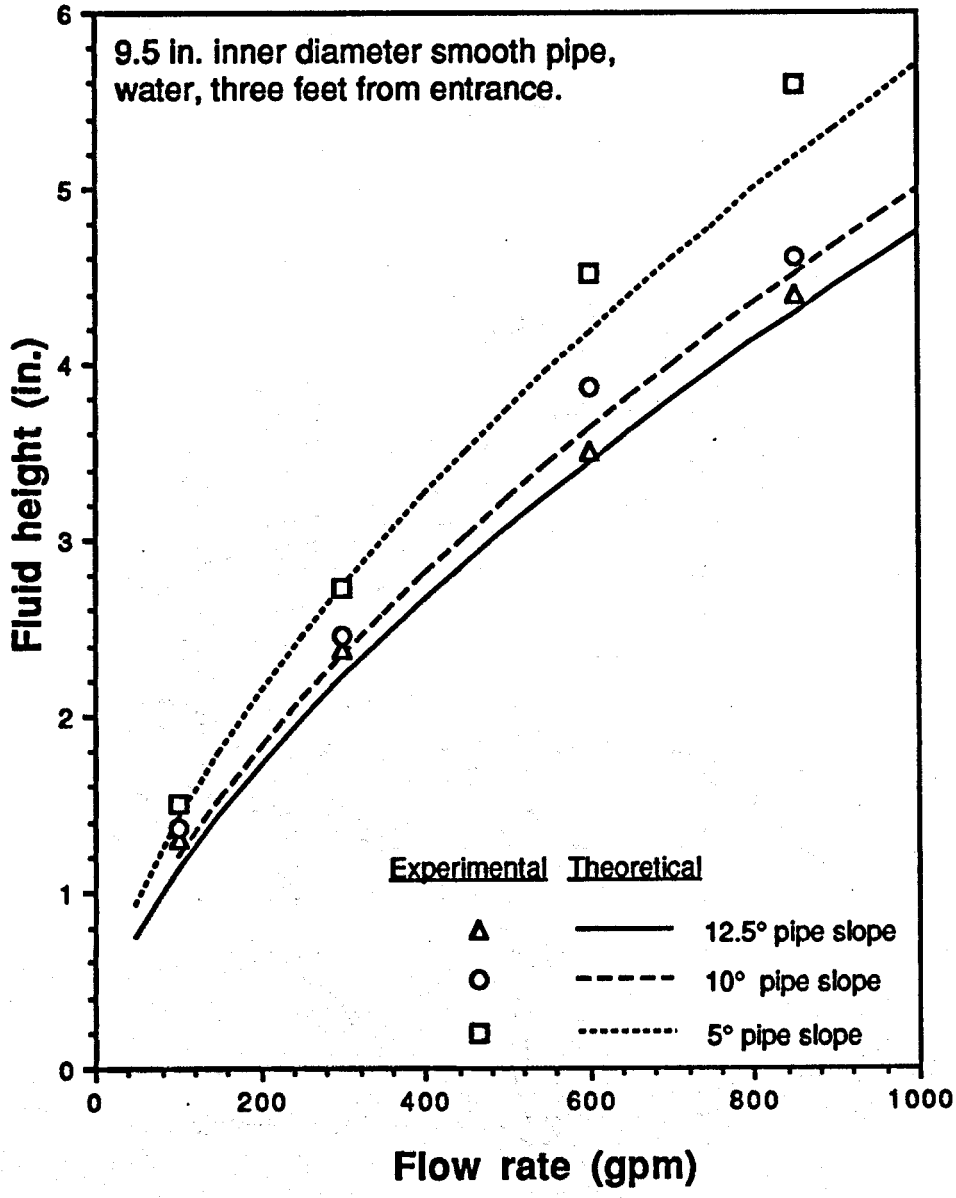

Figure 11 - Comparison of experimental and theoretical fluid height as a function of flow rate in a 9.5-inch inner diameter acrylic pipe with various slopes at a location three feet from the fluid entrance.

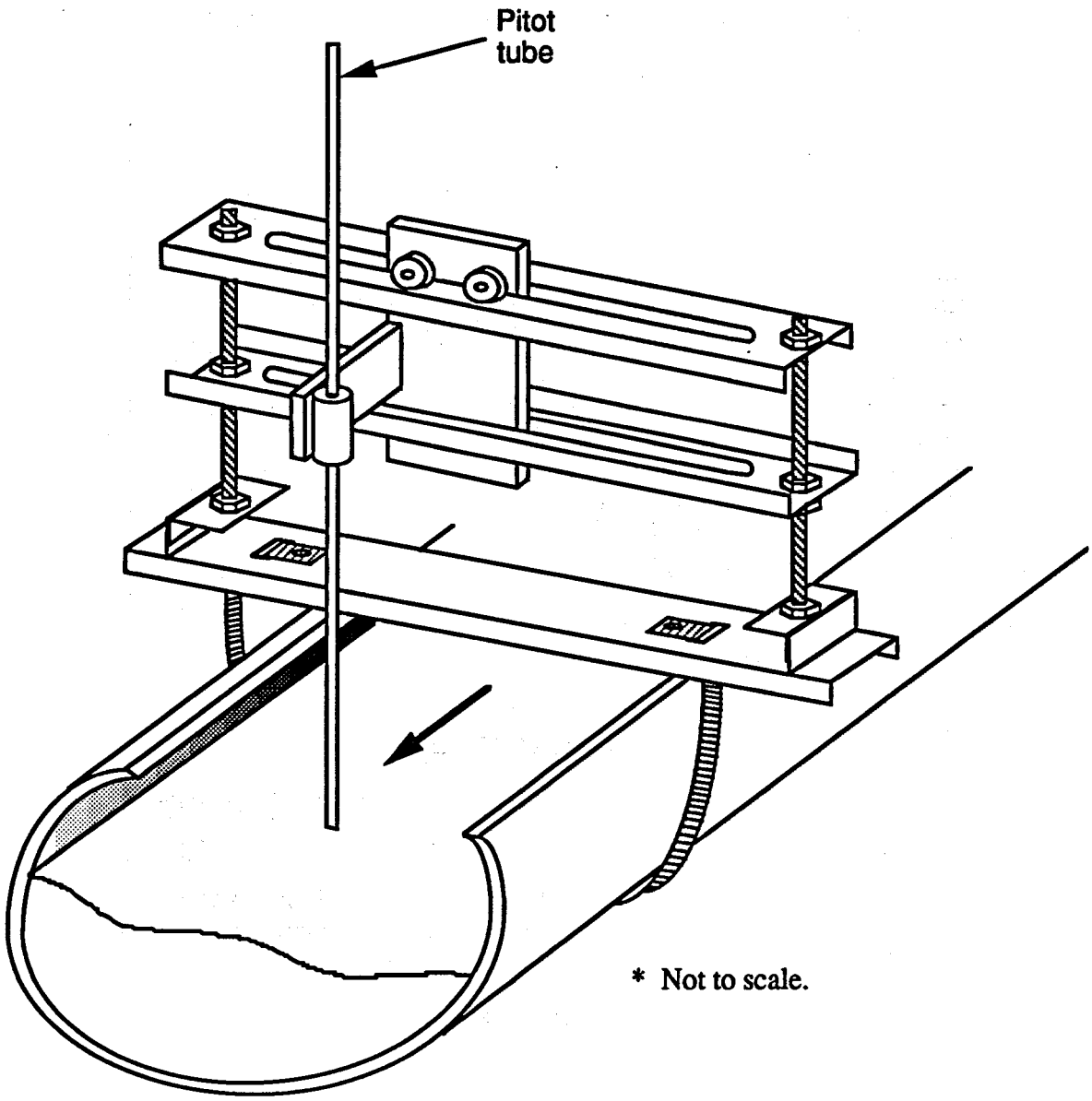

Figure 12 - Schematic of the traversing apparatus used in the measurement of fluid velocity profiles.

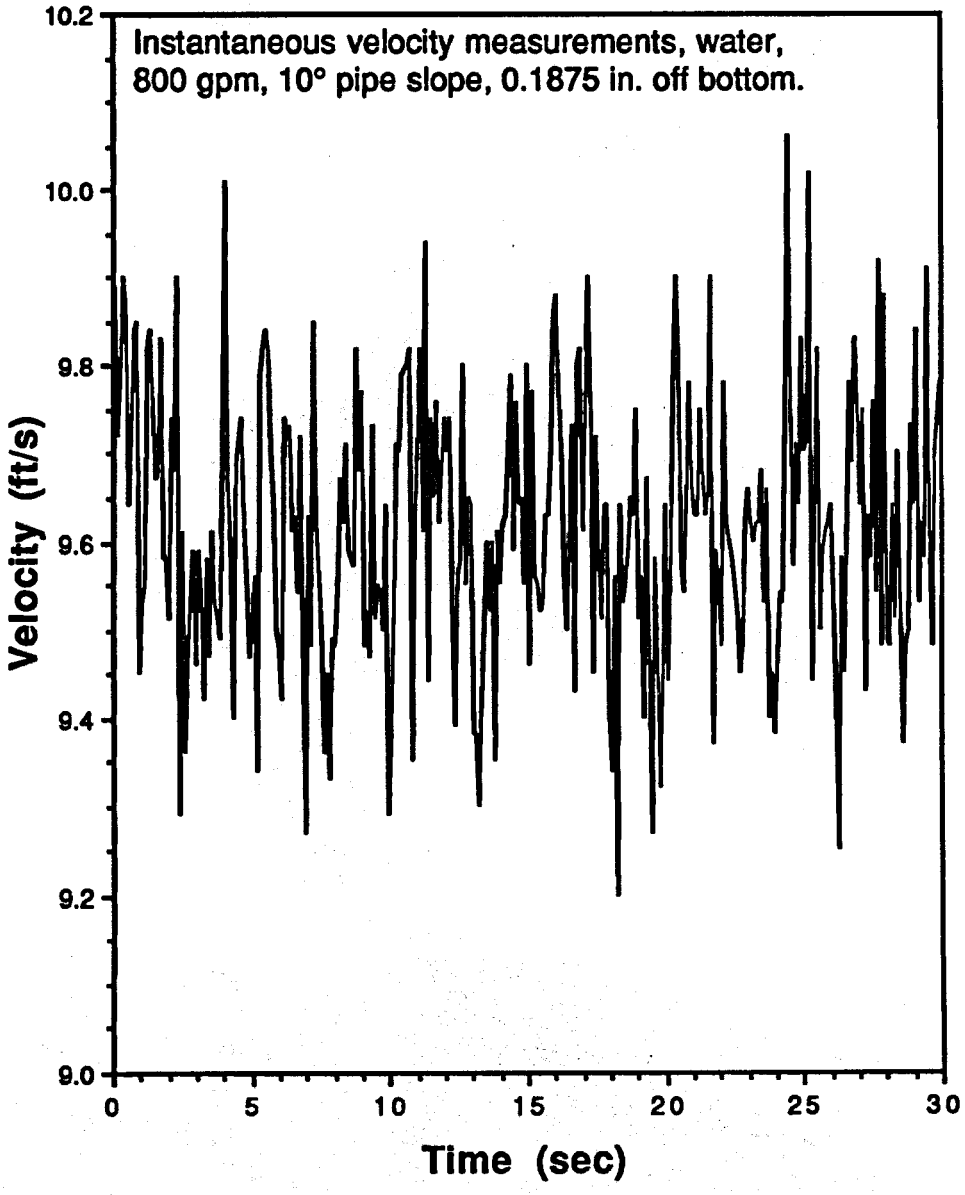

Figure 13 - Instantaneous velocity measurements in a 12-inch steel pipe with a 10° slope at a flow rate of 800 gpm and a location 0.1875 in. off the bottom of the pipe at the pipe's centerline.

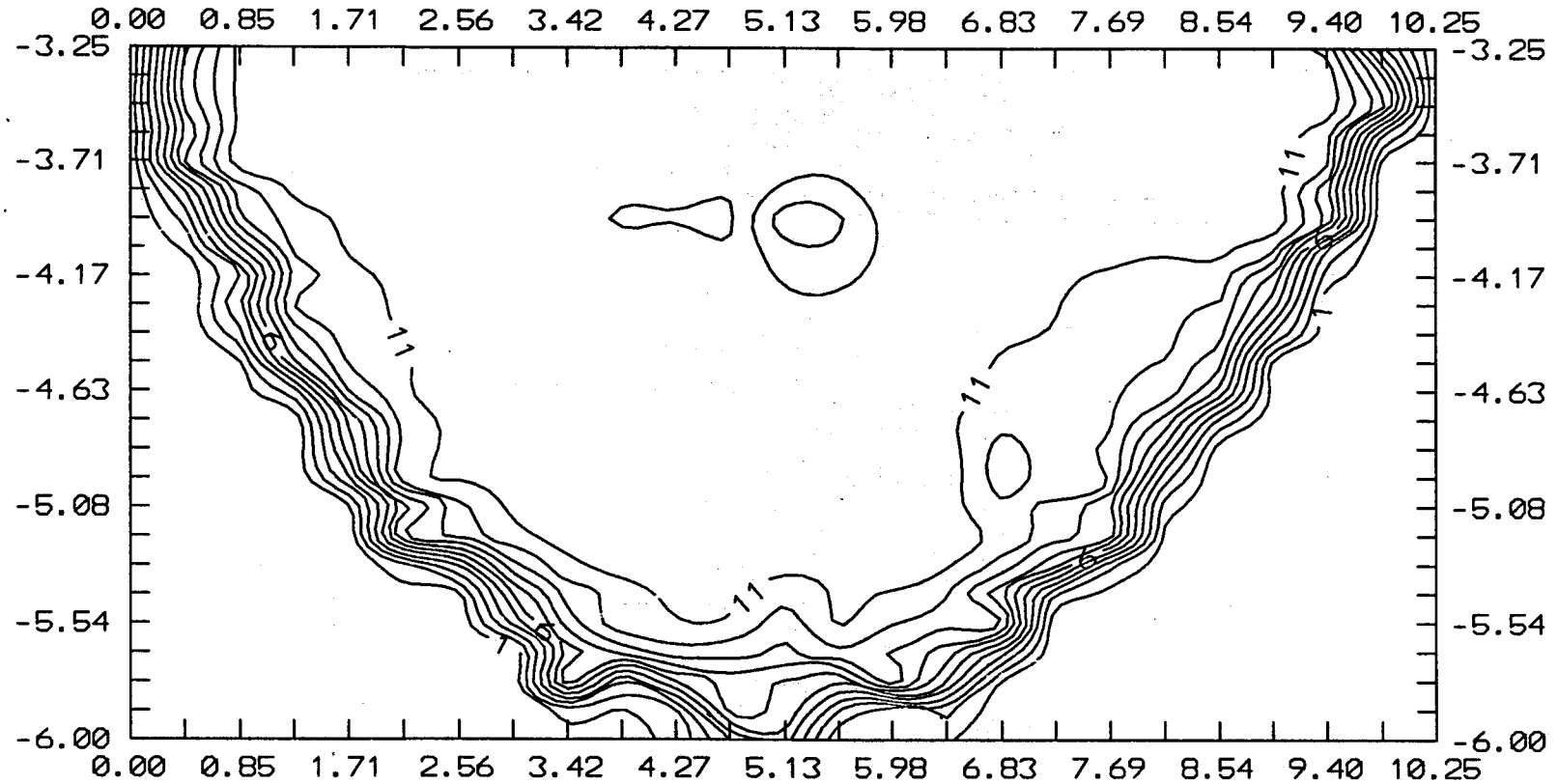

Figure 14 - Contours of equal velocity in a 12-inch steel pipe with a 10° slope at a flow rate of 800 gpm.

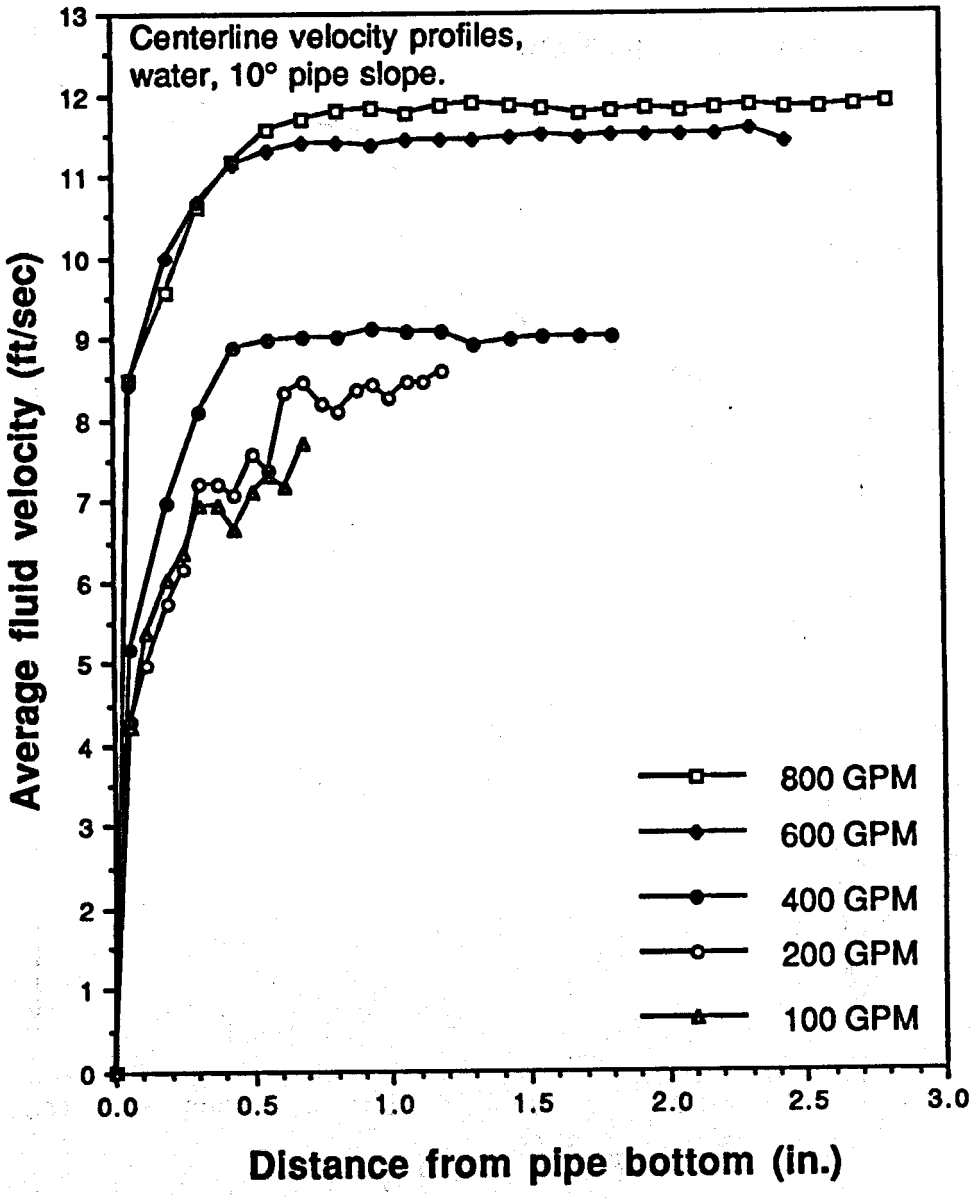

Figure 15 - Centerline velocity profiles at various fluid flow rates in a 12-inch steel pipe with a 10° slope.

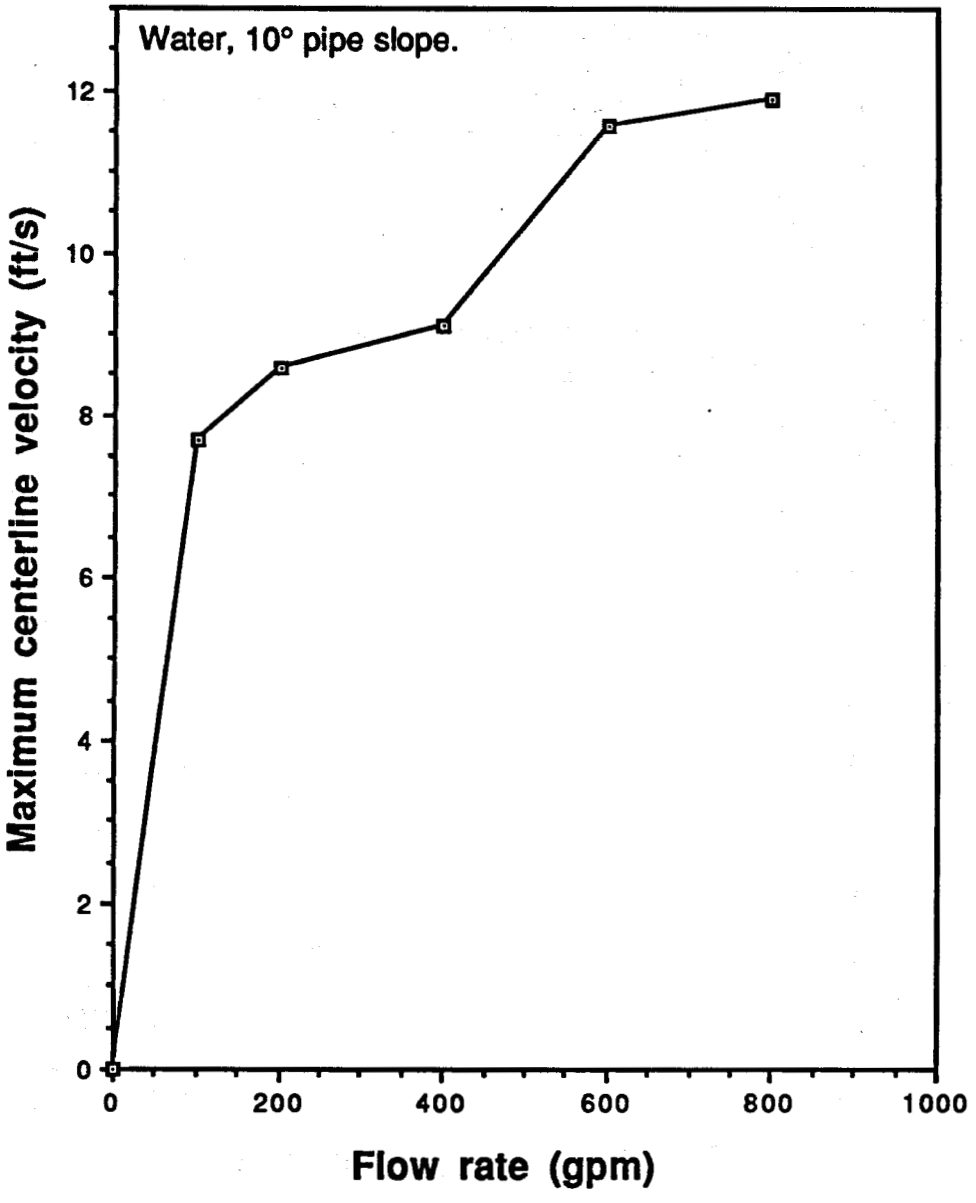

Figure 16 - Maximum centerline velocity as a function of flow rate in a 12-inch steel pipe with a 10° slope.

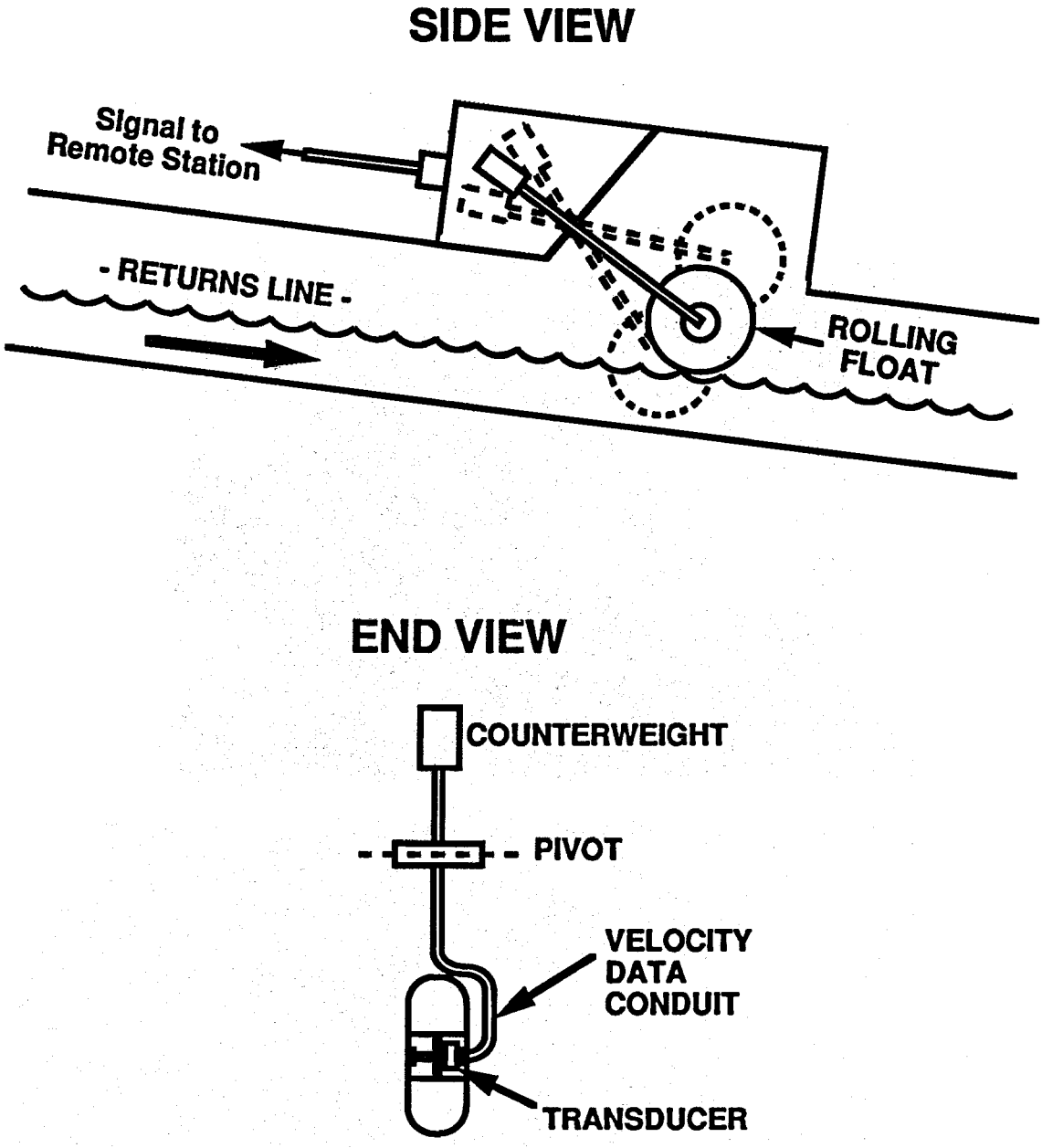

Figure 17 - Schematic of the rolling float meter.

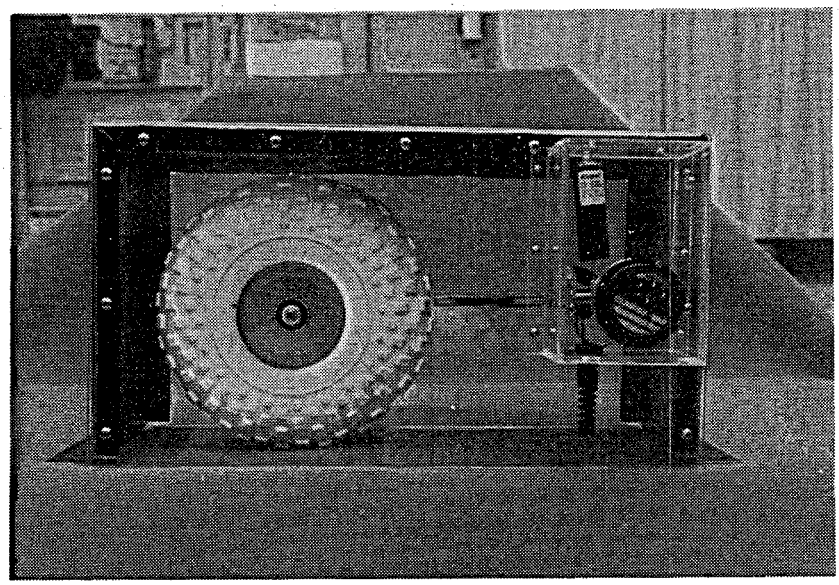

Figure 18 - Photograph of the laboratory prototype rolling float meter.

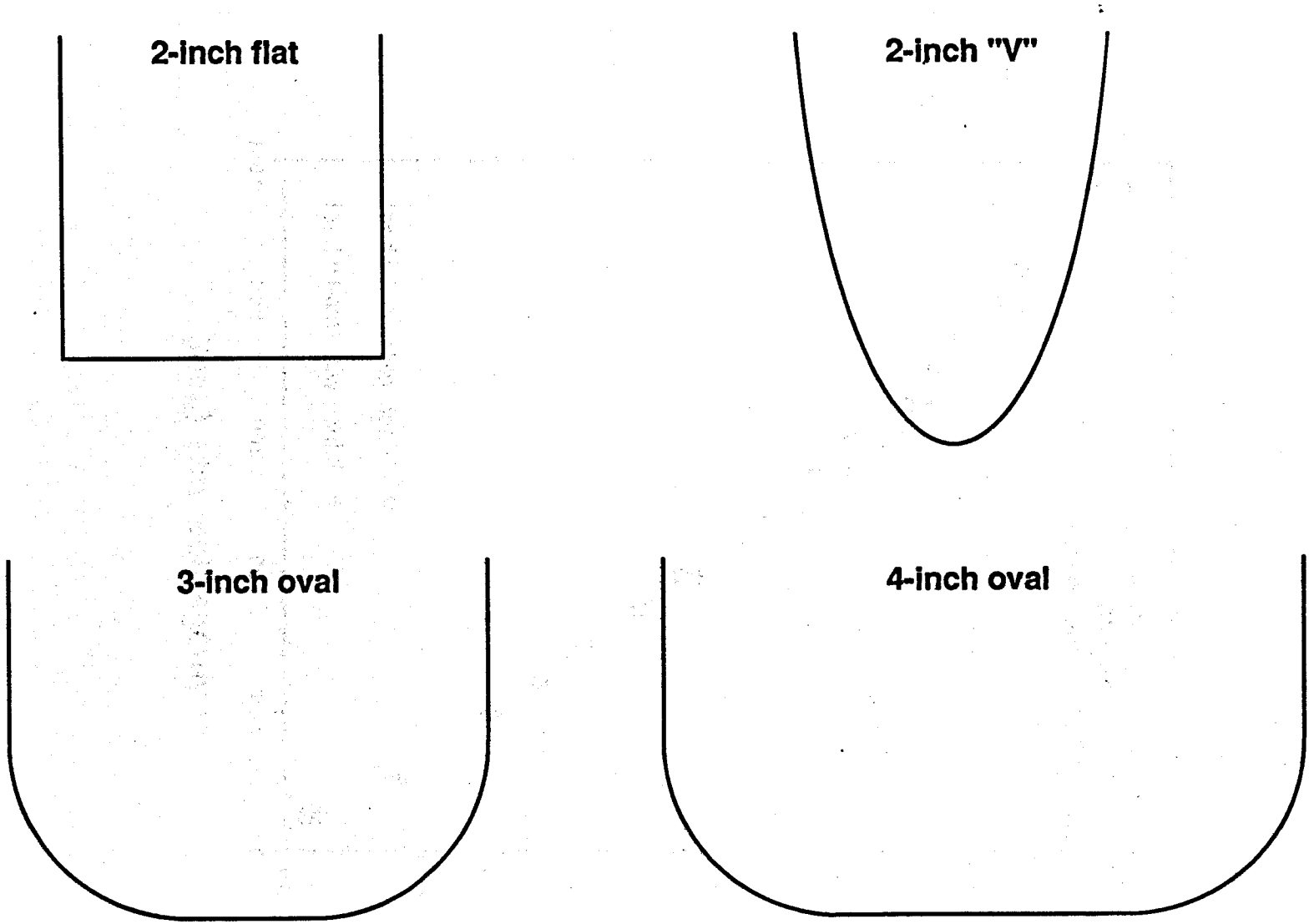

Figure 19 - Schematic of the float profiles tested in the rolling float meter.

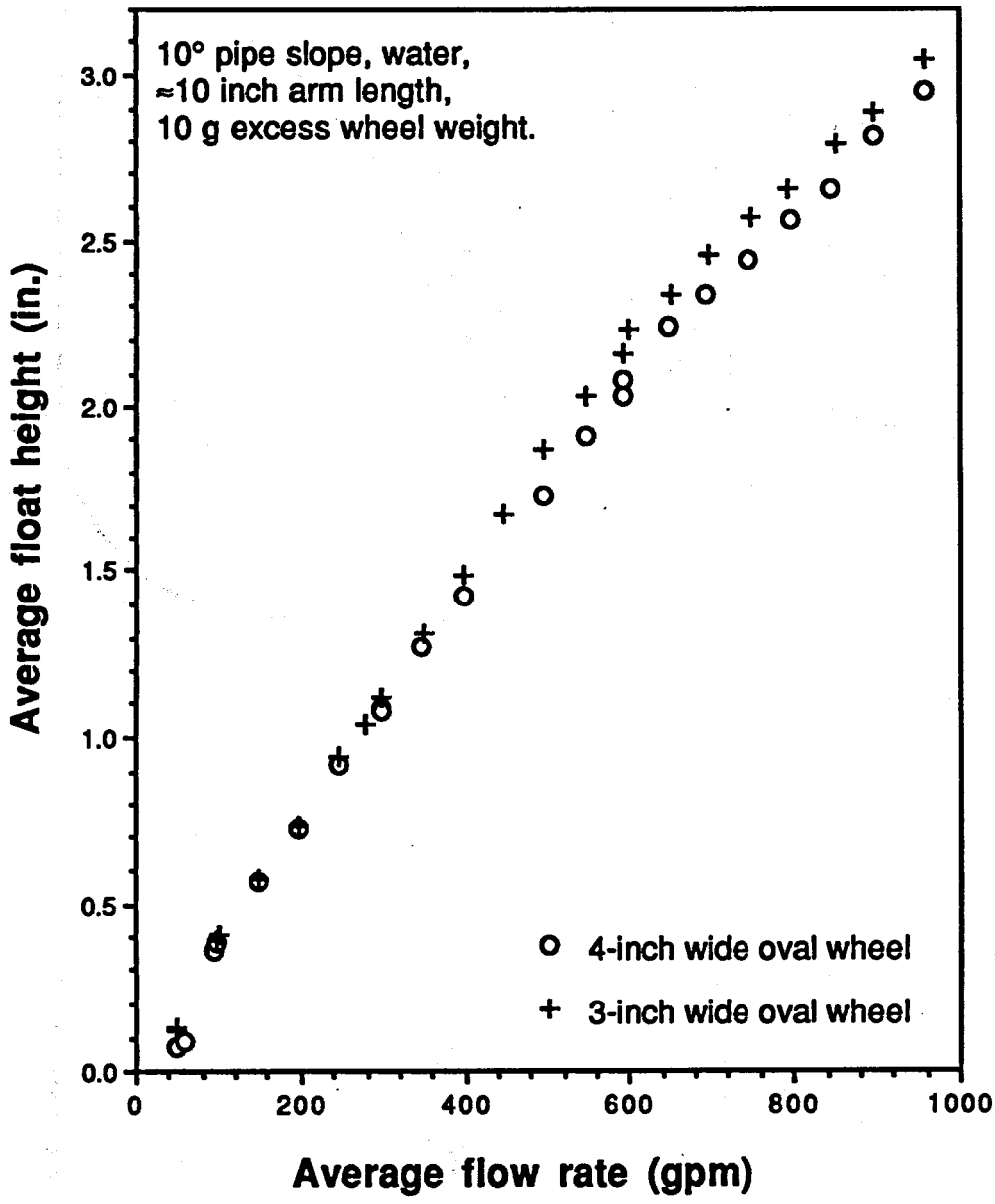

Figure 20 - Average rolling float level as a function of water flow rate for two different float shapes in a 10-inch acrylic pipe with a 10° slope.

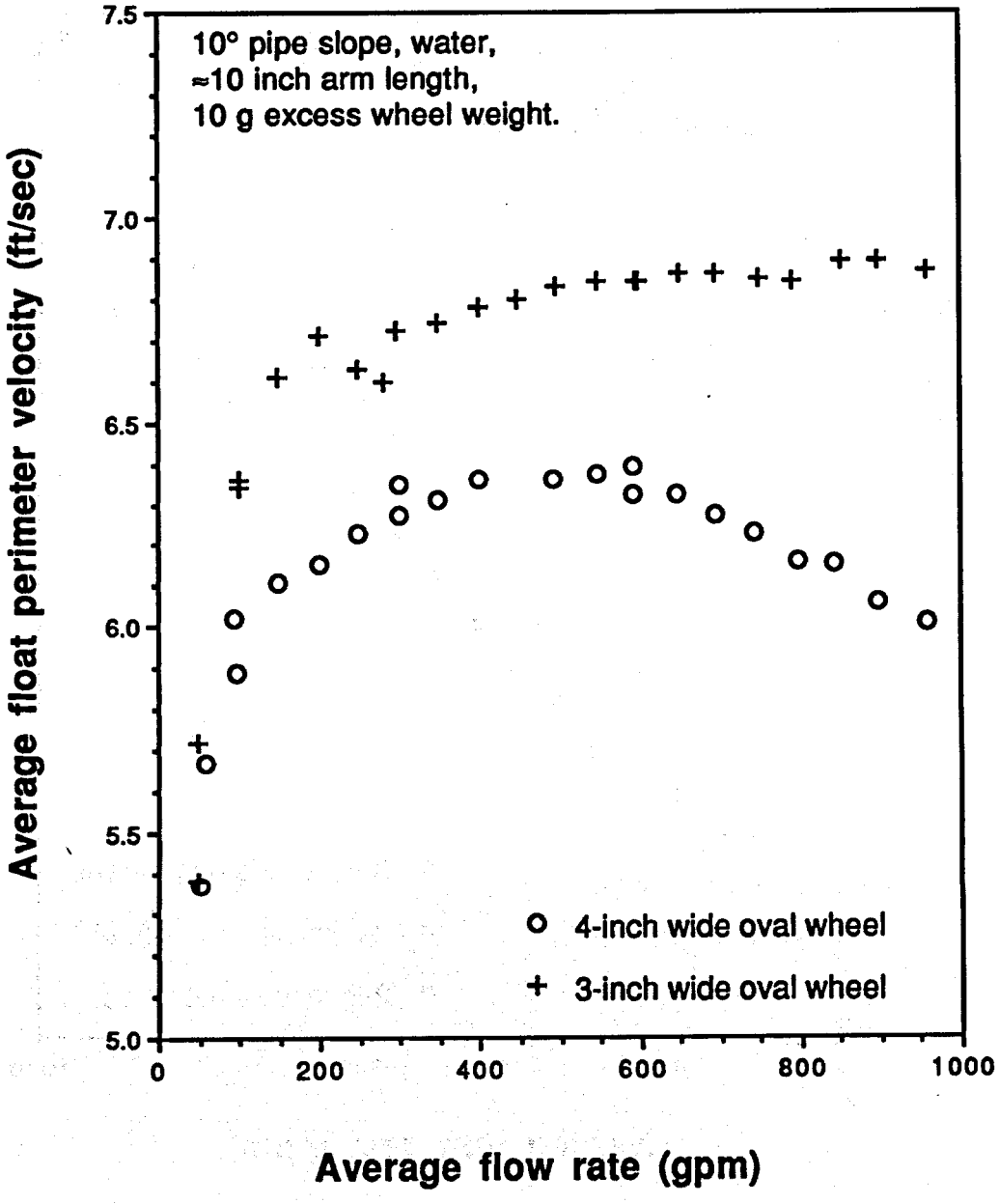

Figure 21 - Average rolling float perimeter velocity as a function of water flow rate for two different float shapes in a 10-inch acrylic pipe with a 10° slope.

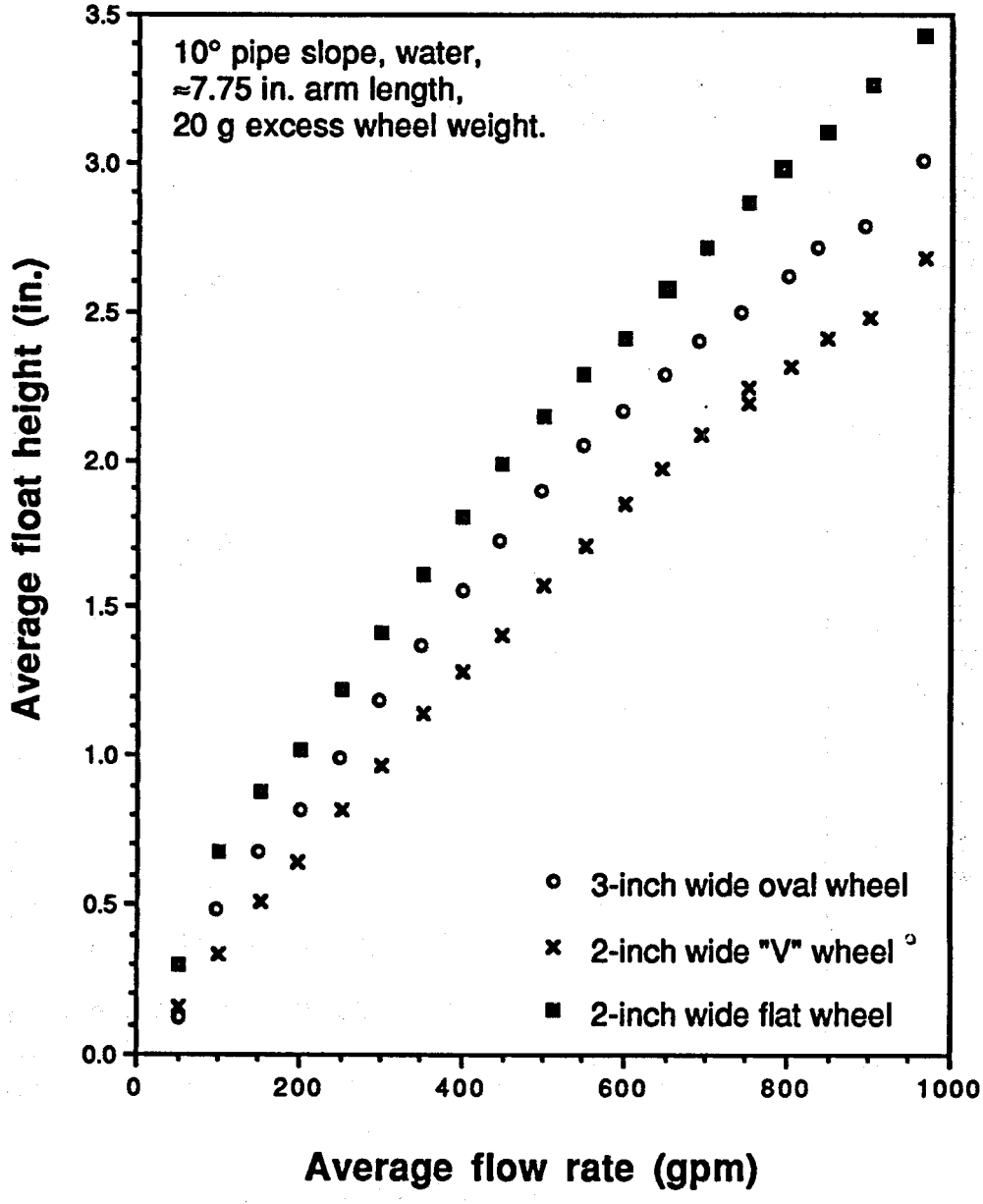

Figure 22 - Average rolling float level as a function of water flow rate for three different float shapes in a 10-inch acrylic pipe with a 10° slope.

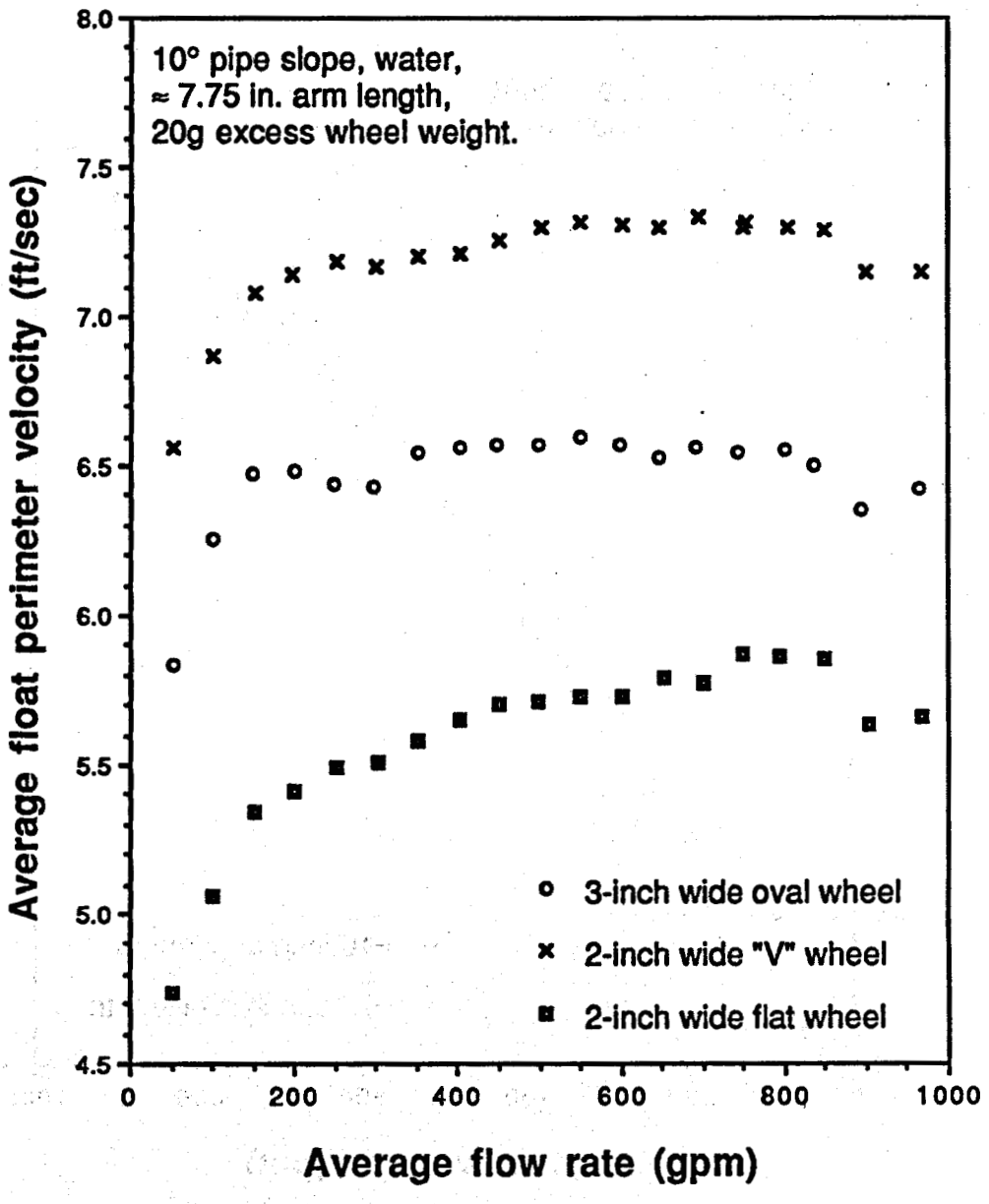

Figure 23 - Average rolling float perimeter velocity as a function of water flow rate for three different float shapes in a 10-inch acrylic pipe with a 10° slope.

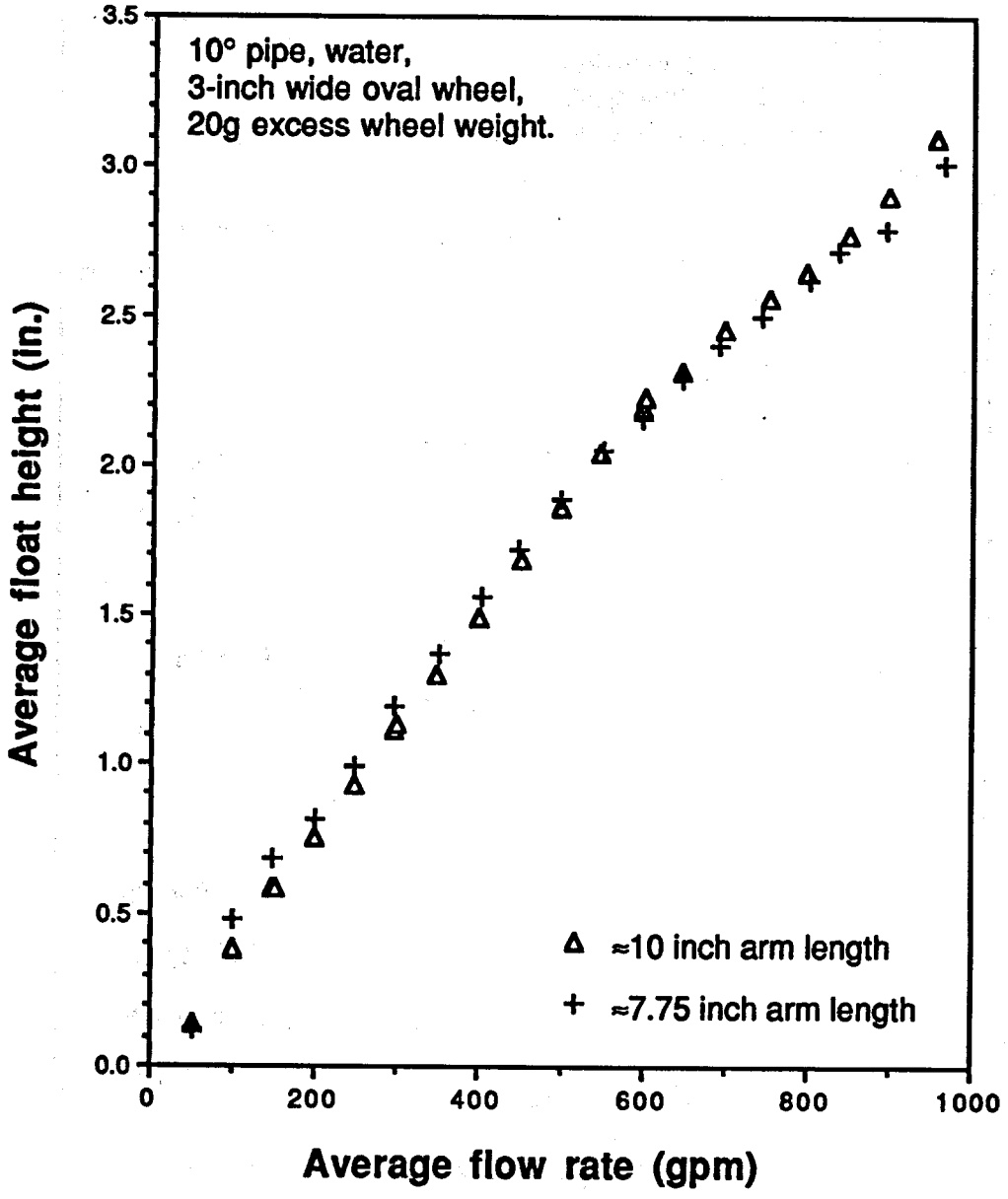

Figure 24 - Average rolling float level as a function of water flow rate for two different pivot arm lengths in a 10-inch acrylic pipe with a 10° slope.

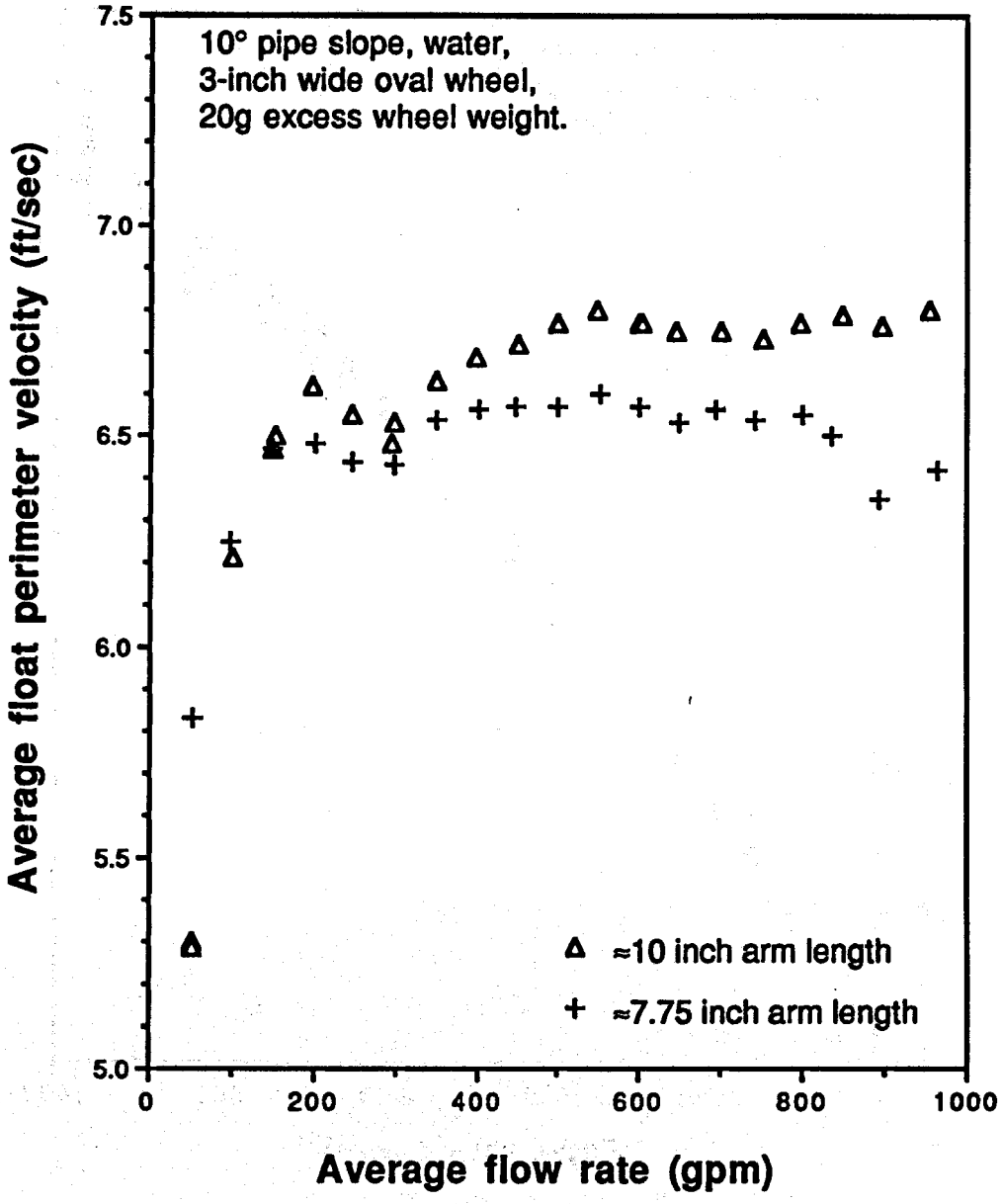

Figure 25 - Average rolling float perimeter velocity as a function of water flow rate for two different pivot arm lengths in a 10-inch acrylic pipe with a 10° slope.

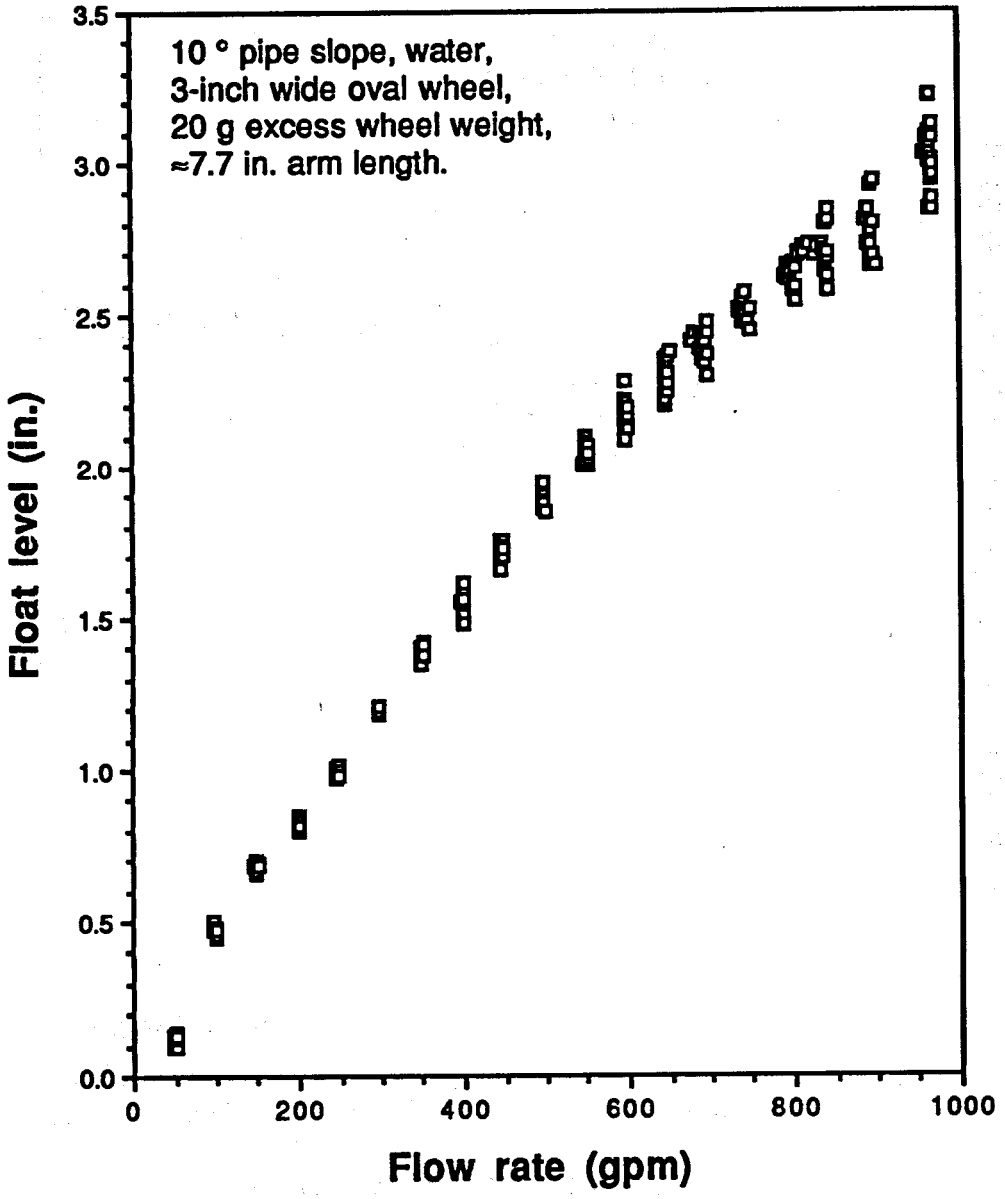

Figure 26 - Instantaneous rolling float level as a function of water flow rate in a 10-inch acrylic pipe with a 10° slope.

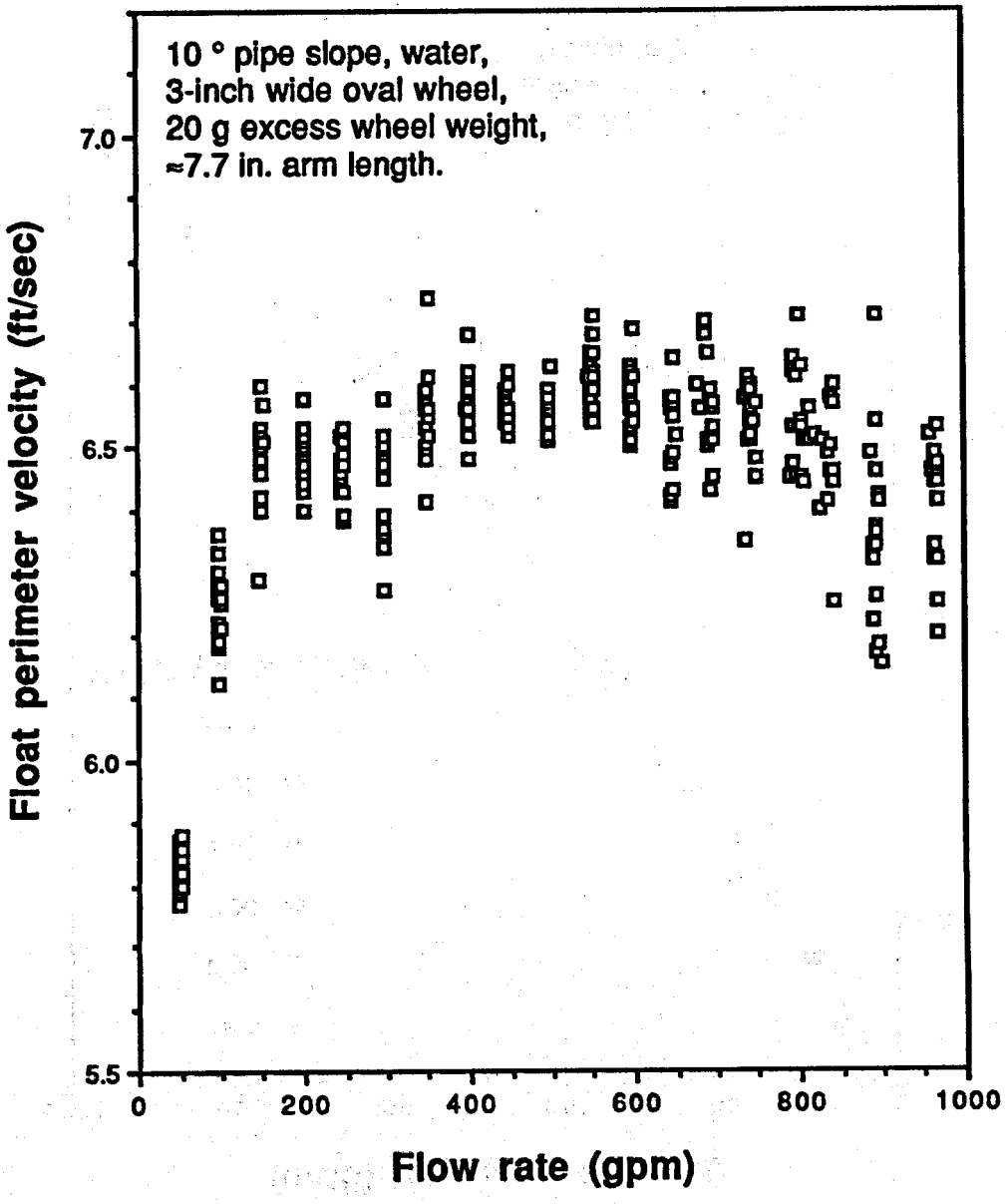

Figure 27 - Instantaneous rolling float perimeter velocity as a function of water flow rate in a 10-inch acrylic pipe with a 10° slope.

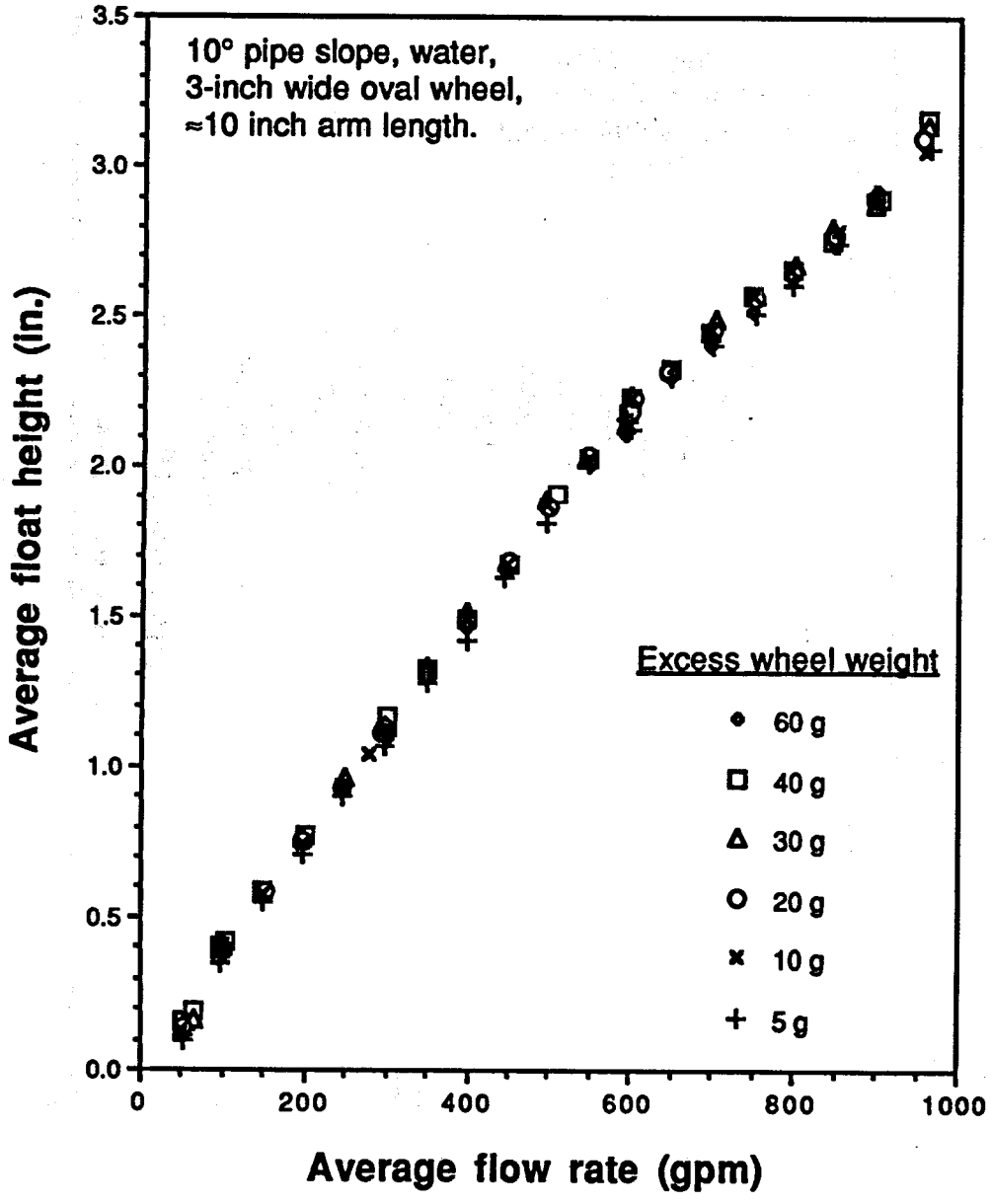

Figure 28 - Effects of excess wheel weight on the average rolling float level in water in a 10-inch acrylic pipe with a 10° slope.

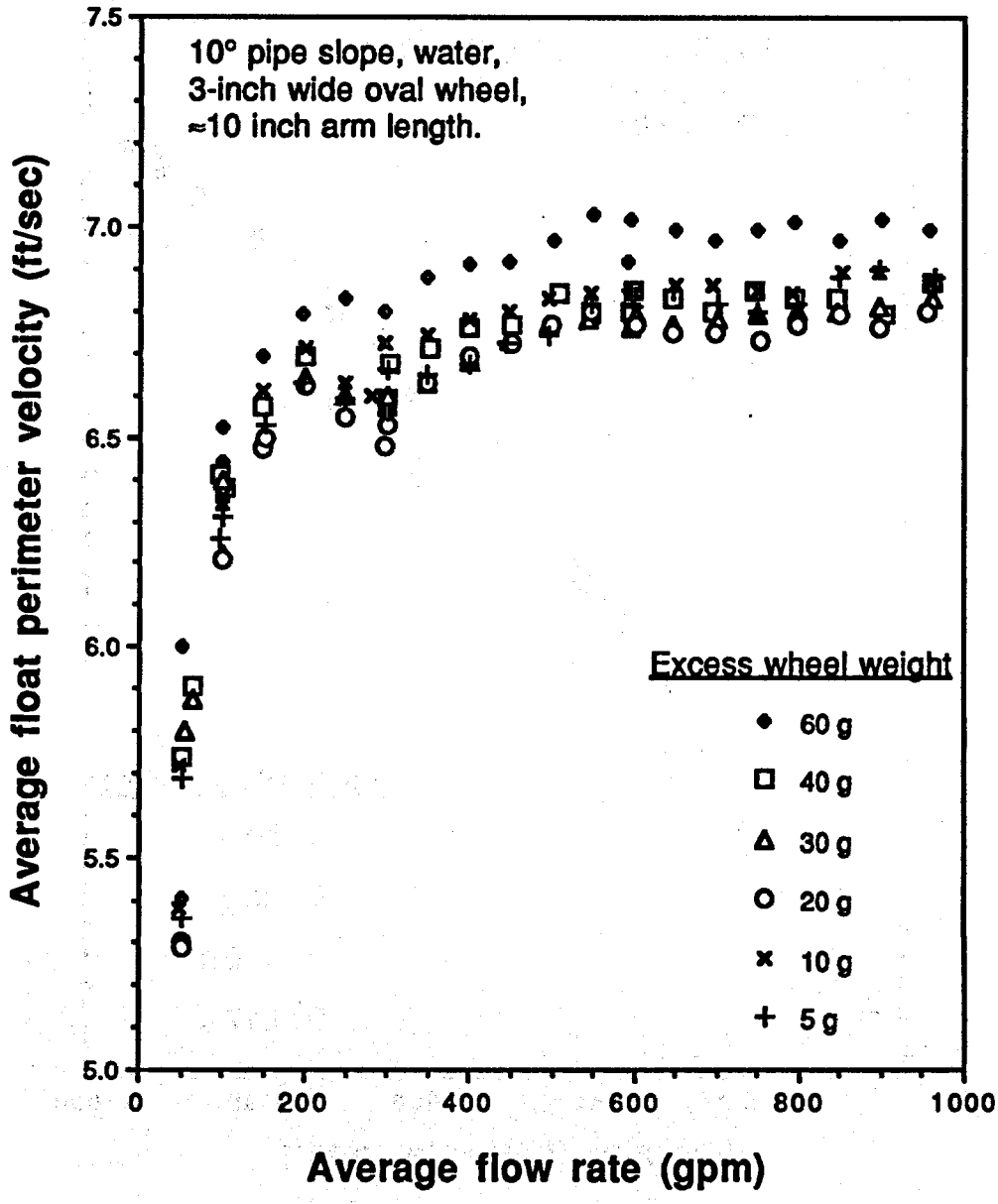

Figure 29 - Effects of excess wheel weight on the average rolling float perimeter velocity in water in a 10-inch acrylic pipe with a 10° slope.

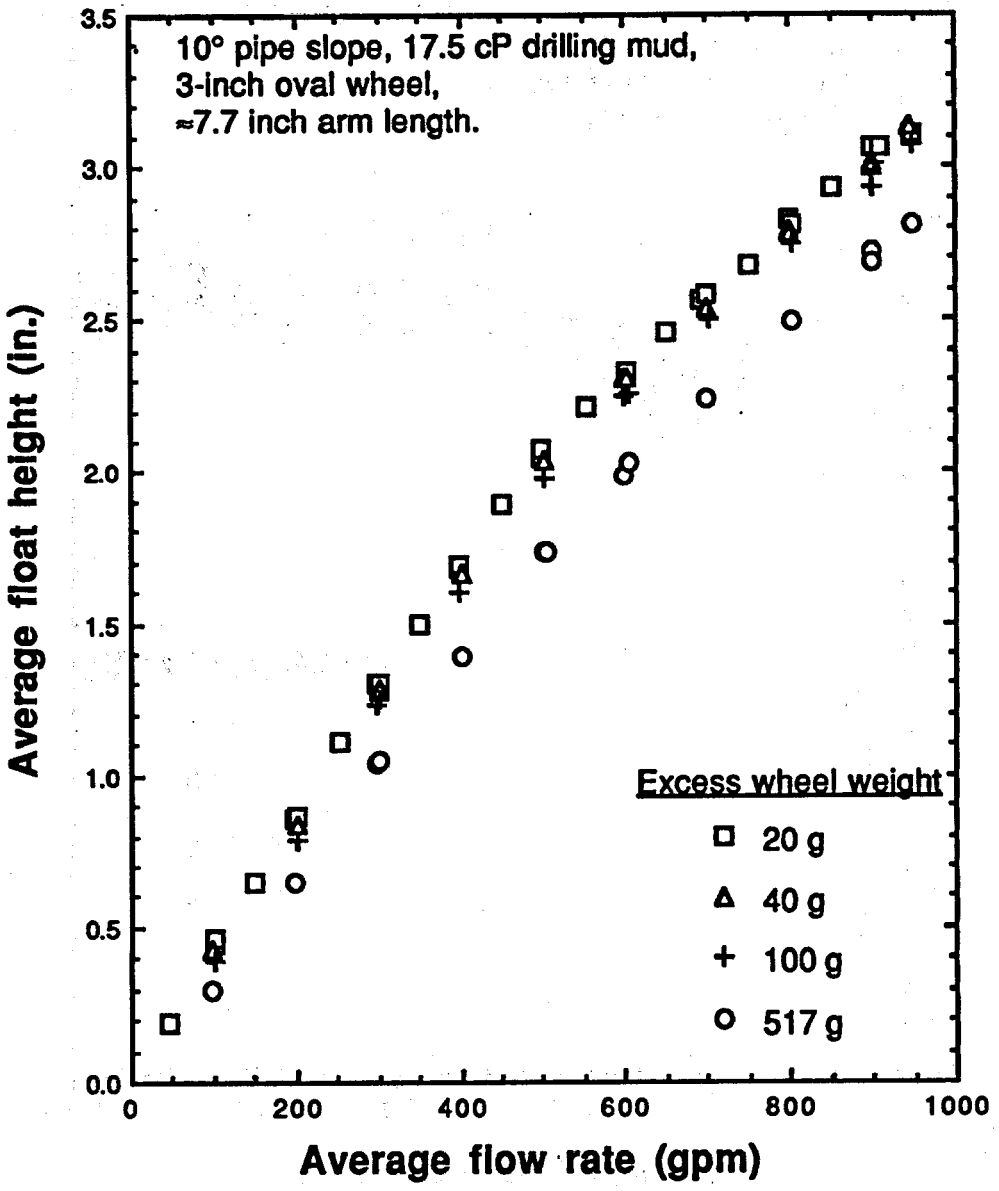

Figure 30 - Effects of excess wheel weight on the average rolling float level in drilling mud in a 10-inch acrylic pipe with a 10° slope.

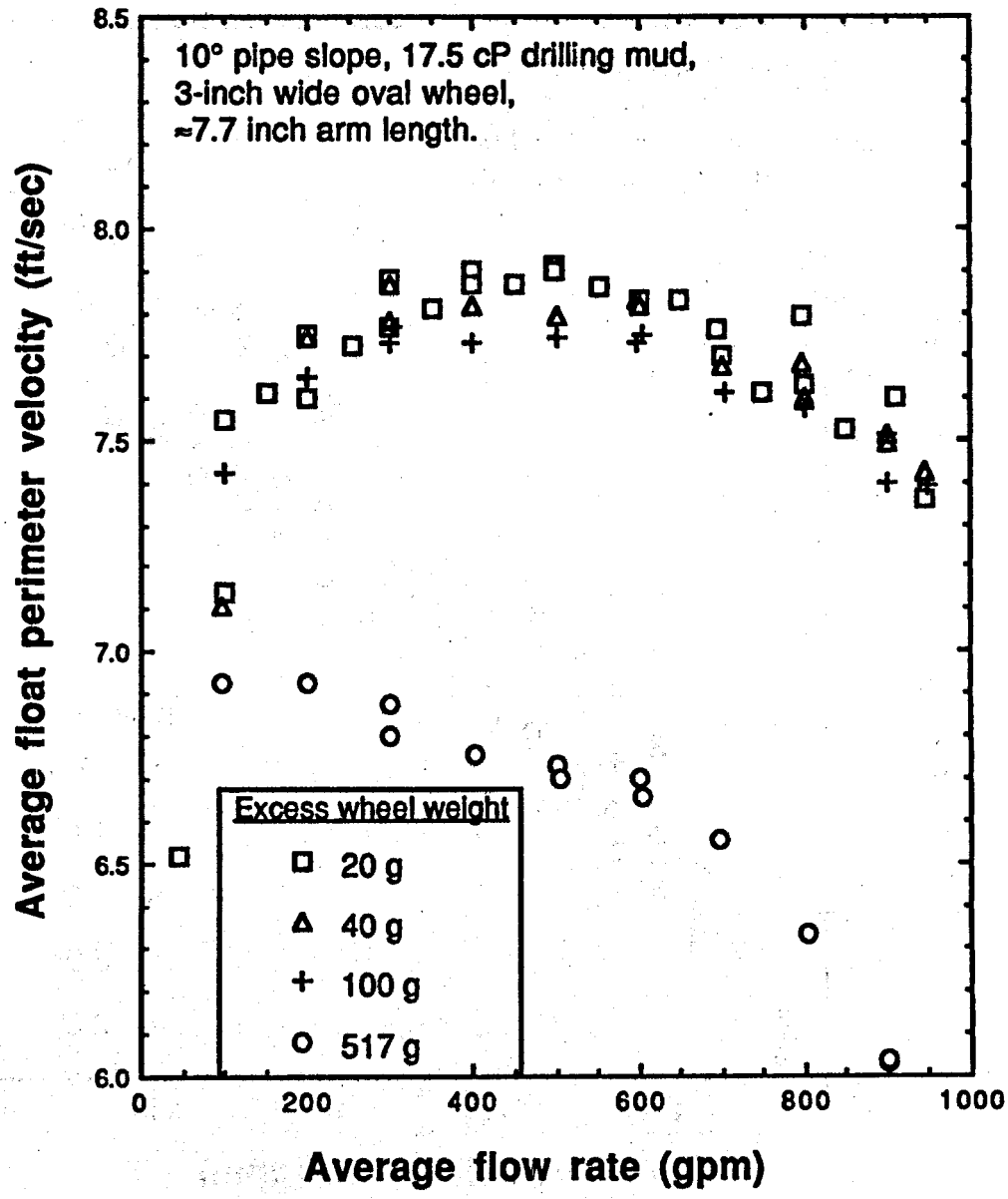

Figure 31 - Effects of excess wheel weight on the average rolling float perimeter velocity in drilling mud in a 10-inch acrylic pipe with a 10° slope.

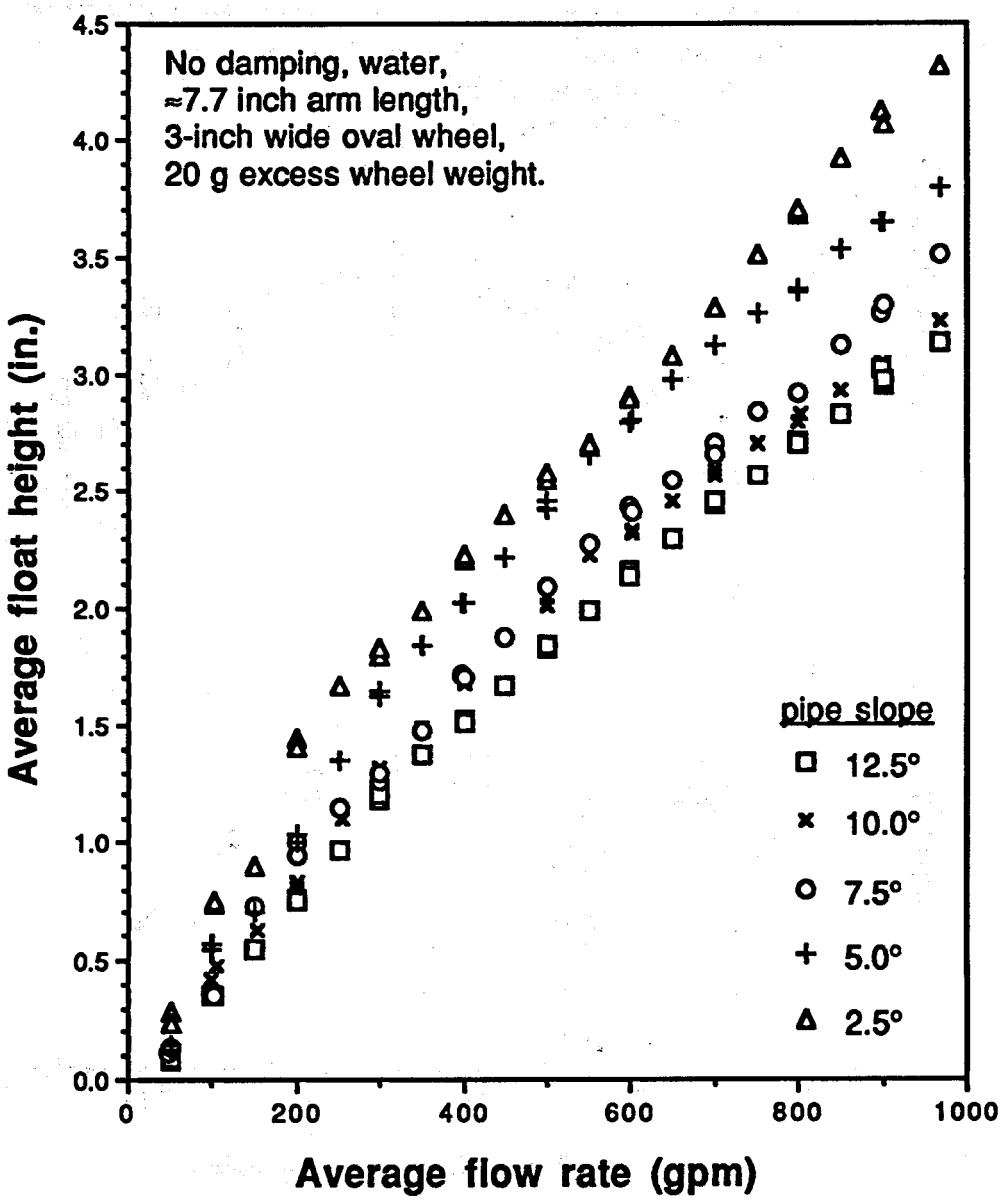

Figure 32 - Effects of pipe slope on the average rolling float level in drilling mud in a 10-inch acrylic pipe with 20 g excess wheel weight.

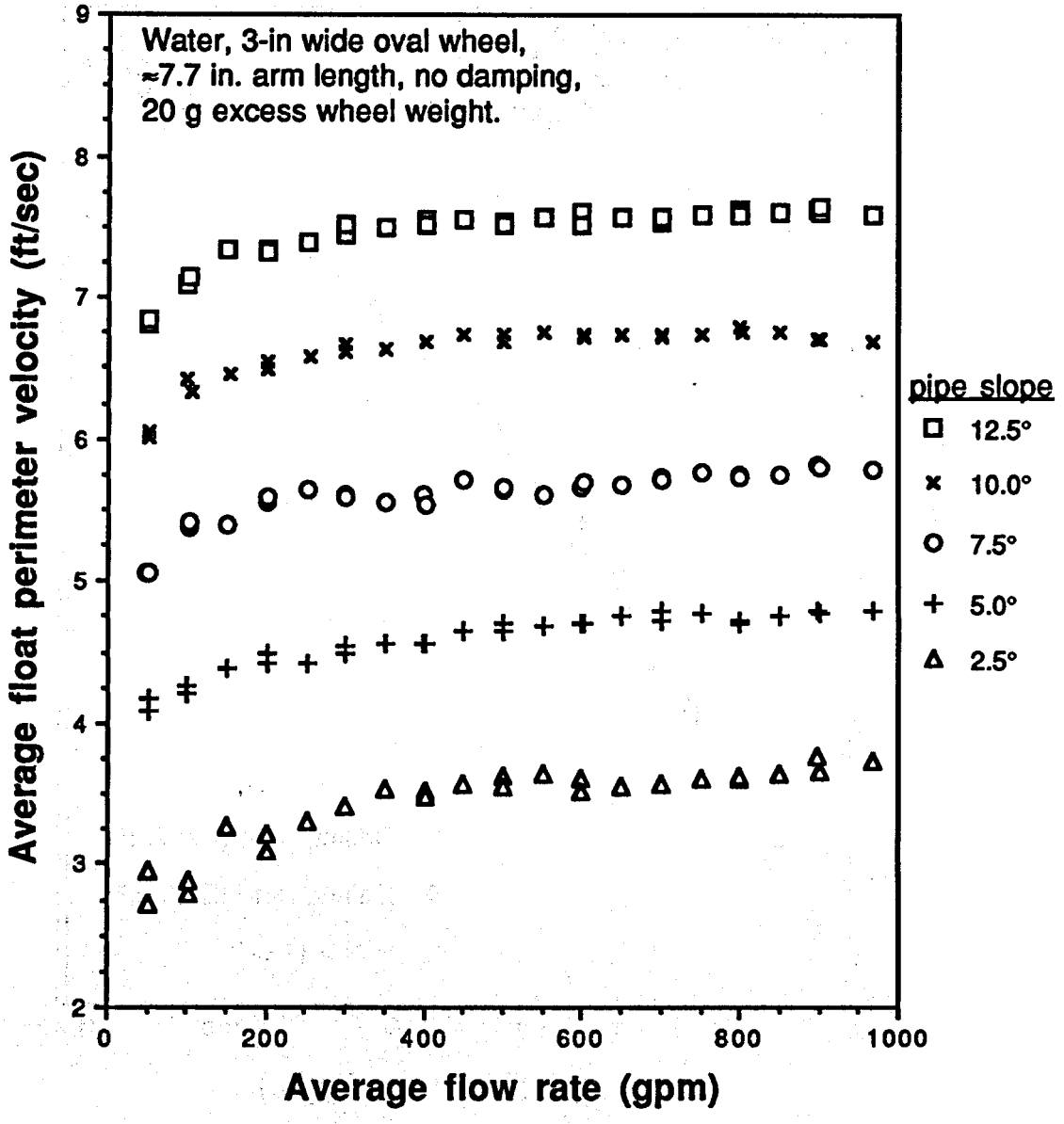

Figure 33 - Effects of pipe slope on the average rolling float perimeter velocity in drilling mud in a 10-inch acrylic pipe with 20 g excess wheel weight.

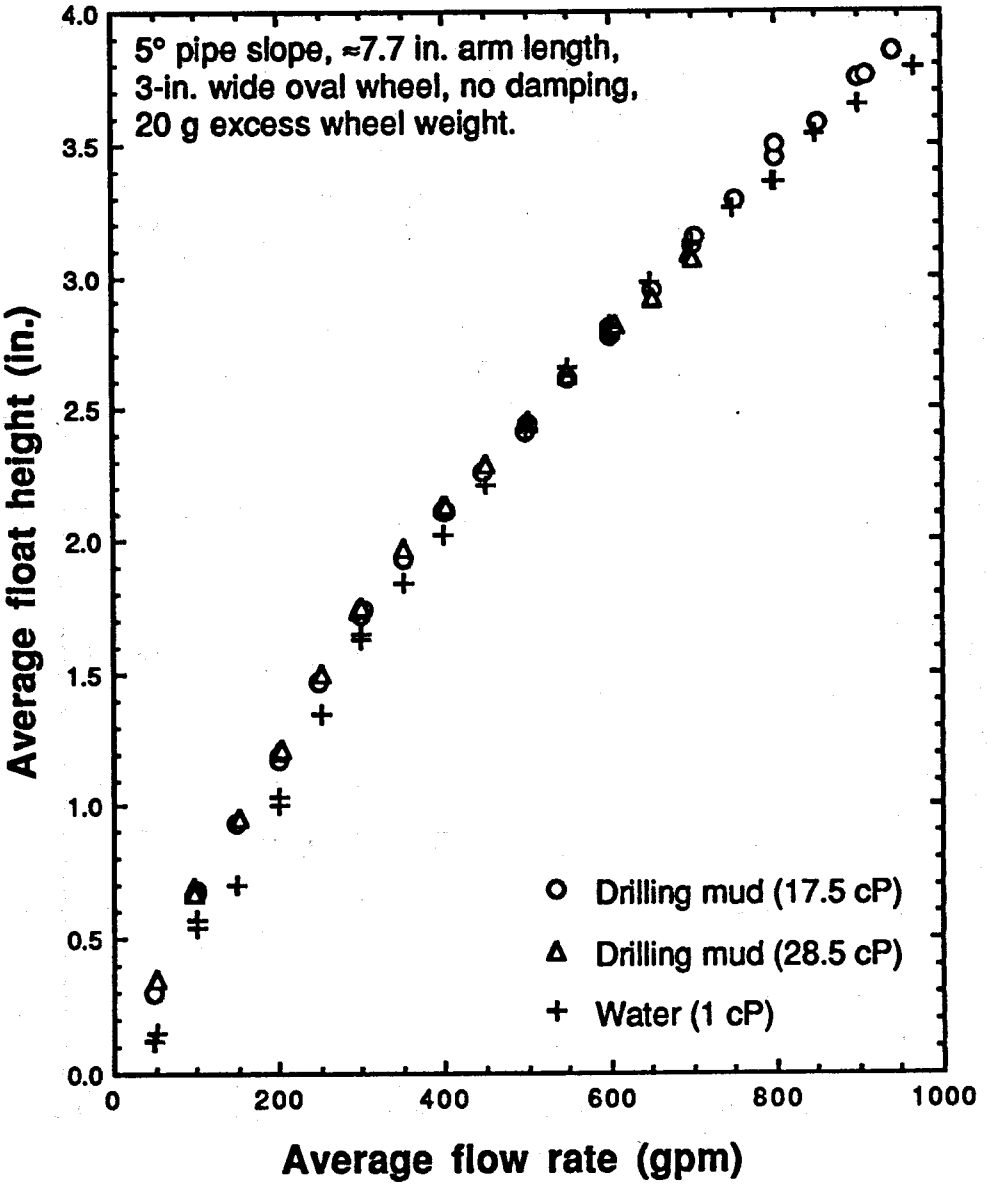

Figure 34 - Effects of fluid viscosity on the average rolling float level in a 12-inch steel pipe with a 5° slope.

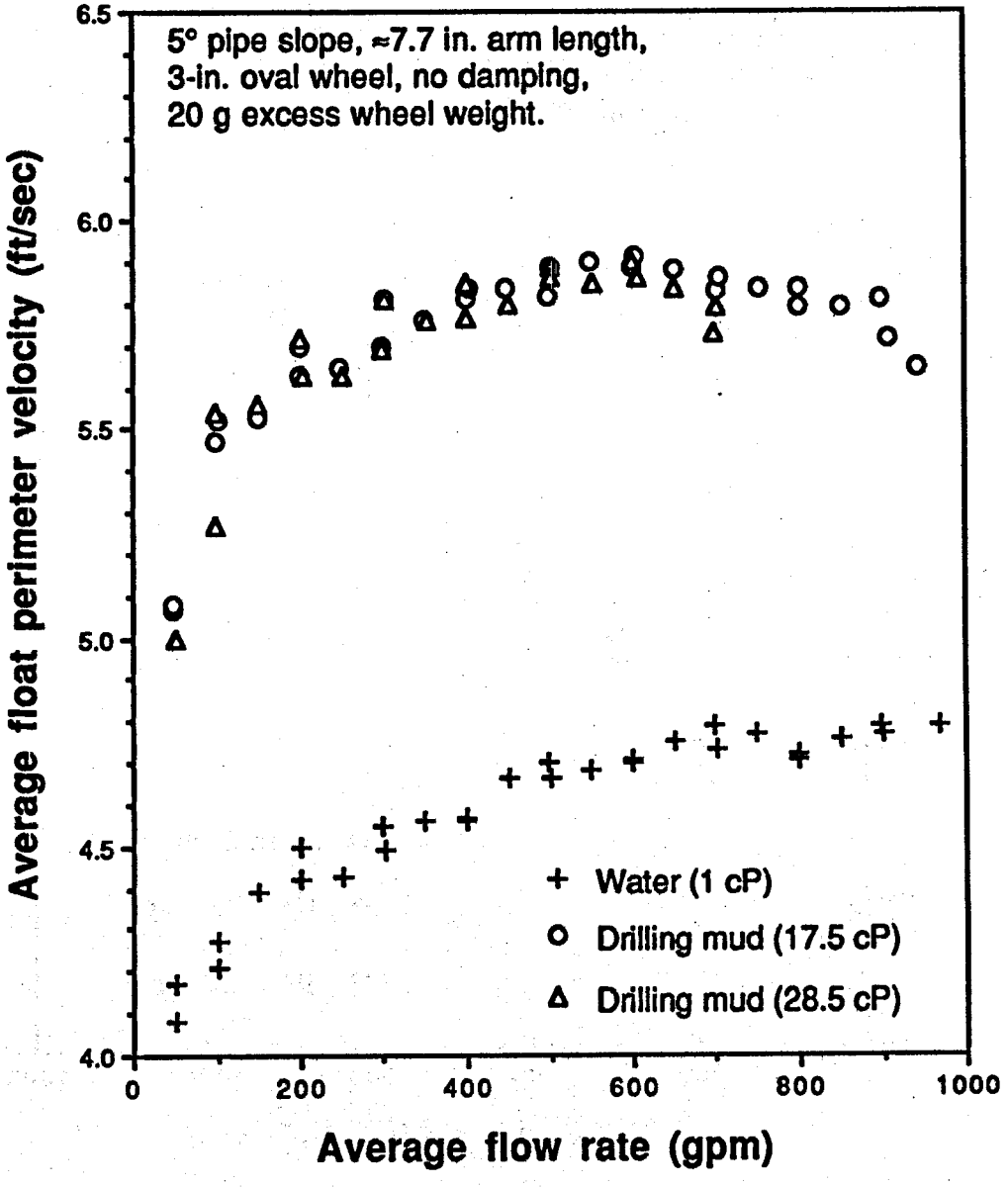

Figure 35 - Effects of fluid viscosity on the average rolling float perimeter velocity in a 12-inch steel pipe with a 5° slope.

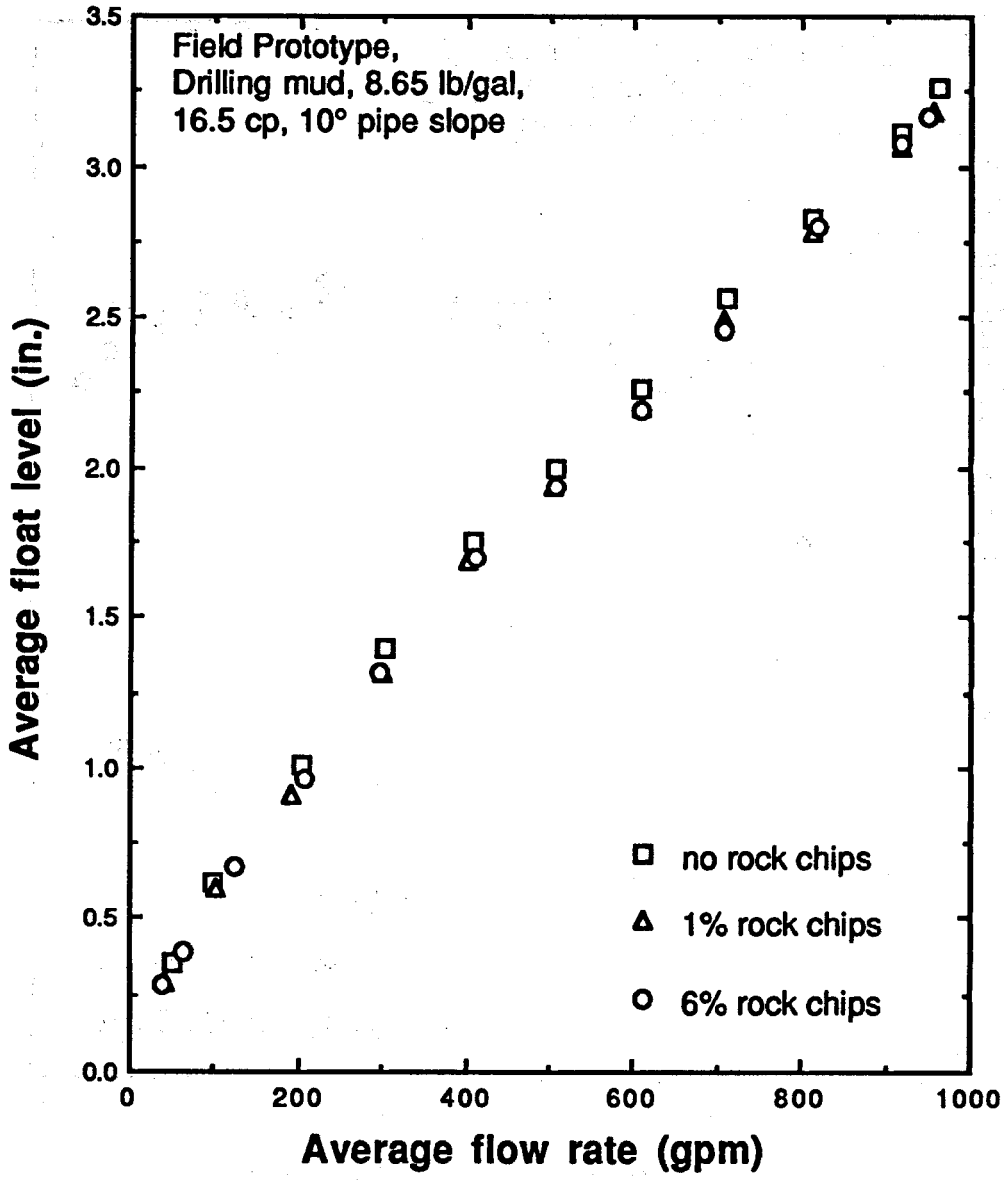

Figure 36 - Effects of rock chips on the average rolling float level in drilling mud in a 12-inch steel pipe with a 10° slope.

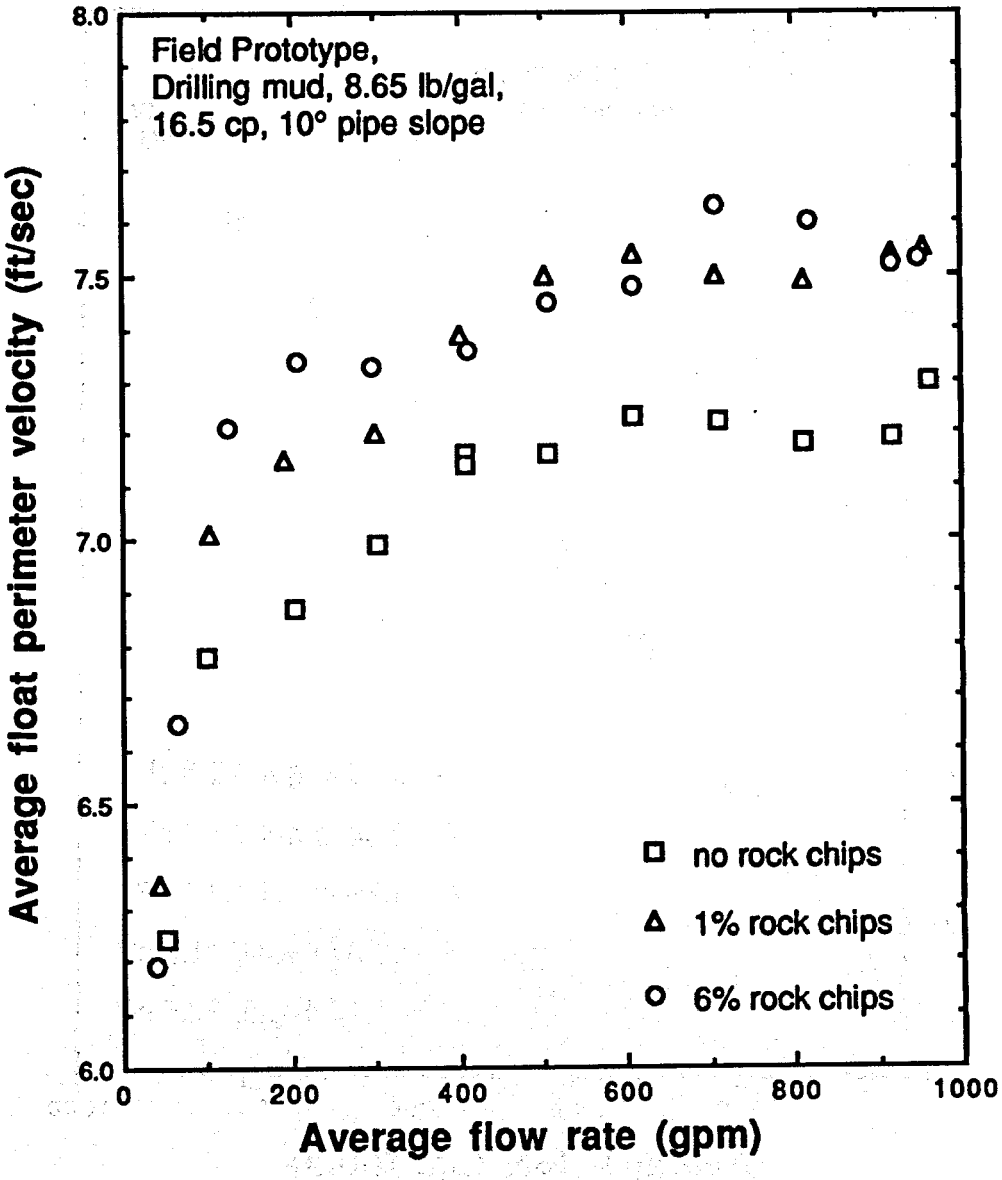

Figure 37 - Effects of rock chips on the average rolling float perimeter velocity in drilling mud in a 12-inch steel pipe with a 10° slope.

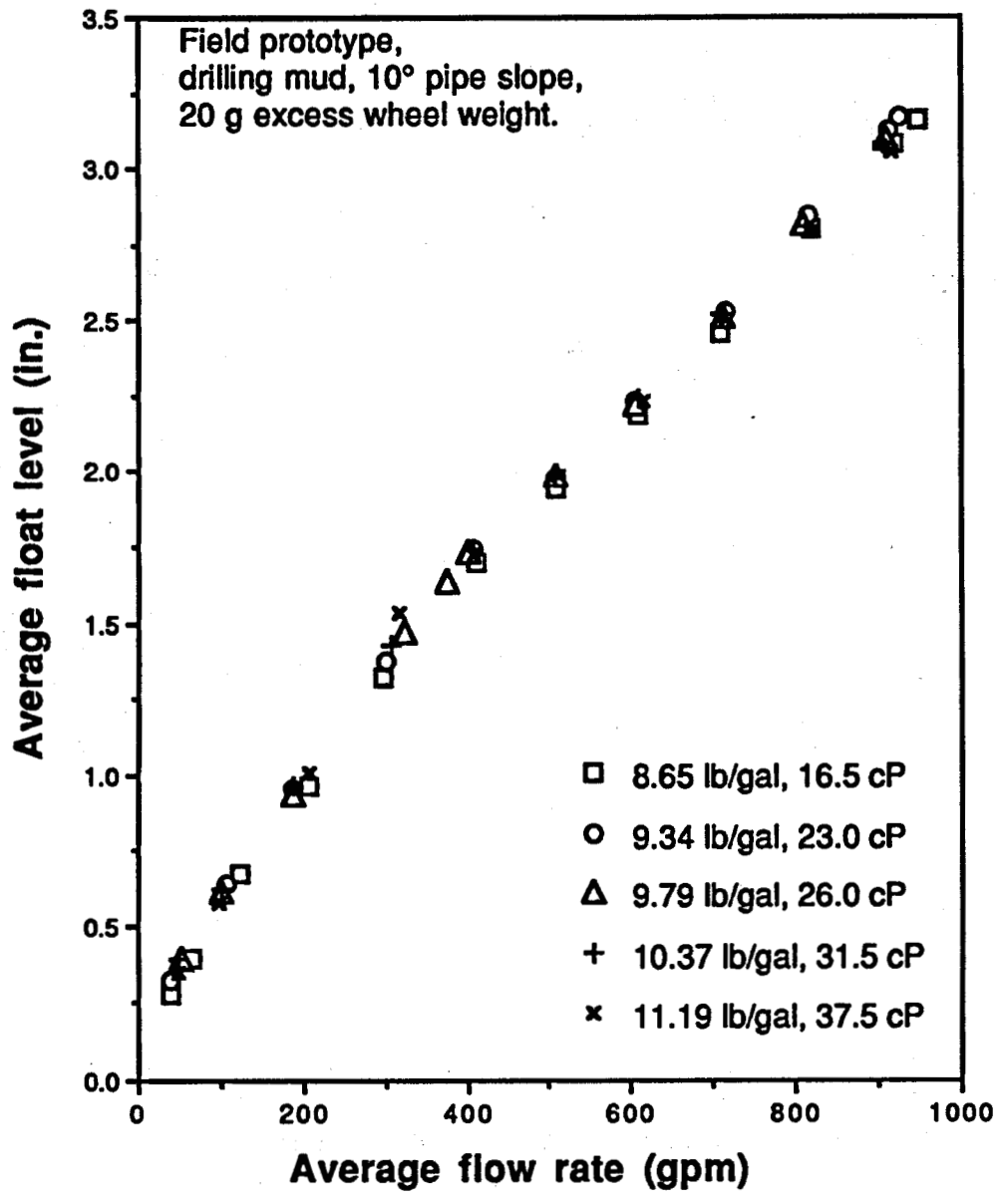

Figure 38 - Effects of fluid viscosity and density on the average field prototype rolling float level in a 12-inch steel pipe with a 10° slope.

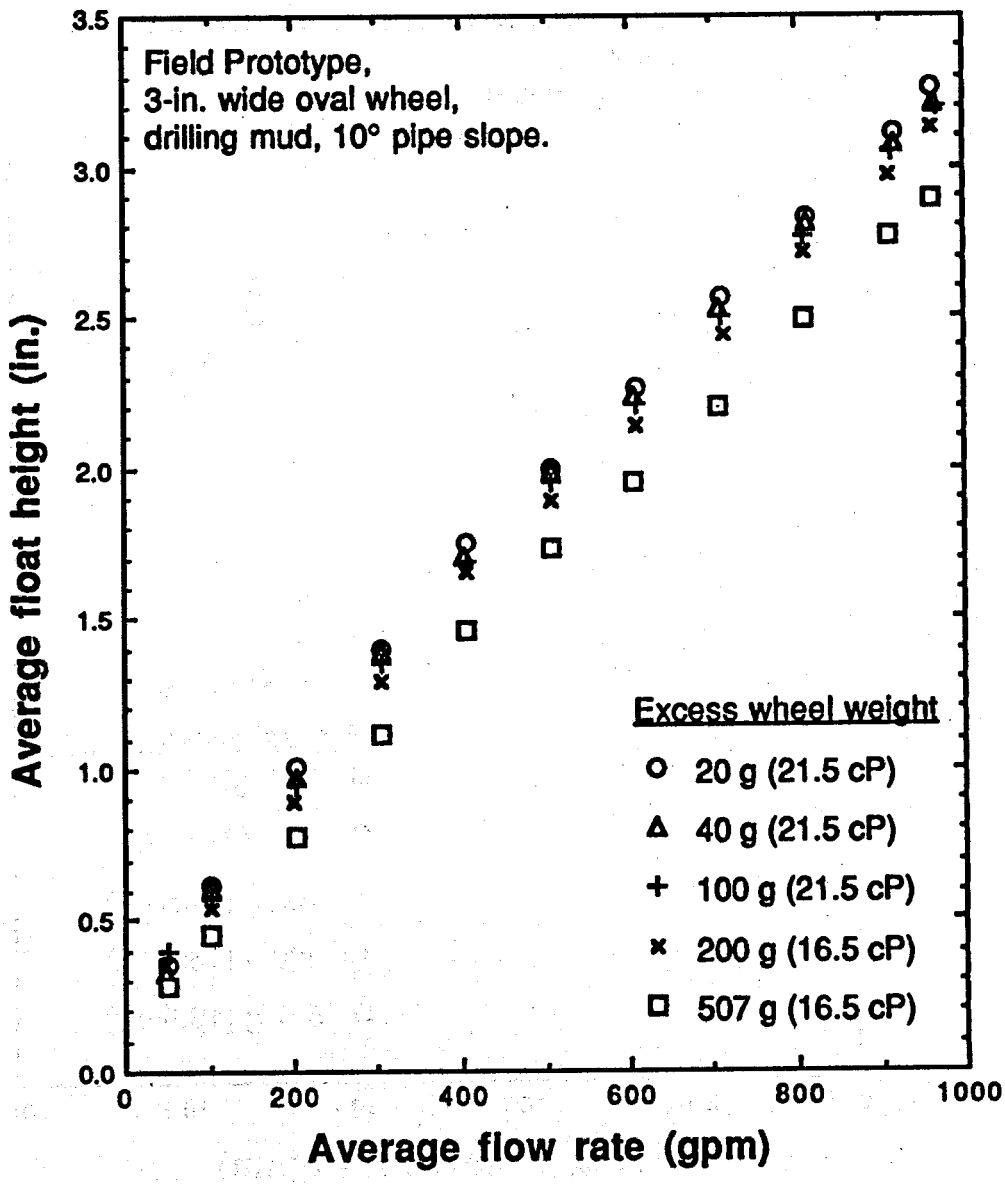

Figure 39 - Effects of excess wheel weight on the average field prototype rolling float level in drilling mud in a 12-inch steel pipe with a 10° slope.

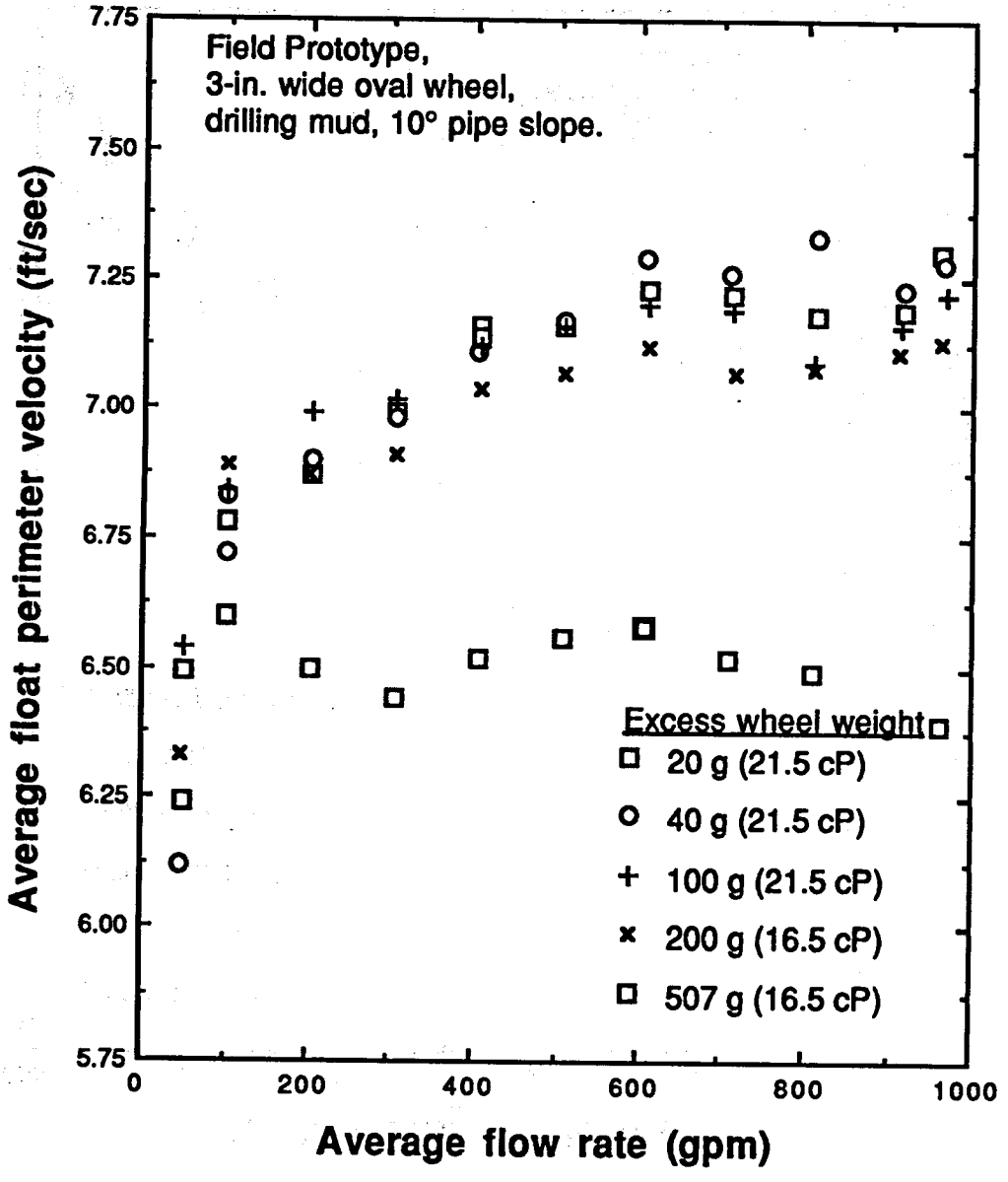

Figure 40 - Effects of excess wheel weight on the average field prototype rolling float perimeter velocity in drilling mud in a 12-inch steel pipe with a 10° slope.

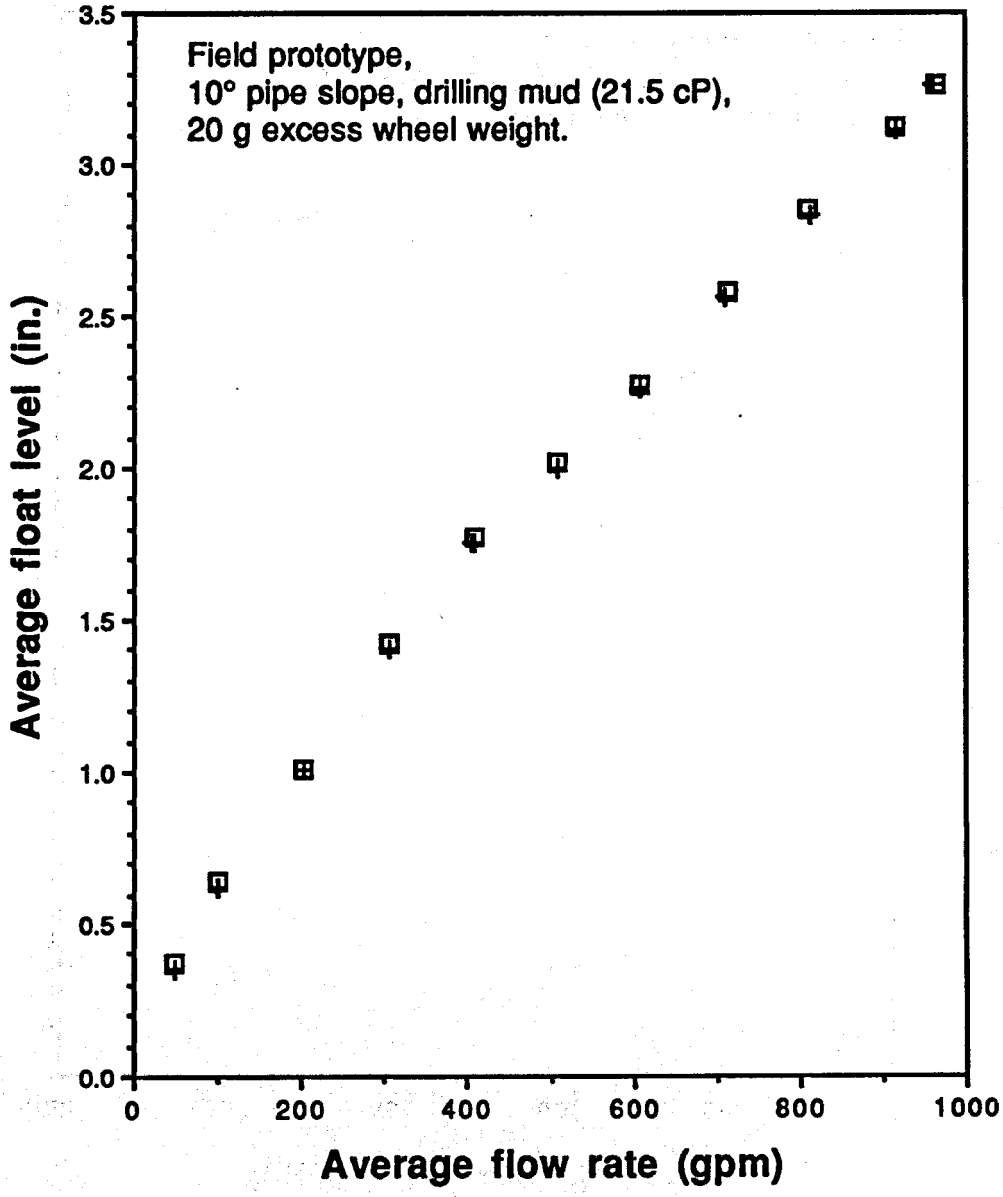

Figure 41 - Repeatability of the field prototype average rolling float level in drilling mud in a 12-inch steel pipe with a 10° slope.

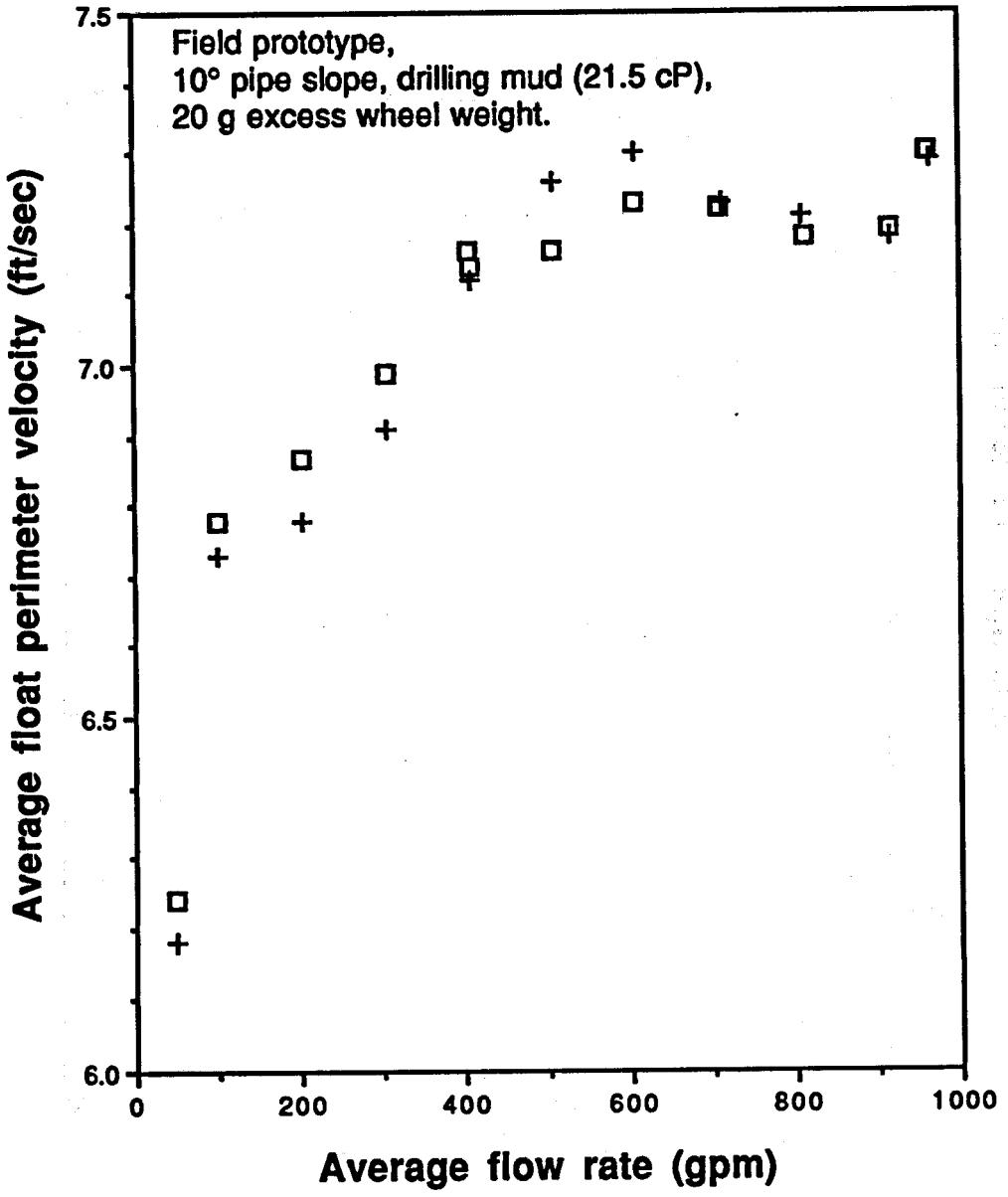

Figure 42 - Repeatability of the field prototype average rolling float perimeter velocity in drilling mud in a 12-inch steel pipe with a 10° slope.

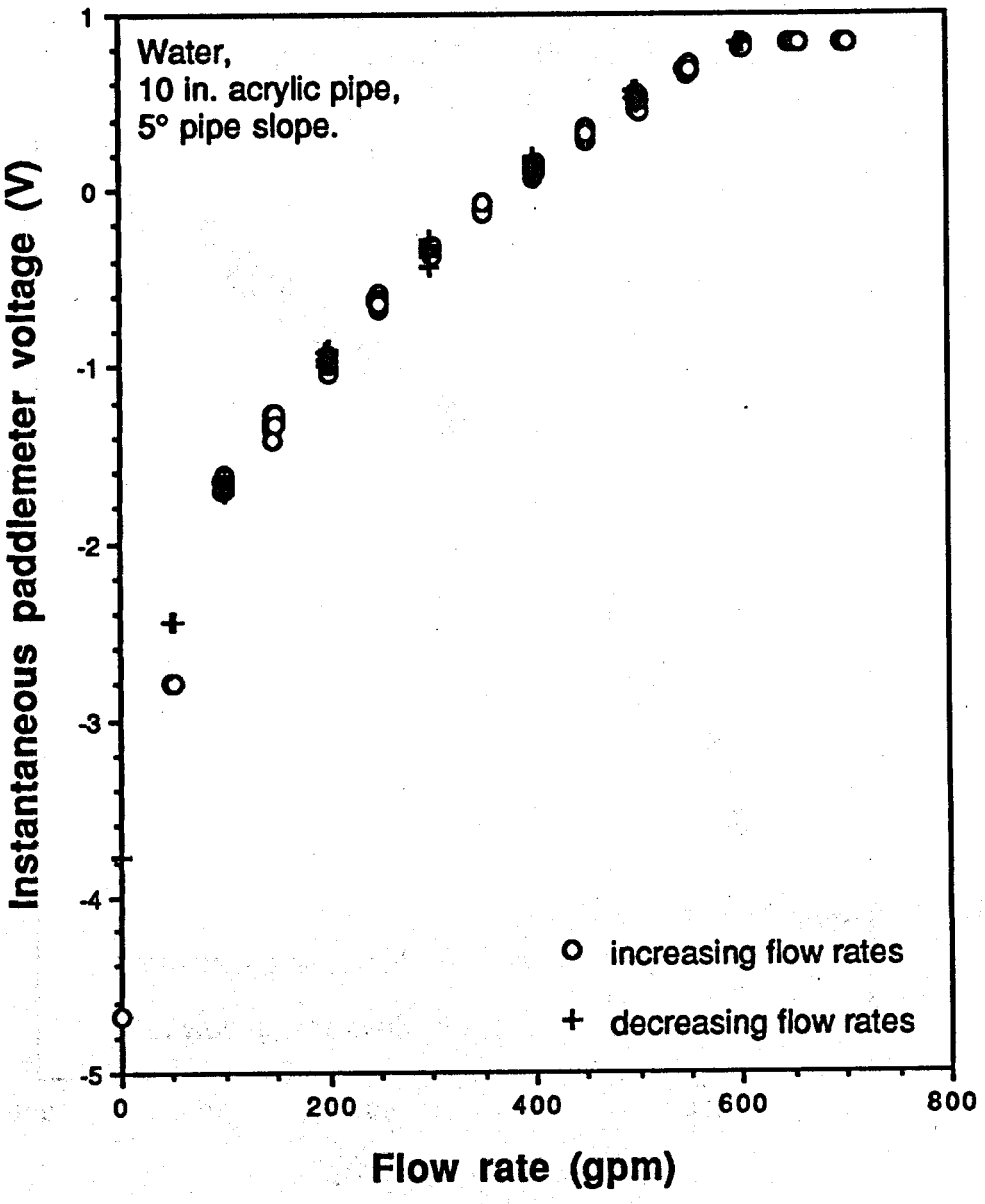

Figure 43 - Paddlemeter response as a function of flow rate in water in a 10-inch acrylic pipe with a 5° slope.

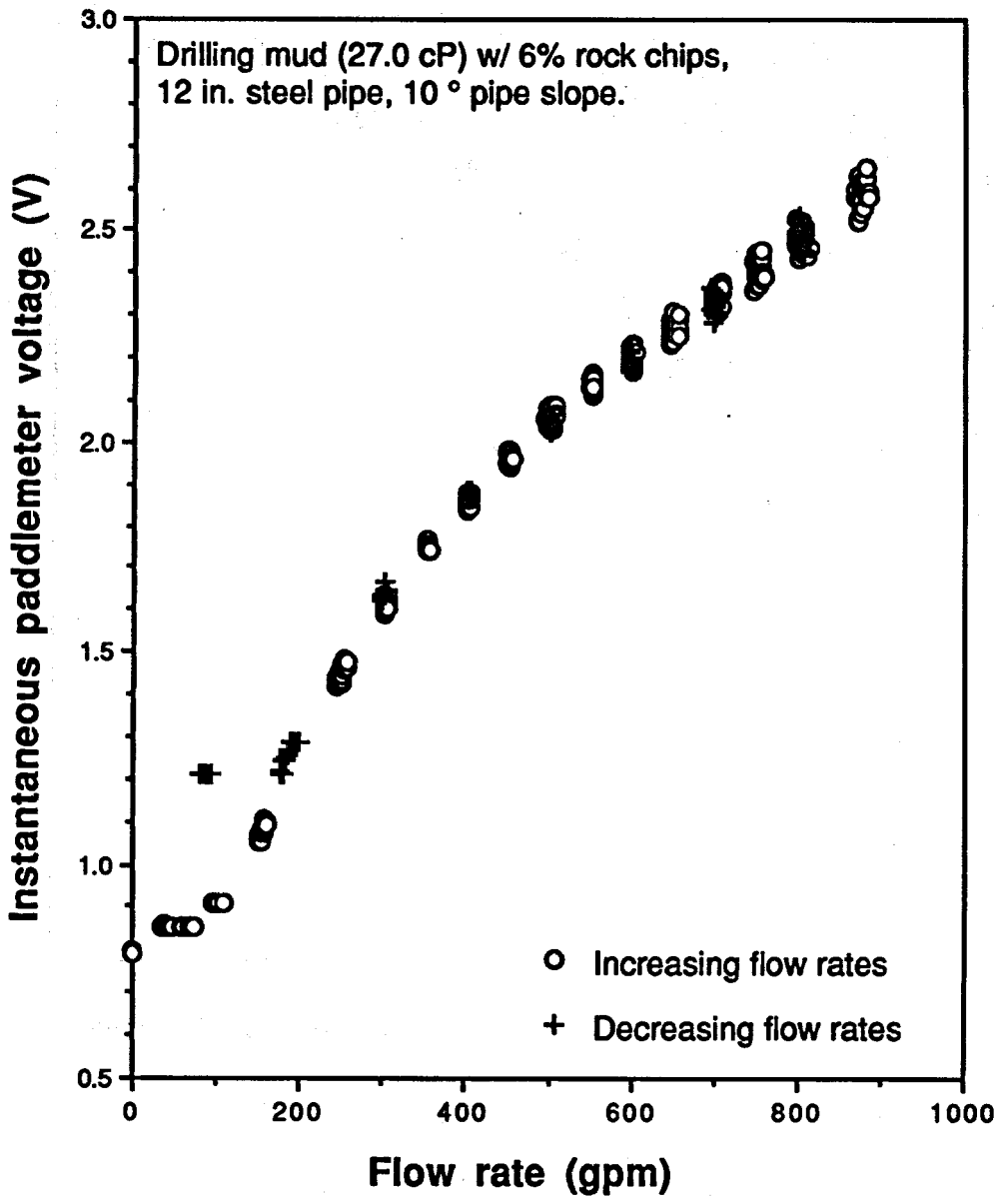

Figure 44 - Paddlemeter response as a function of flow rate in weighted drilling mud with rock chips in a 12-inch steel pipe with a 10° slope.

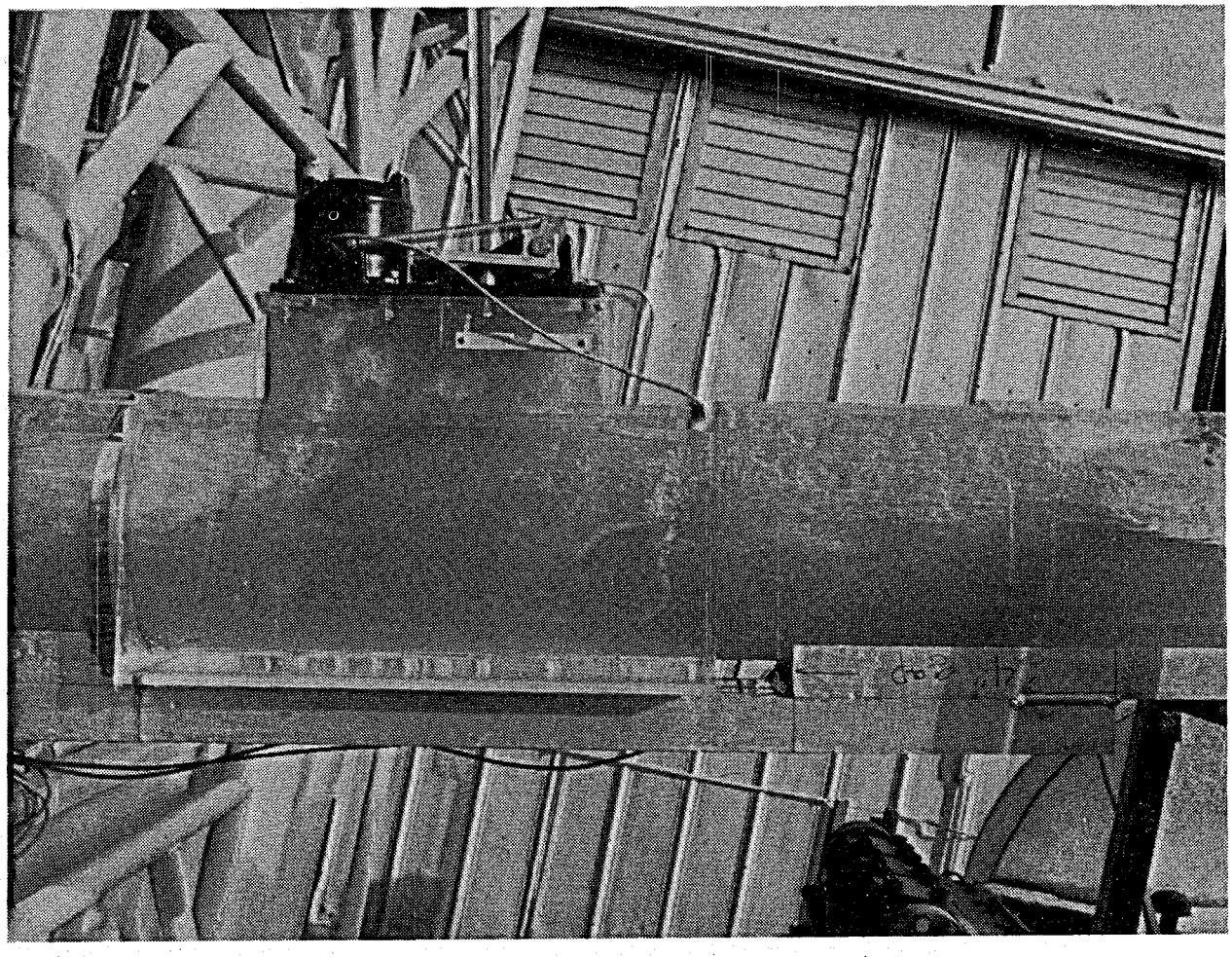

Figure 45 - Photograph of the flow disturbance caused by the paddlemeter in a 10-inch acrylic pipe.

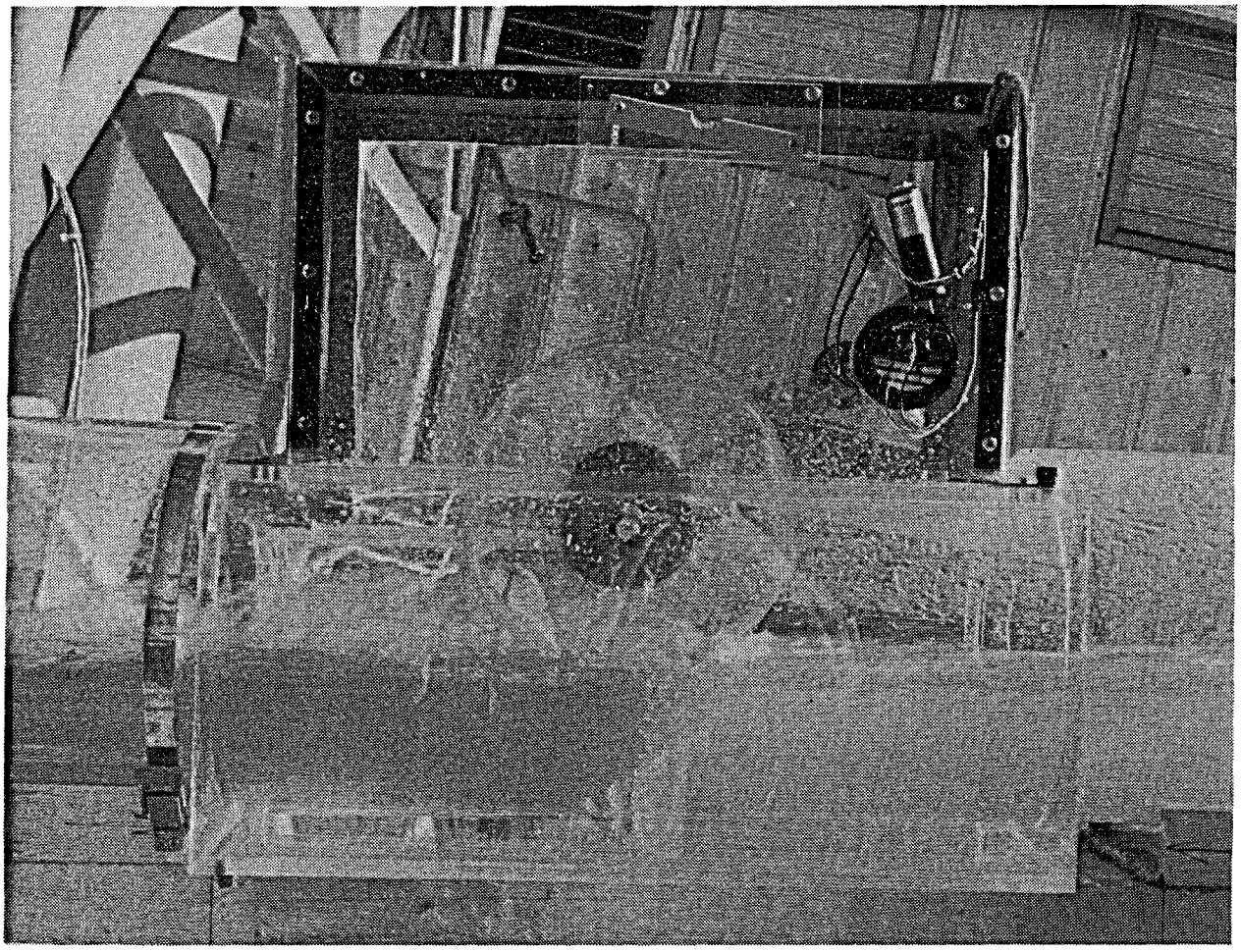

Figure 46 - Photograph of the flow disturbance caused by the rolling float meter in a 10-inch acrylic pipe.

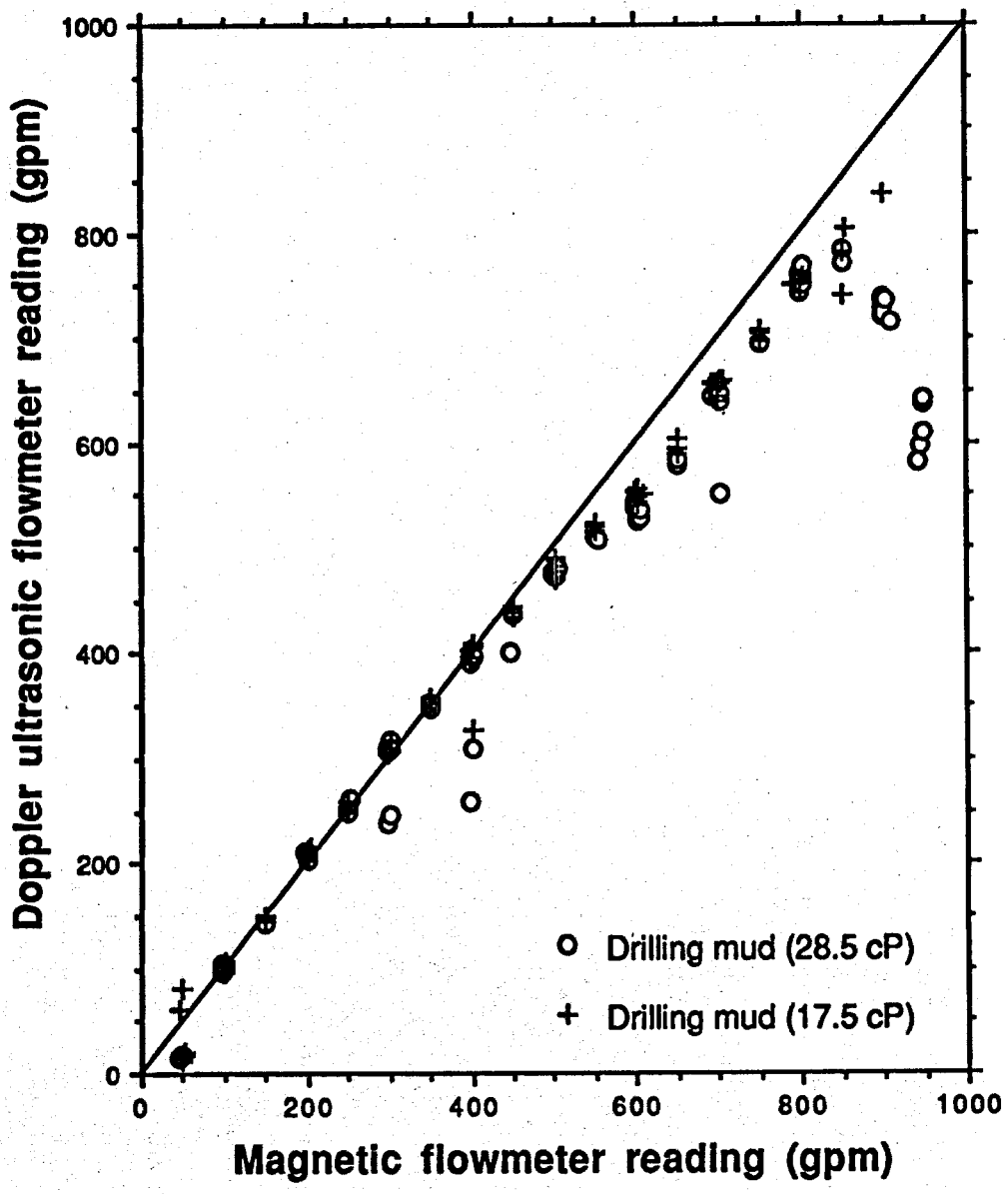

Figure 47 - Comparison of drilling mud flow rates measured by the magnetic flowmeter and Doppler ultrasonic flowmeter in the Wellbore Hydraulics Flow Facility.

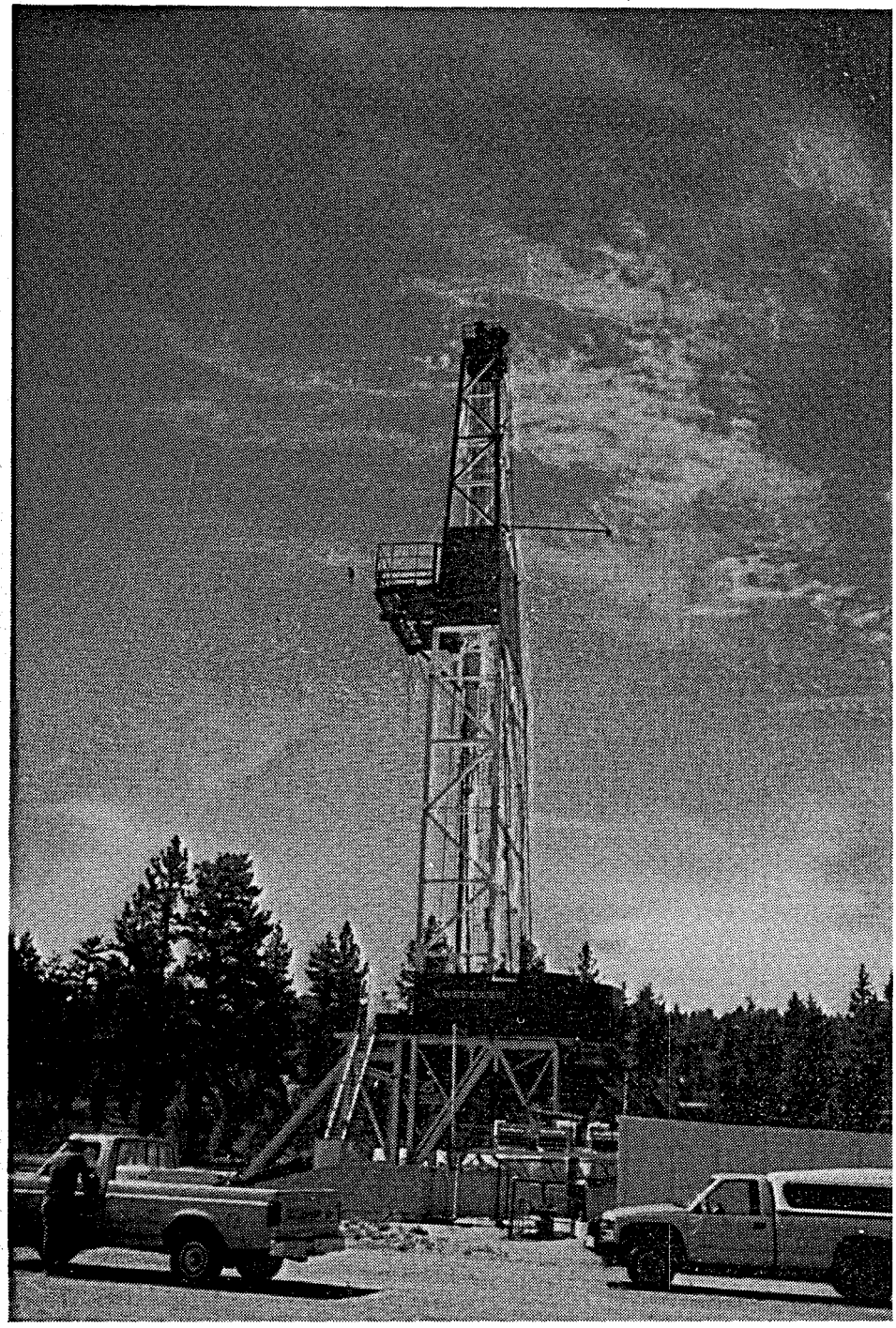

Figure 48 - Photograph of the Long Valley Exploratory Well drill site.

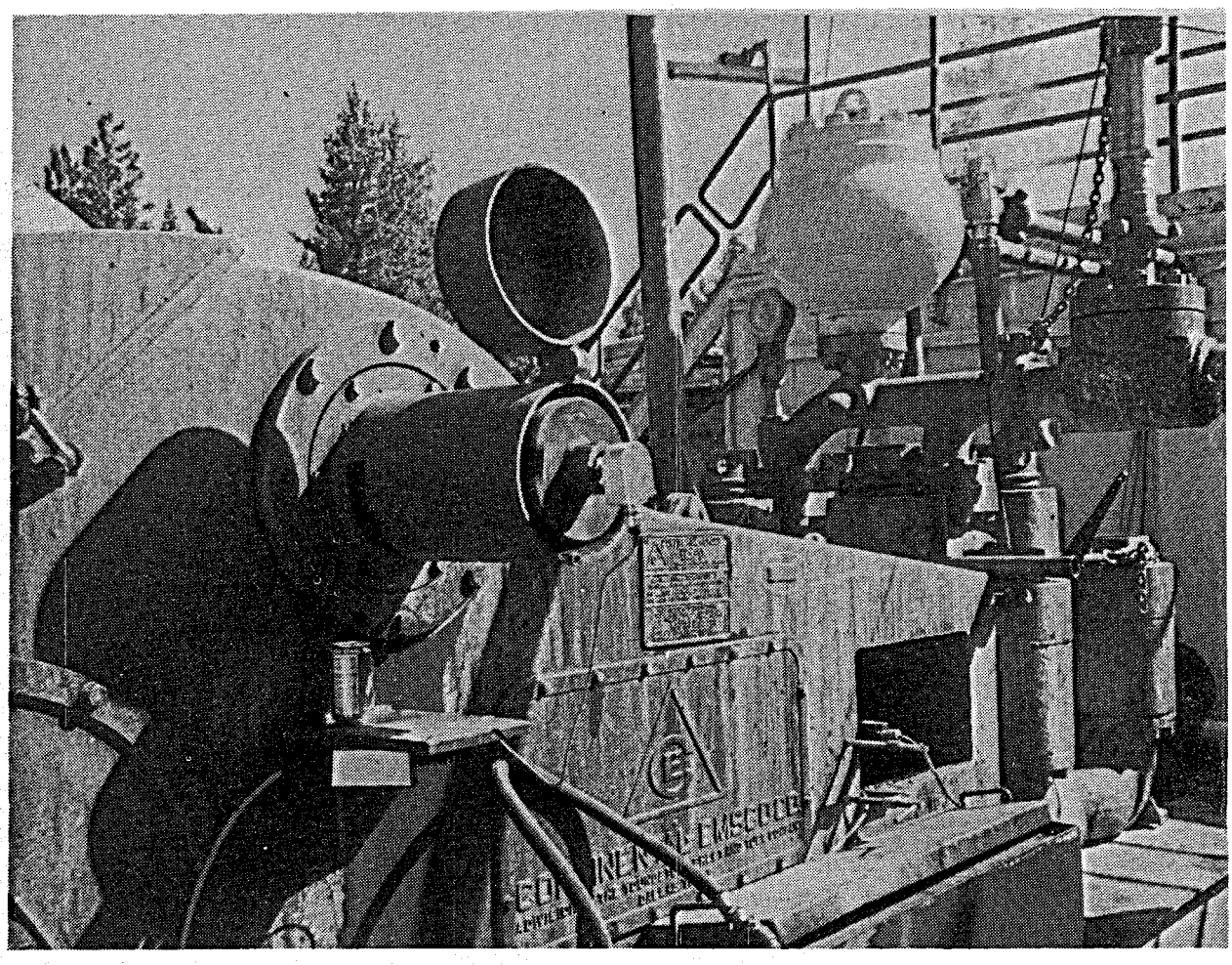

Figure 49 - Photograph of the rotary speed transducer and stroke-counter limit switch on a mud pump at the Long Valley Exploratory Well.

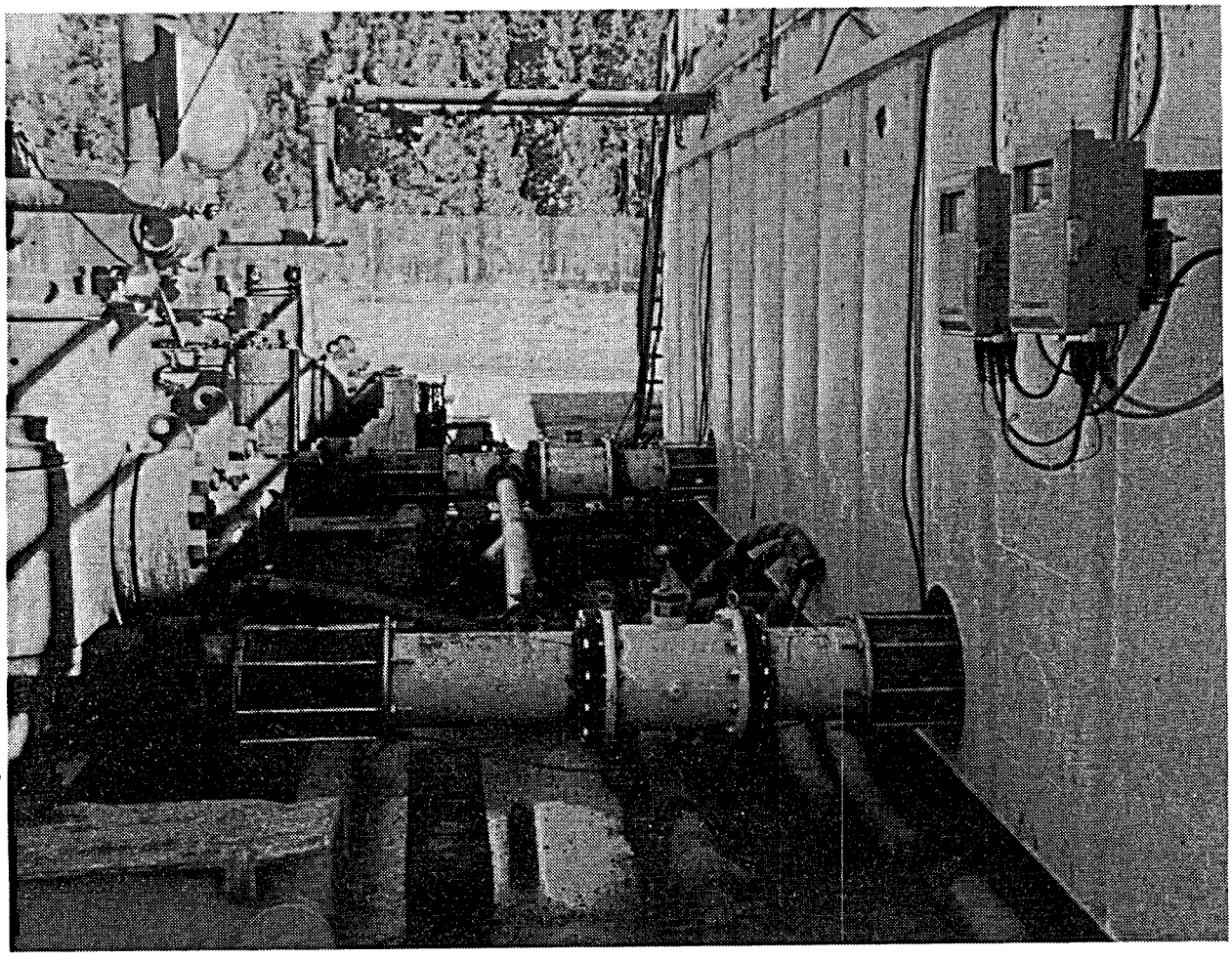

Figure 50 - Photograph of the 10-inch magnetic flowmeters on the inlet lines to the mud pumps at the Long Valley Exploratory Well.

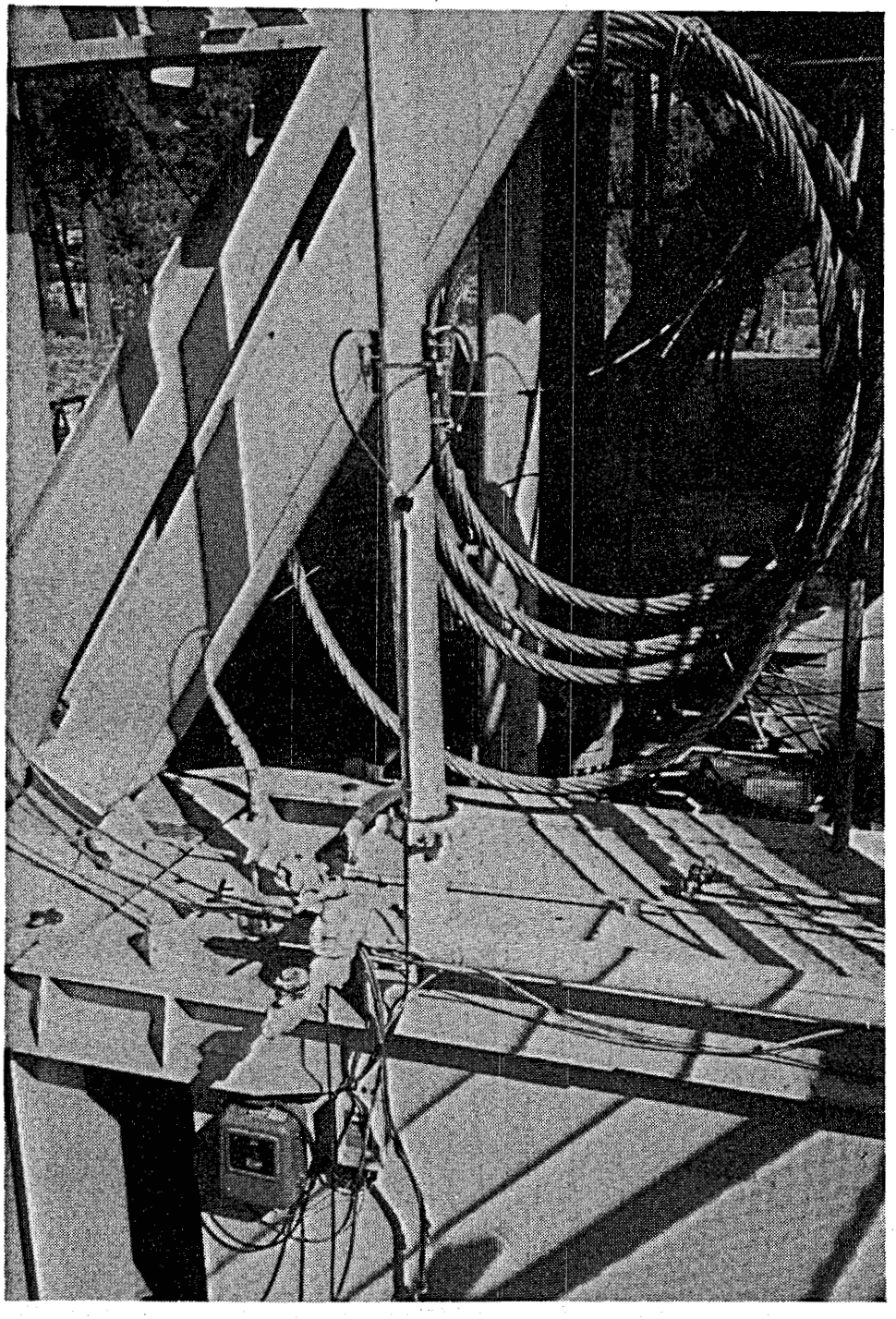

Figure 51 - Photograph of the Doppler ultrasonic flowmeter at the Long Valley Exploratory Well.

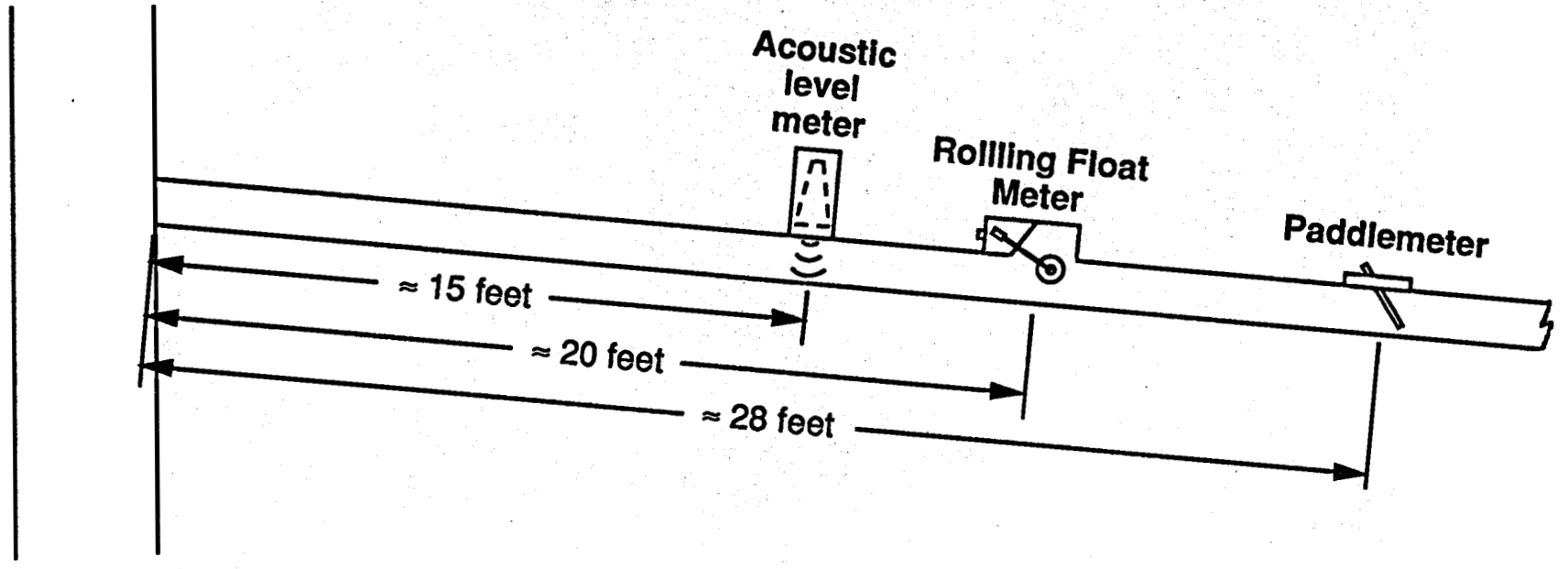

Figure 52 - Schematic of the drilling fluid return line at the Longvalley Exploratory Well

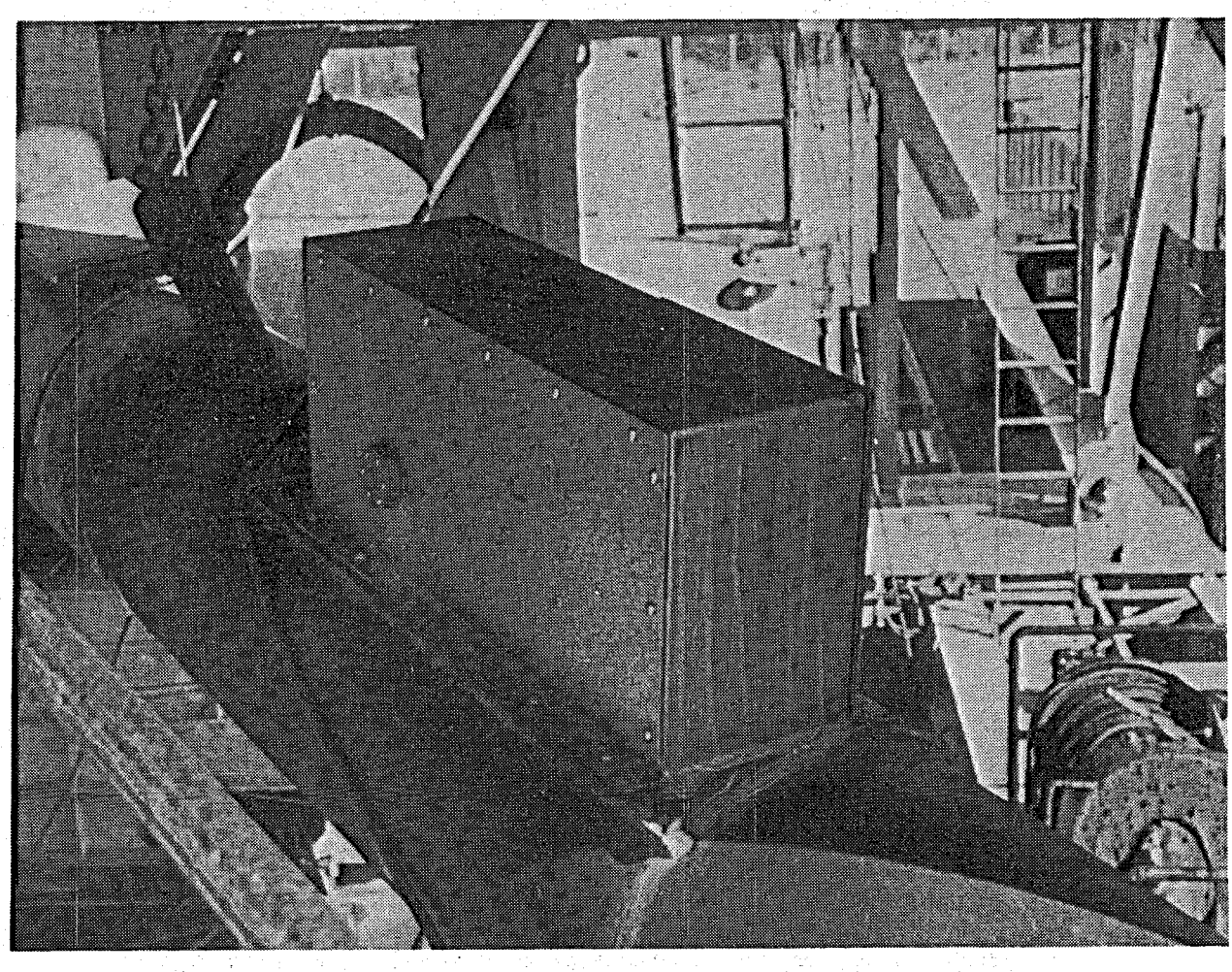

Figure 53 - Photograph of the acoustic level meter on the return line at the Long Valley Exploratory Well.

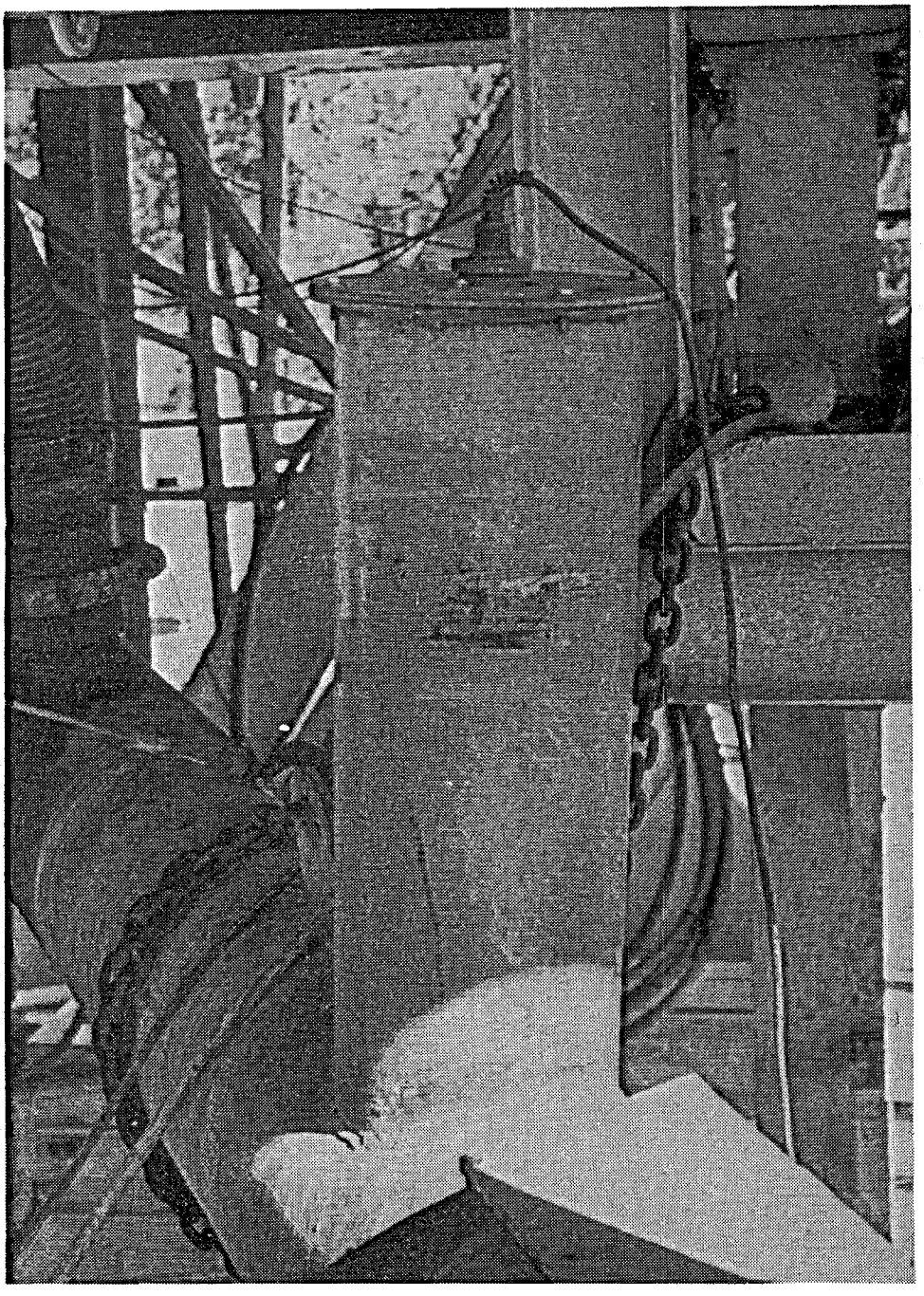

Figure 54 - Photograph of the rolling float meter on the return line at the Long Valley Exploratory Well.

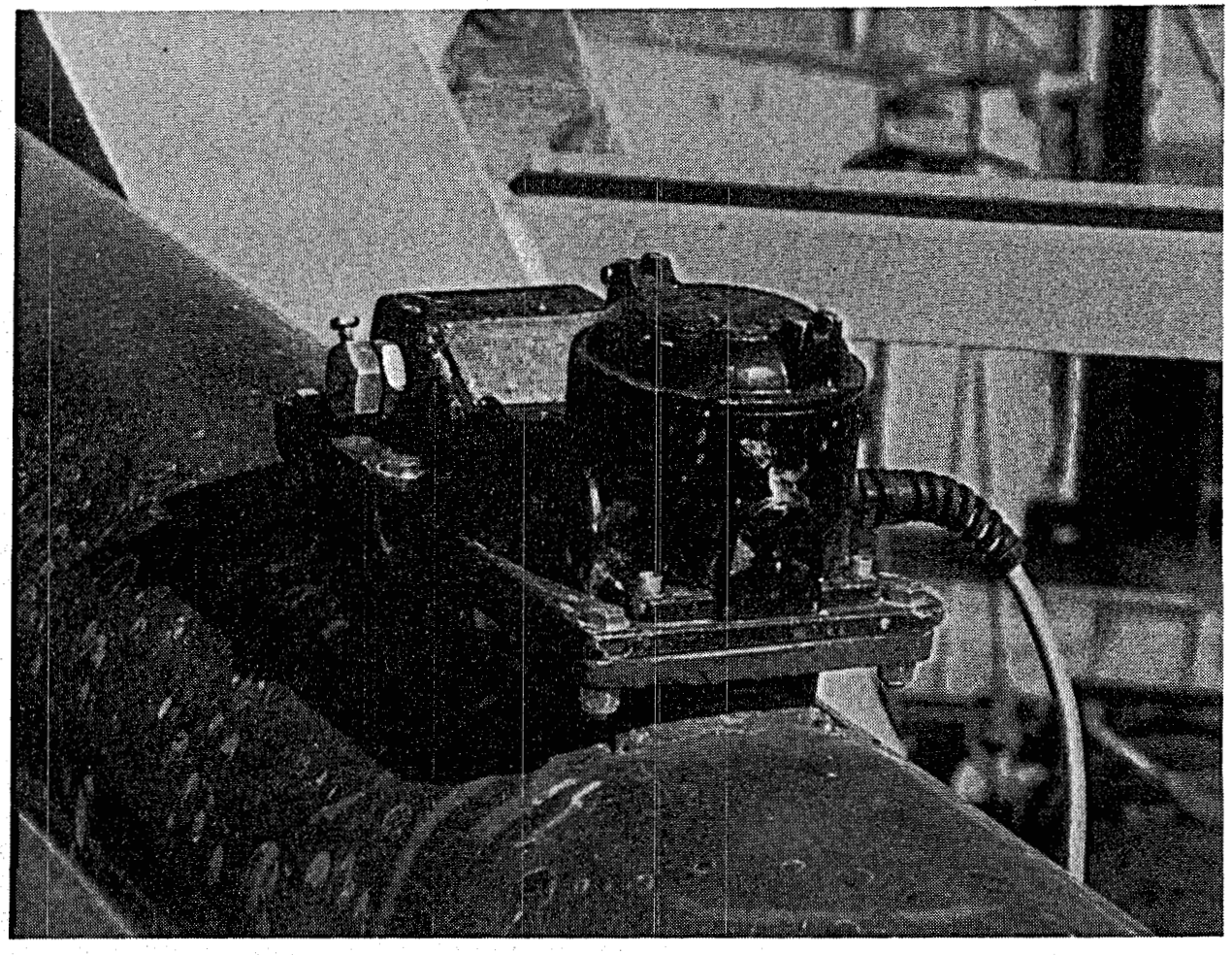

Figure 55 - Photograph of the paddlemeter on the return line at the Long Valley Exploratory Well.

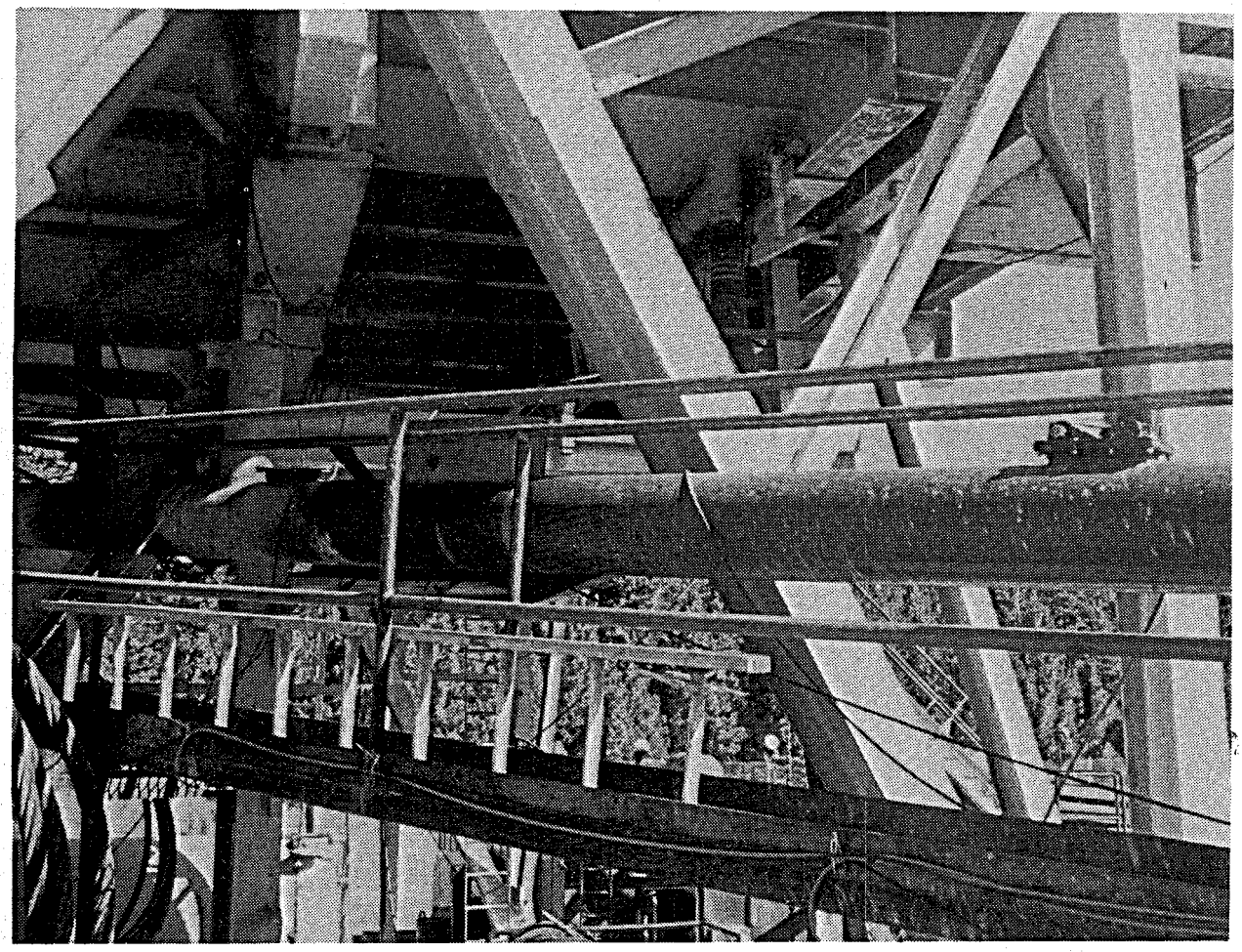

Figure 56 - Photograph of the return flow line at the Long Valley Exploratory Well.

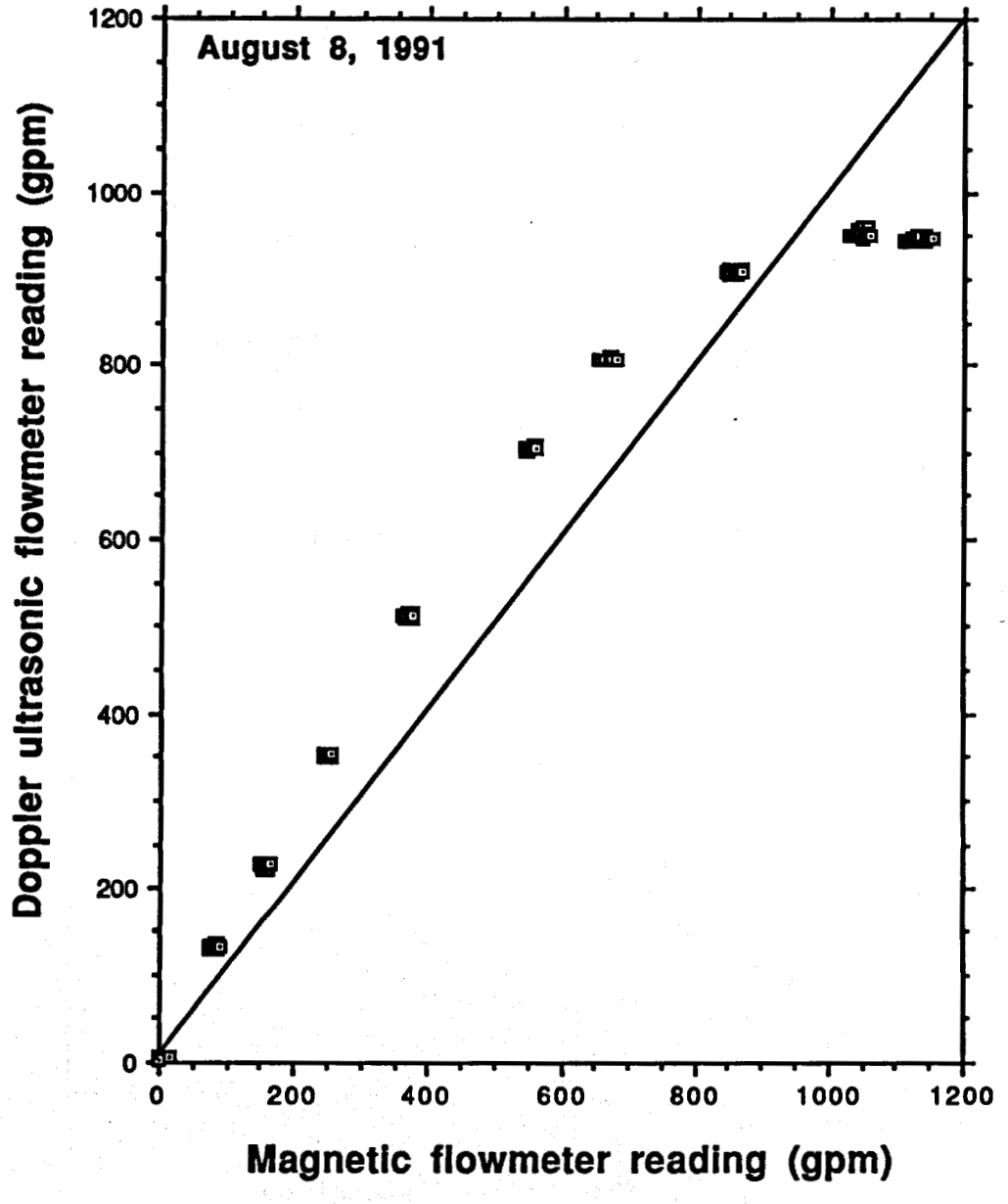

Figure 57 - Comparison of drilling mud flow rates measured by the magnetic flowmeter and Doppler ultrasonic flowmeter at the Long Valley Exploratory Well.

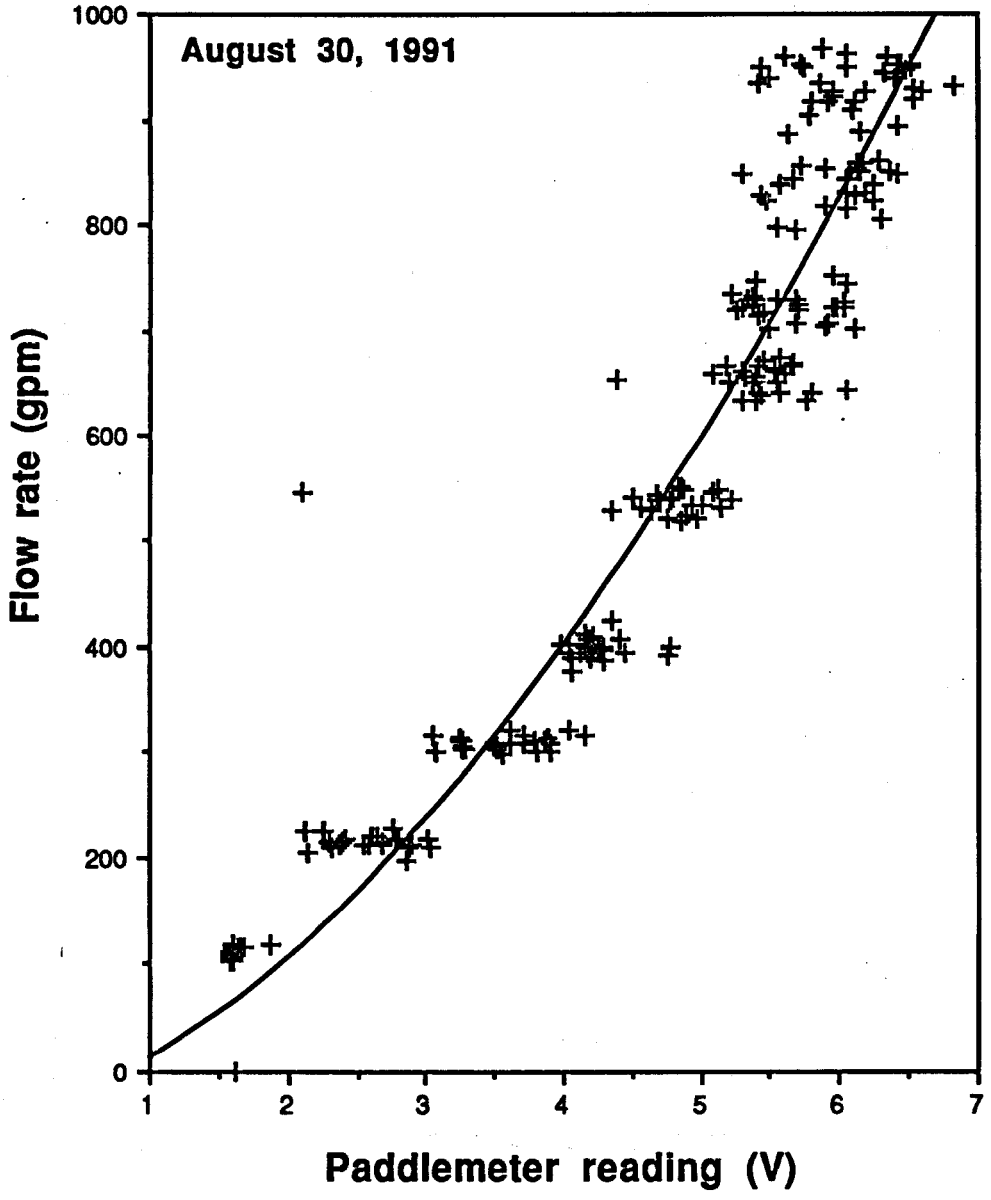

Figure 58 - Flow rate calibration of the paddlemeter at the Long Valley Exploratory Well.

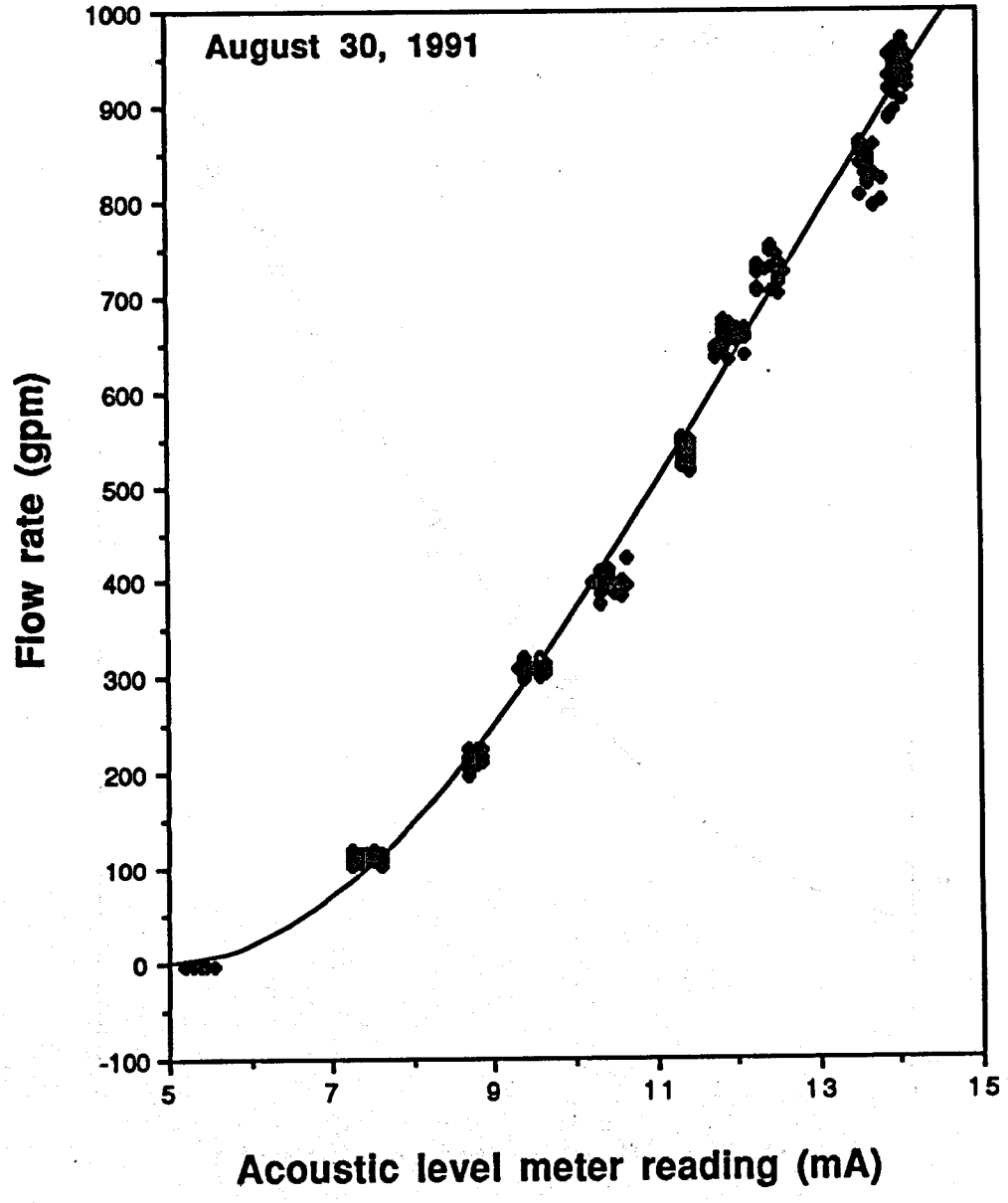

Figure 59 - Flow rate calibration of the acoustic level meter at the Long Valley Exploratory Well.

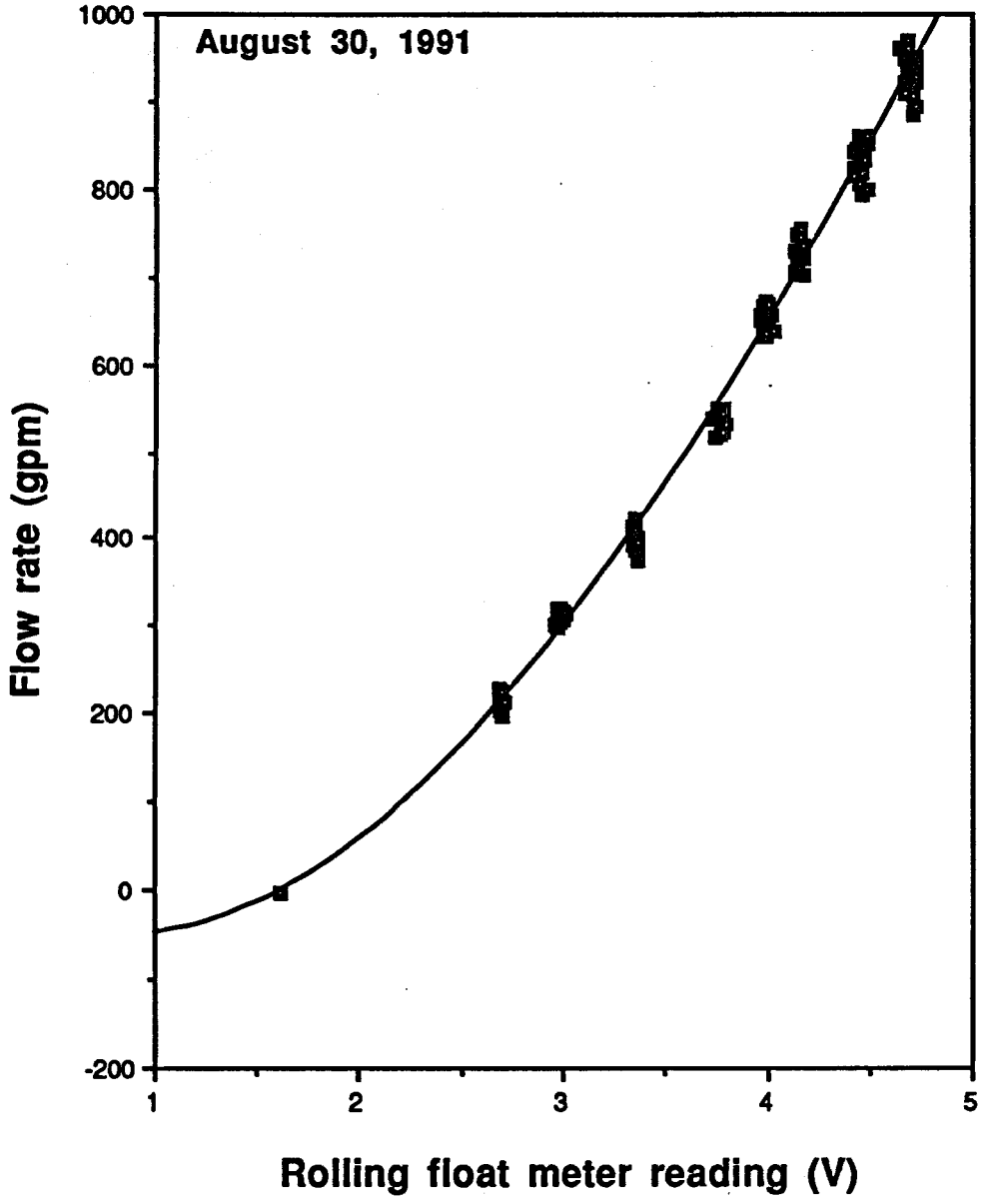

Figure 60 - Flow rate calibration of the rolling float meter at the Long Valley Exploratory Well.

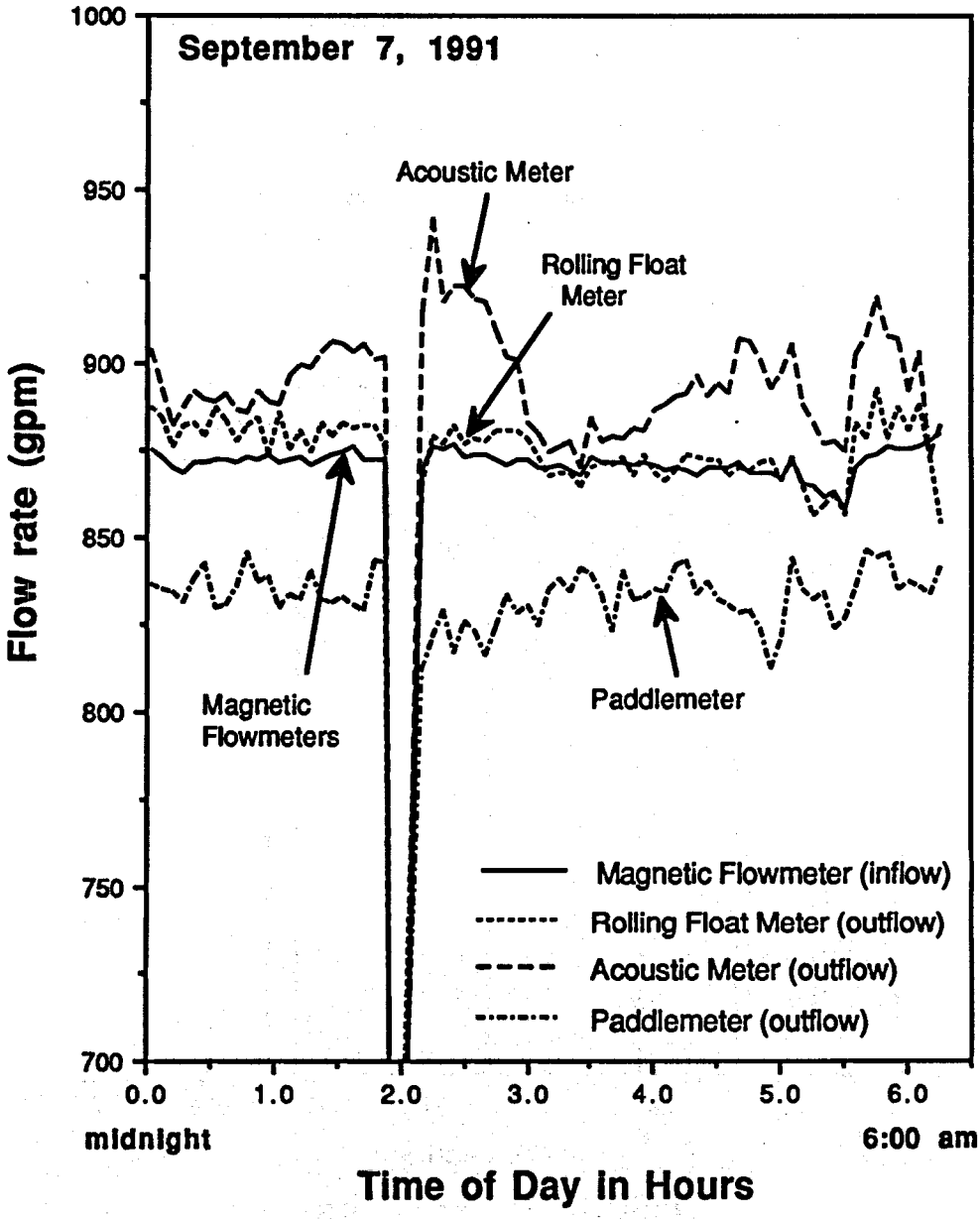

Figure 61 - Comparison of drilling fluid inflow and outflow rates during normal drilling at the Long Valley Exploratory Well.

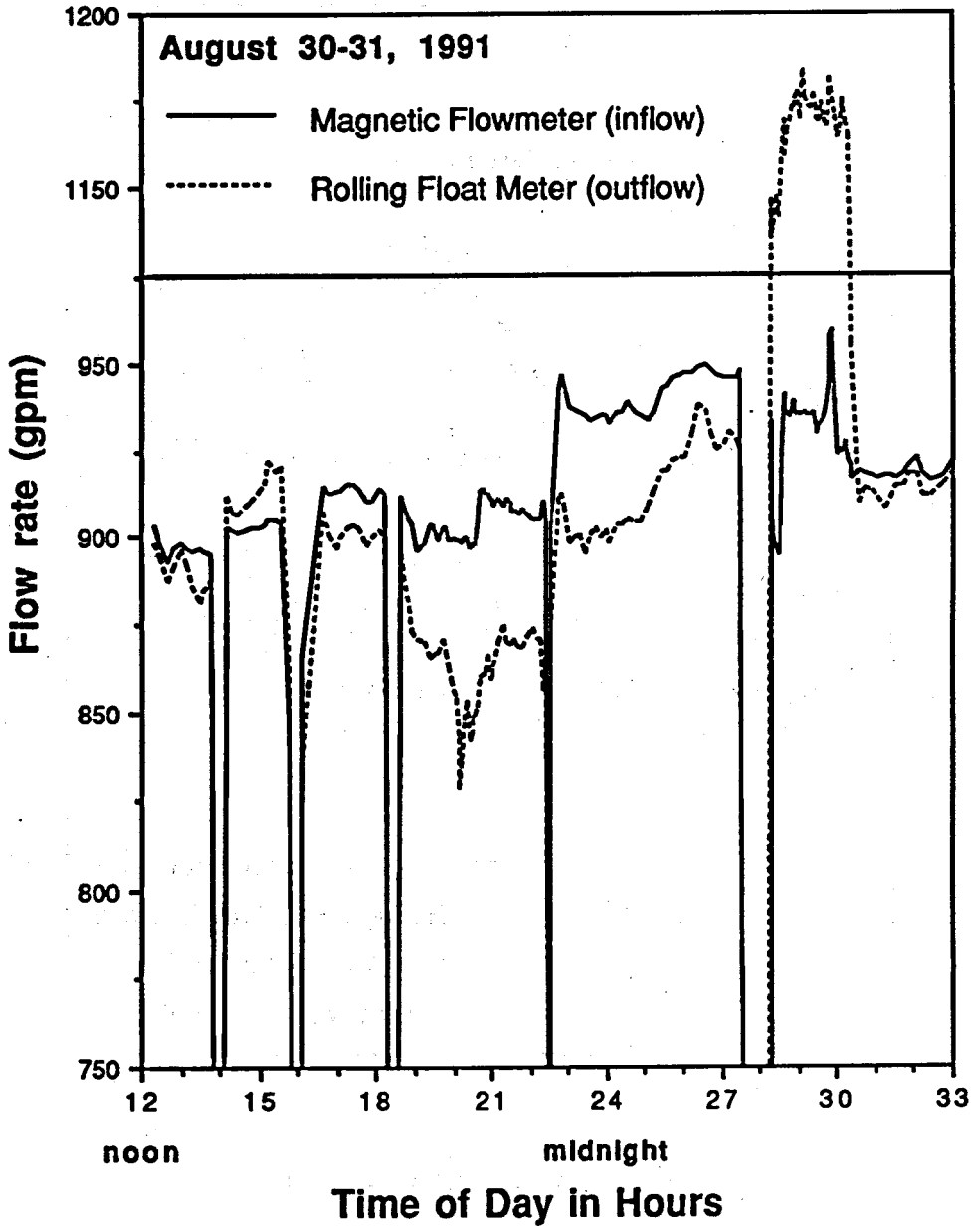

Figure 62 - Comparison of magnetic flowmeter inflow and rolling float meter outflow rates during lost circulation at the Long Valley Exploratory Well.

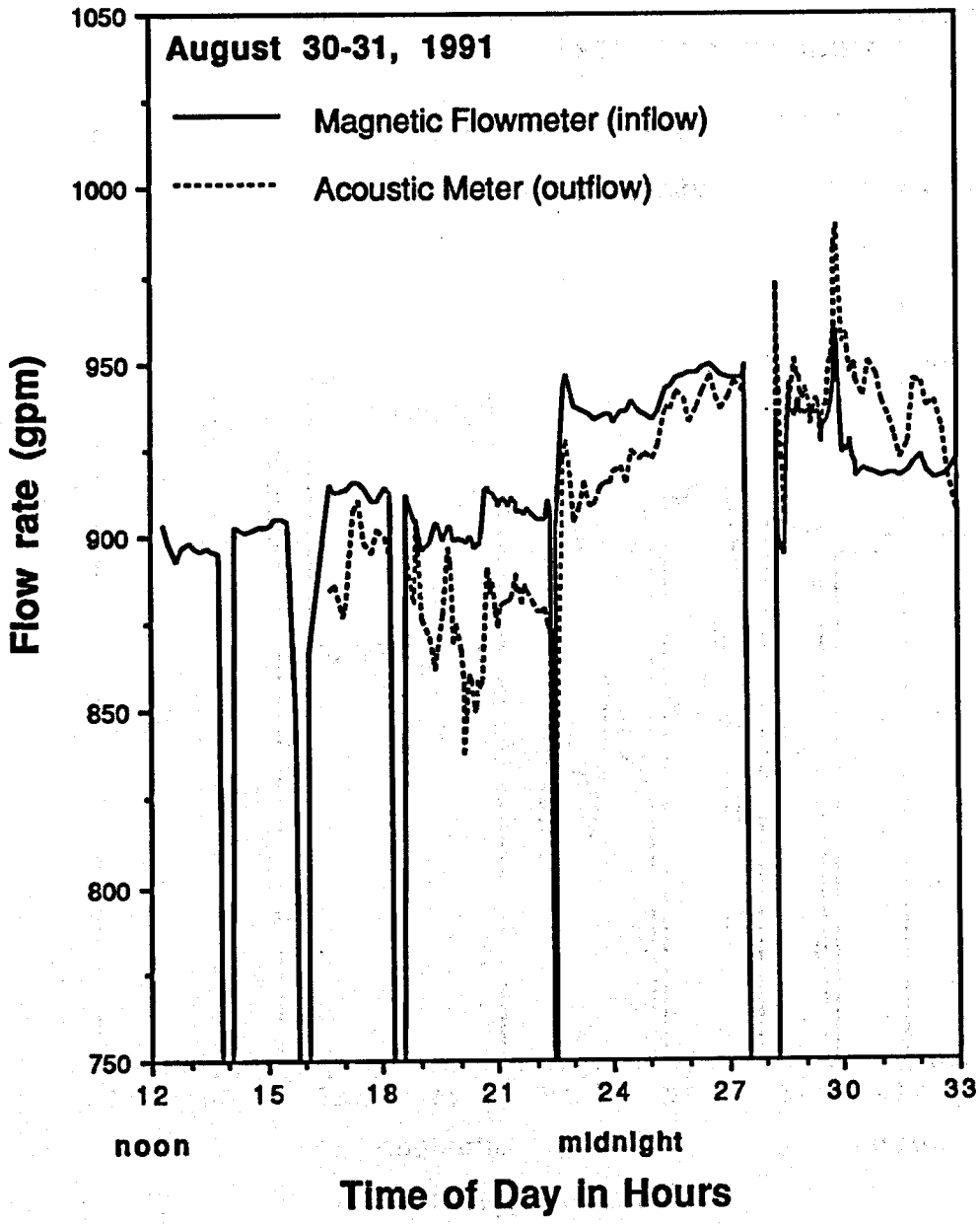

Figure 63 - Comparison of magnetic flowmeter inflow and acoustic meter outflow rates during lost circulation at the Long Valley Exploratory Well.

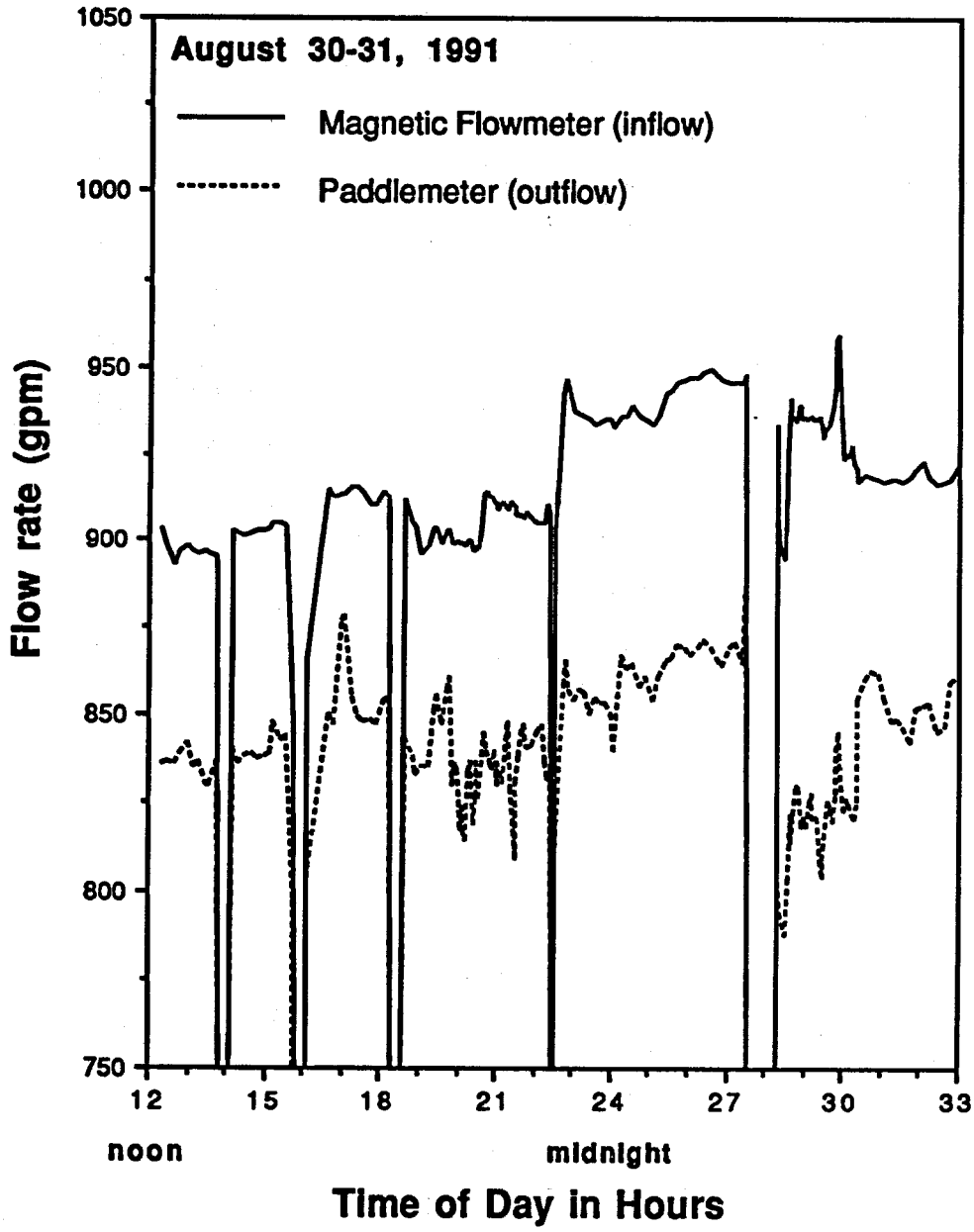

Figure 64 - Comparison of magnetic flowmeter inflow and paddlemeter outflow rates during lost circulation at the Long Valley Exploratory Well.

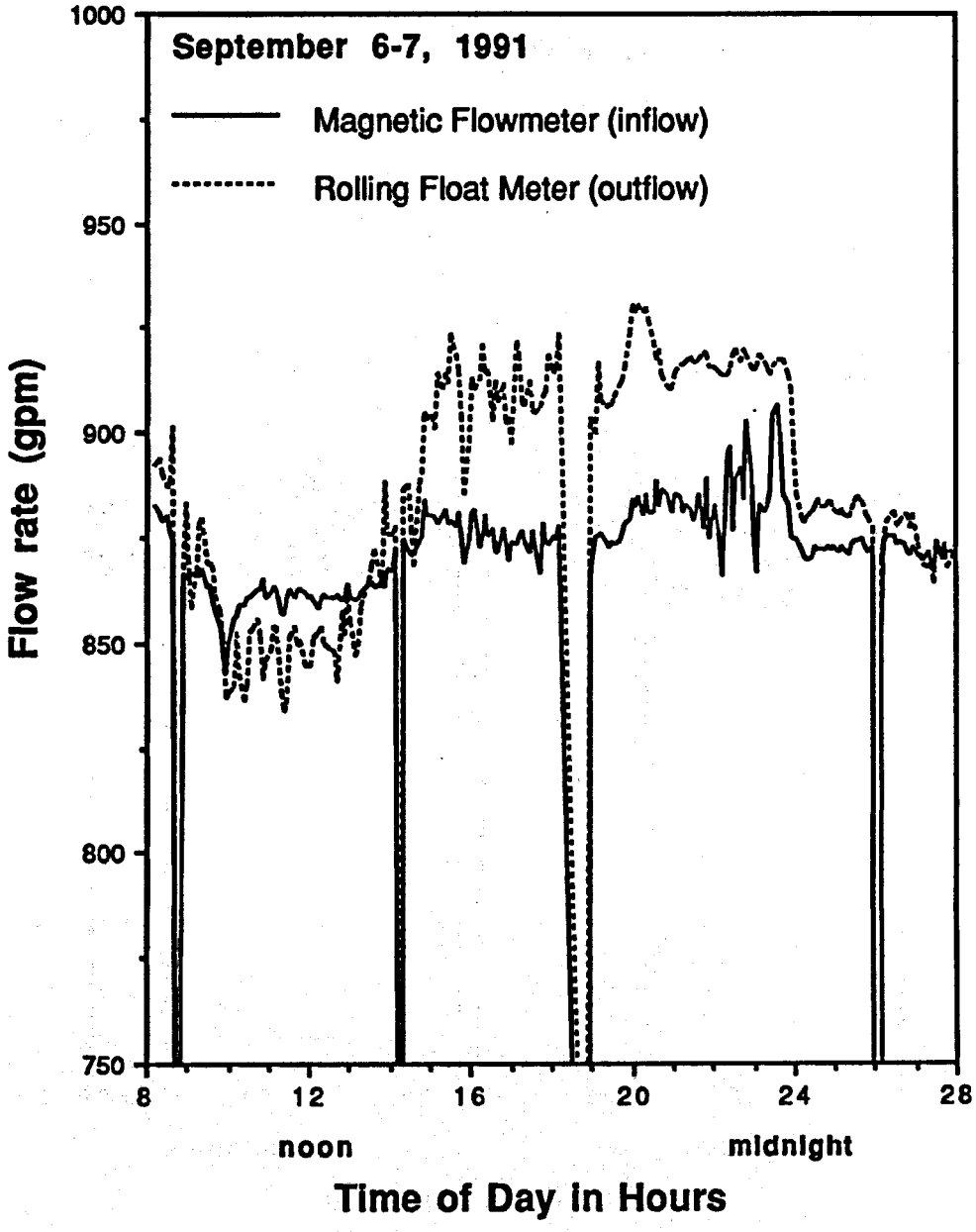

Figure 65 - Comparison of magnetic flowmeter inflow and rolling float meter outflow rates during wellbore fluid production at the Long Valley Exploratory Well.

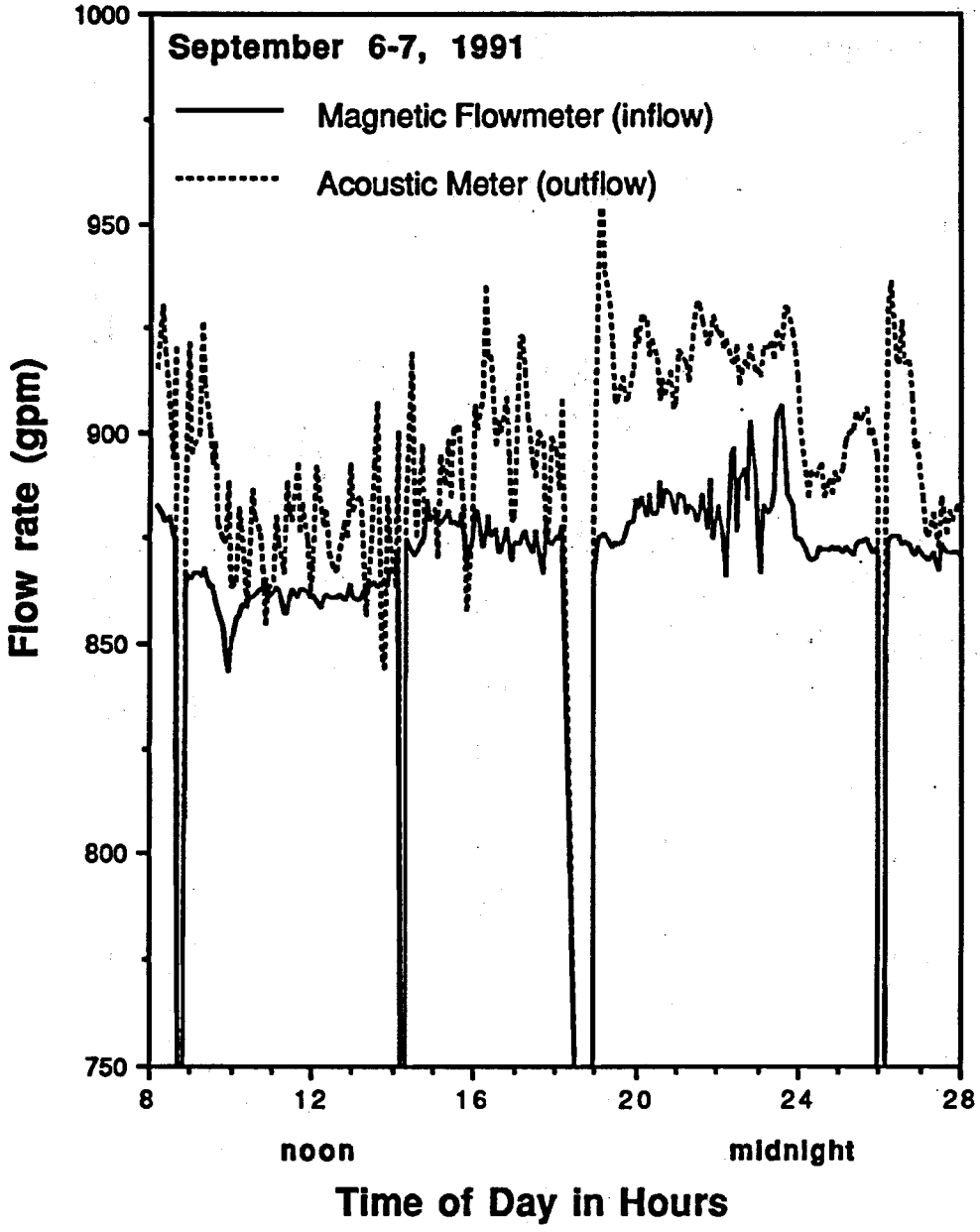

Figure 66 - Comparison of magnetic flowmeter inflow and acoustic meter outflow rates during wellbore fluid production at the Long Valley Exploratory Well.

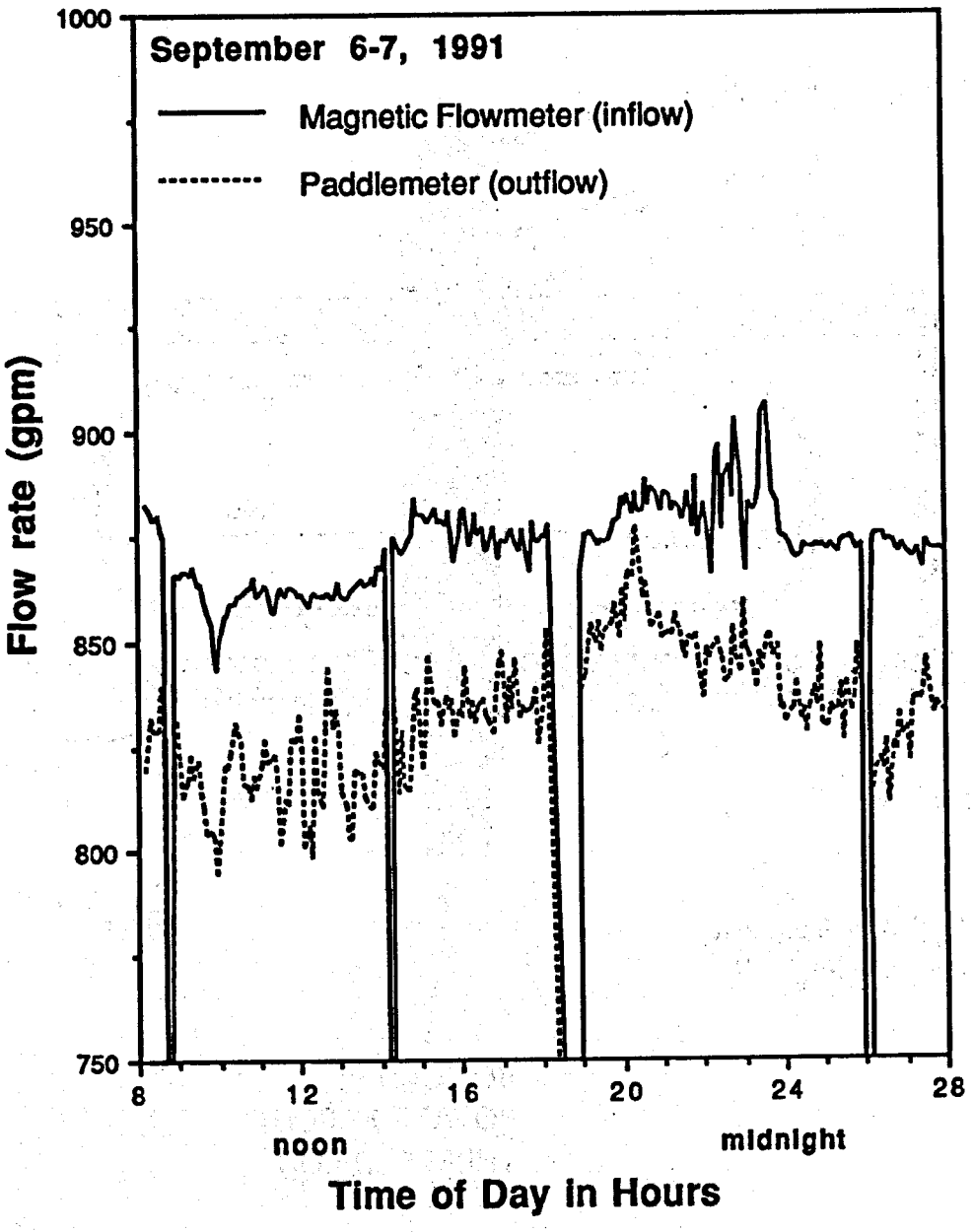

Figure 67 - Comparison of magnetic flowmeter inflow and paddlemeter outflow rates during wellbore fluid production at the Long Valley Exploratory Well.

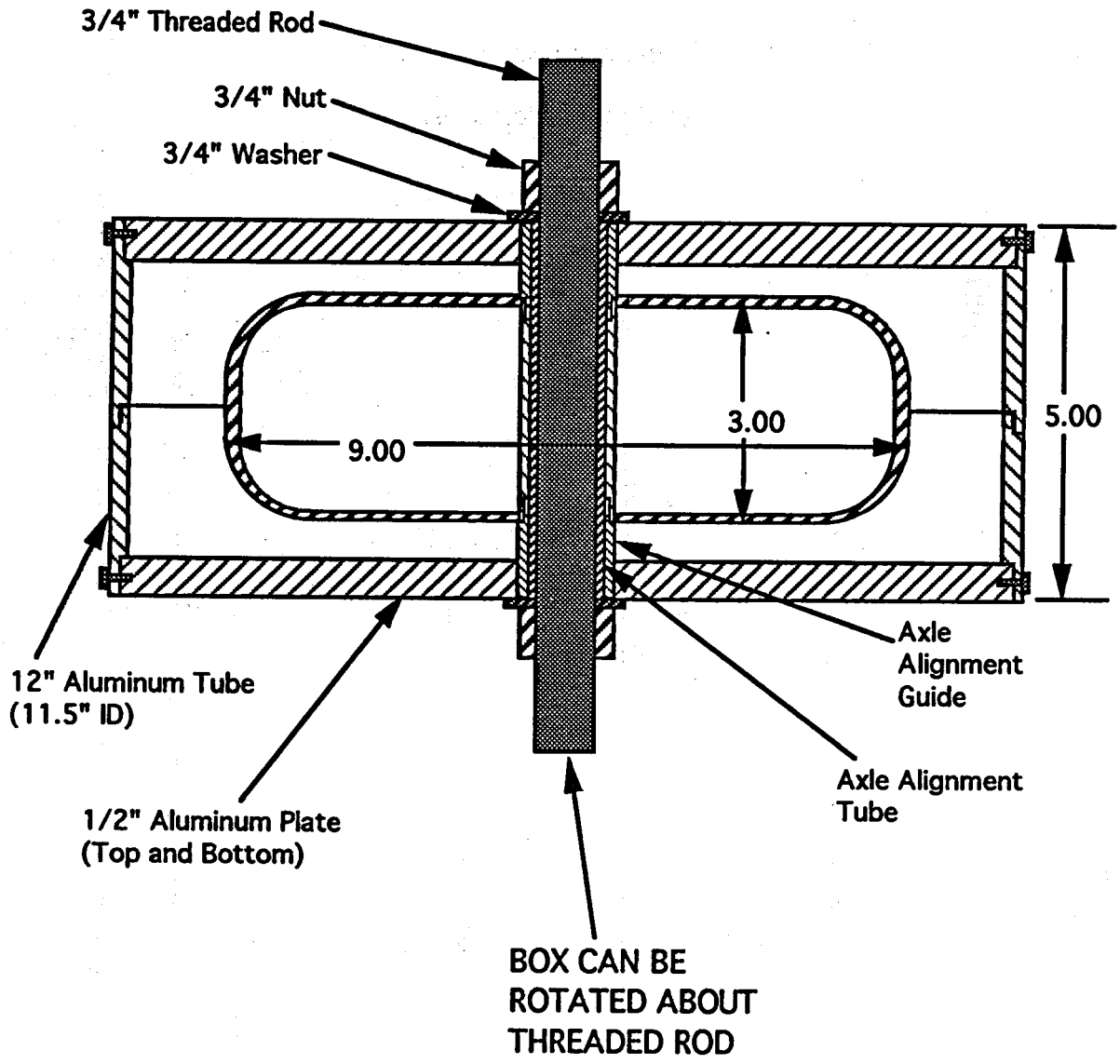

Figure 68 - Aluminum circular box used to form the mold for the polyurethane foam float.

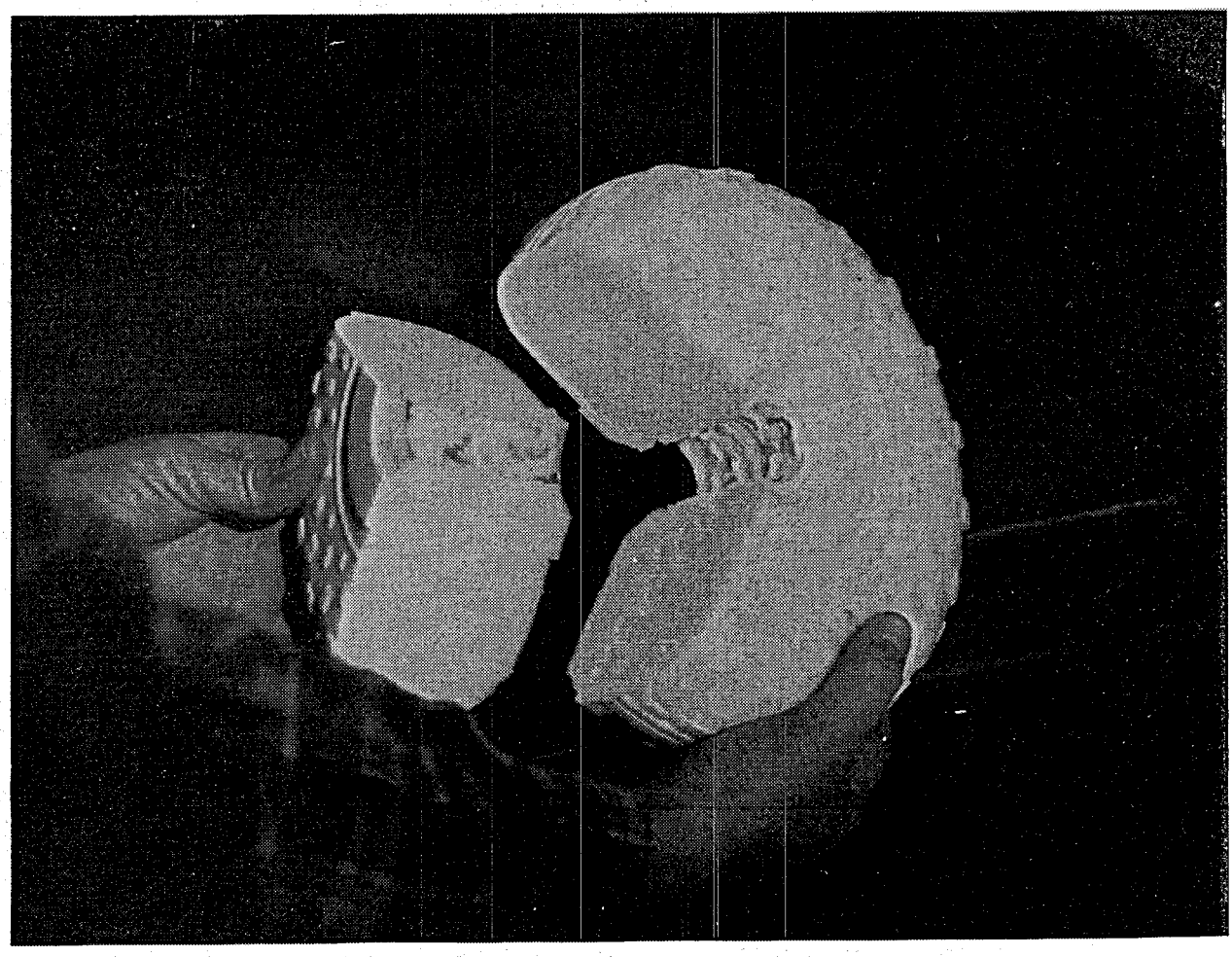

Figure 69 - Photograph of the polyurethane foam float.

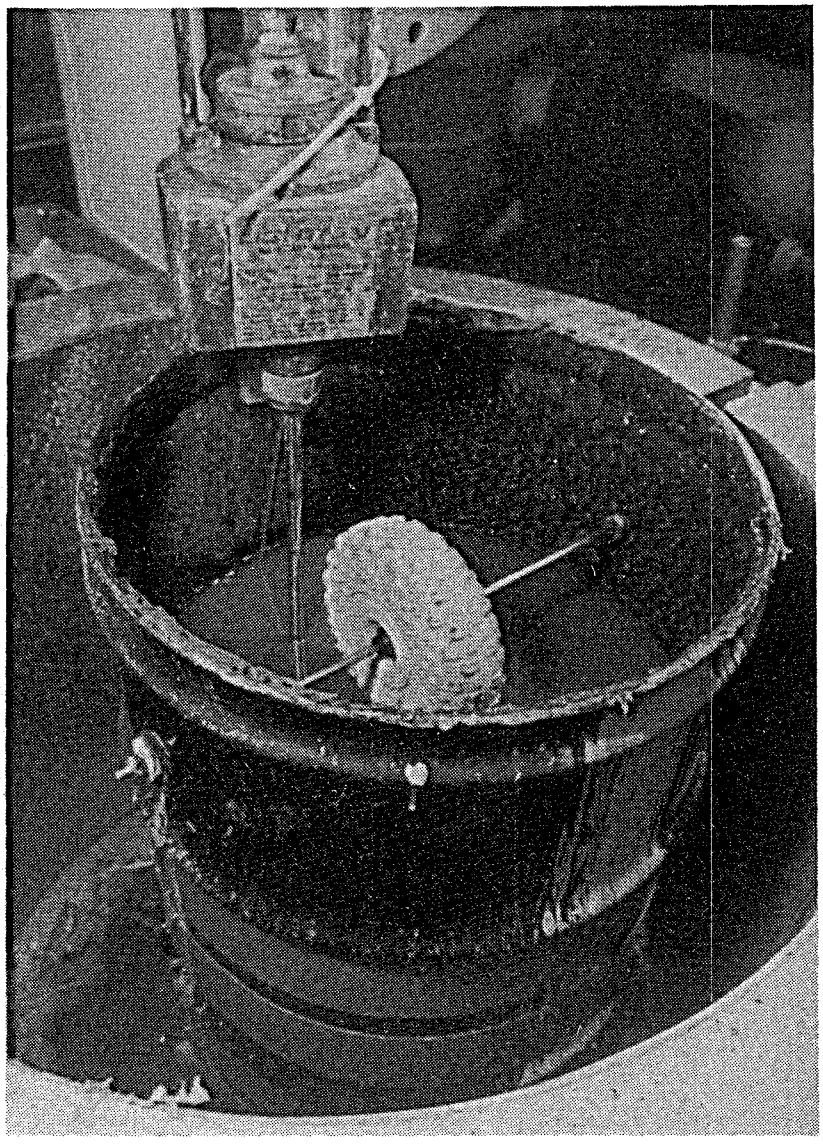

Figure 70 - Photograph of the float durability testing apparatus.

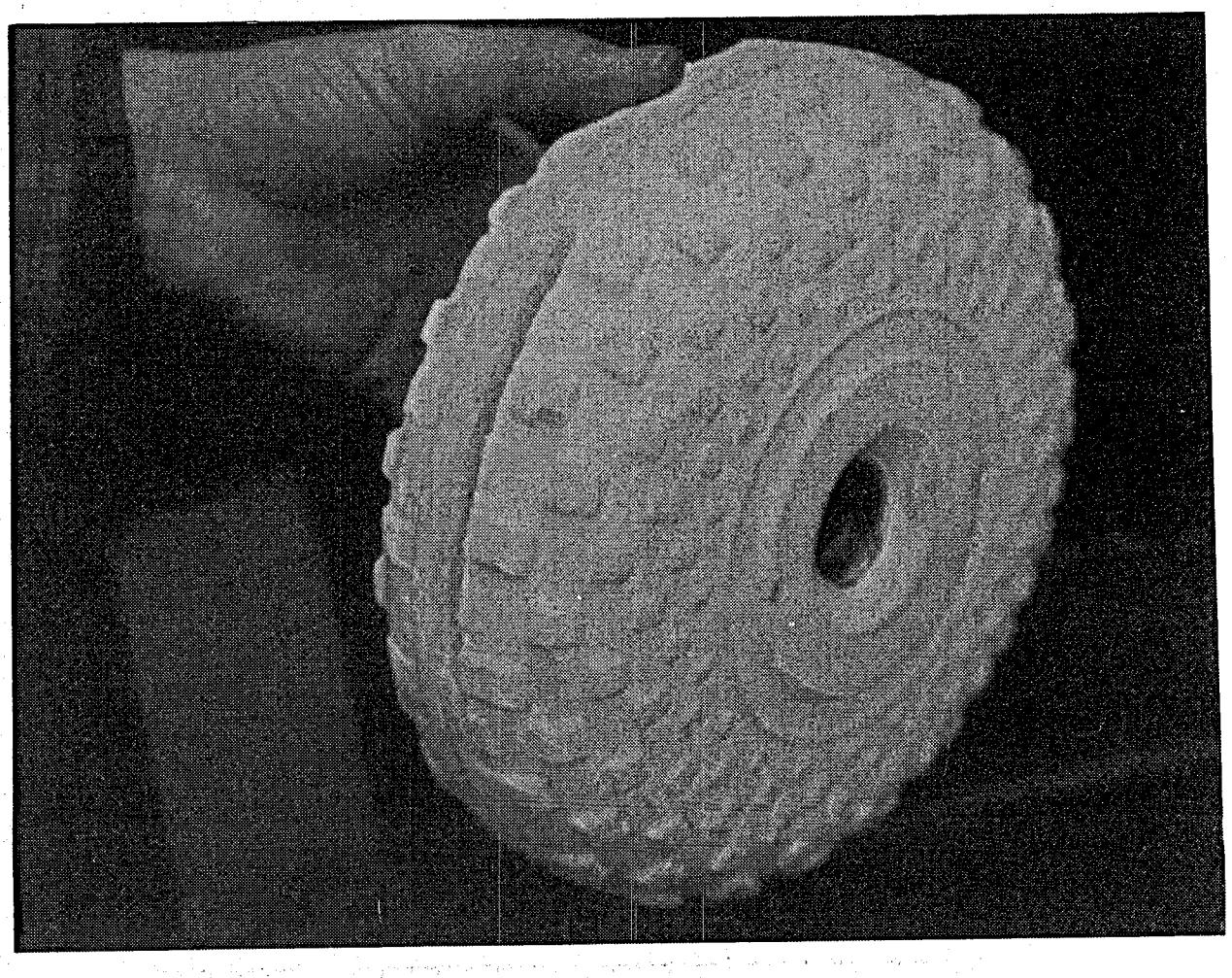

Figure 71 - Photograph of the failure of the first polyurethane foam float after testing for three days at 180 °F.

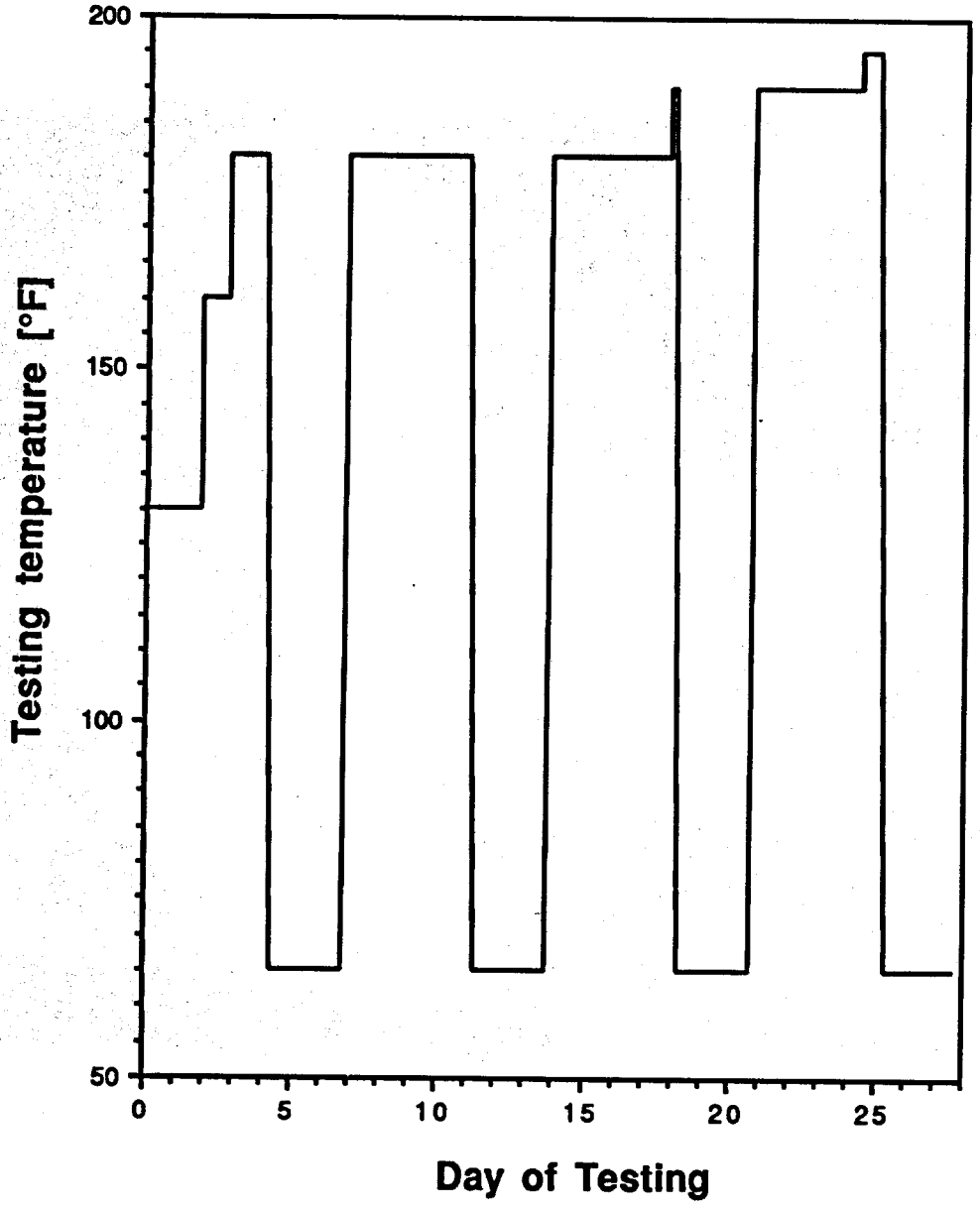

Figure 72 - Temperature cycle used in the testing of the second polyurethane foam float in the float durability testing apparatus.

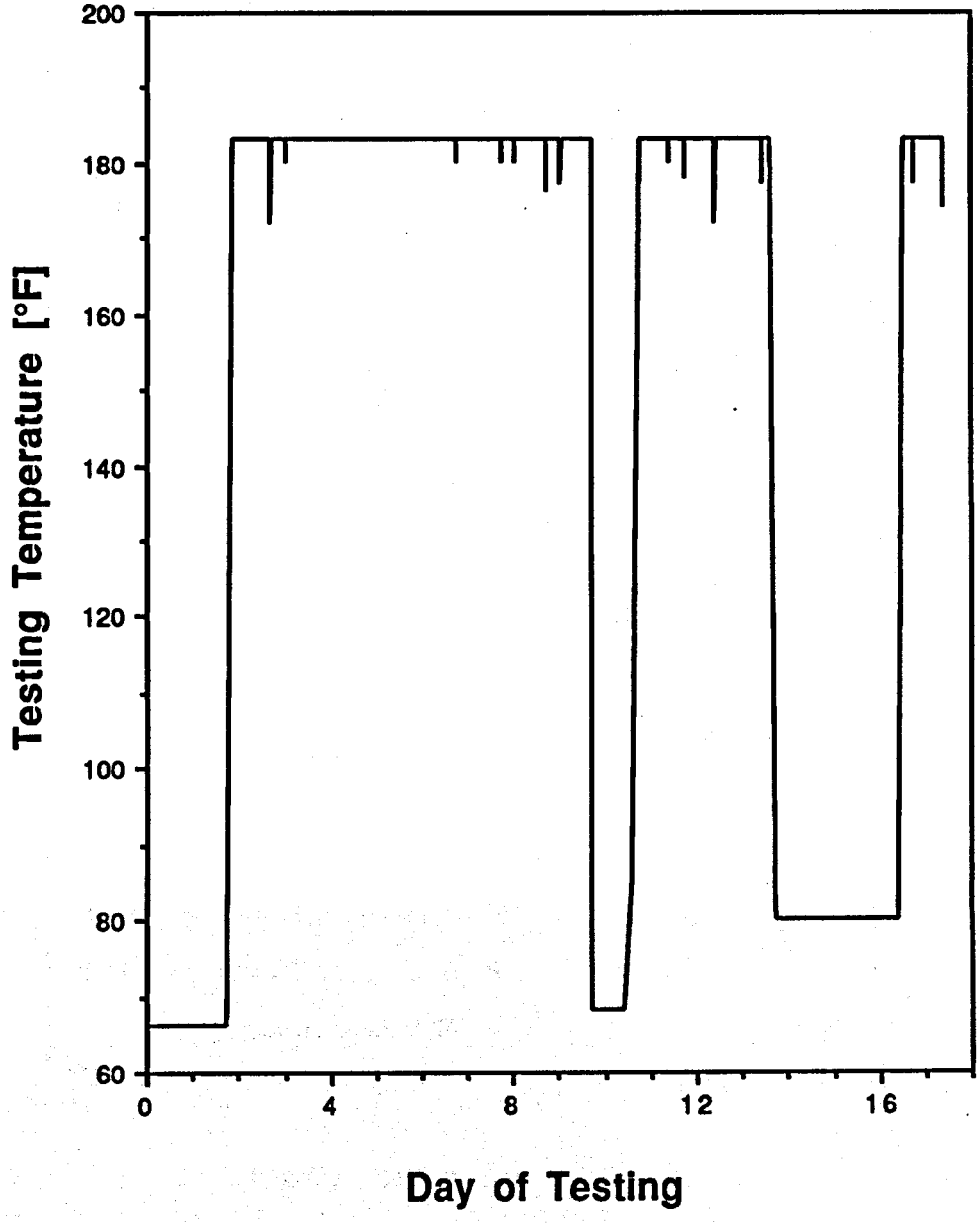

Figure 73 - Temperature cycle used in the testing of the bearing assembly in the float durability testing apparatus.

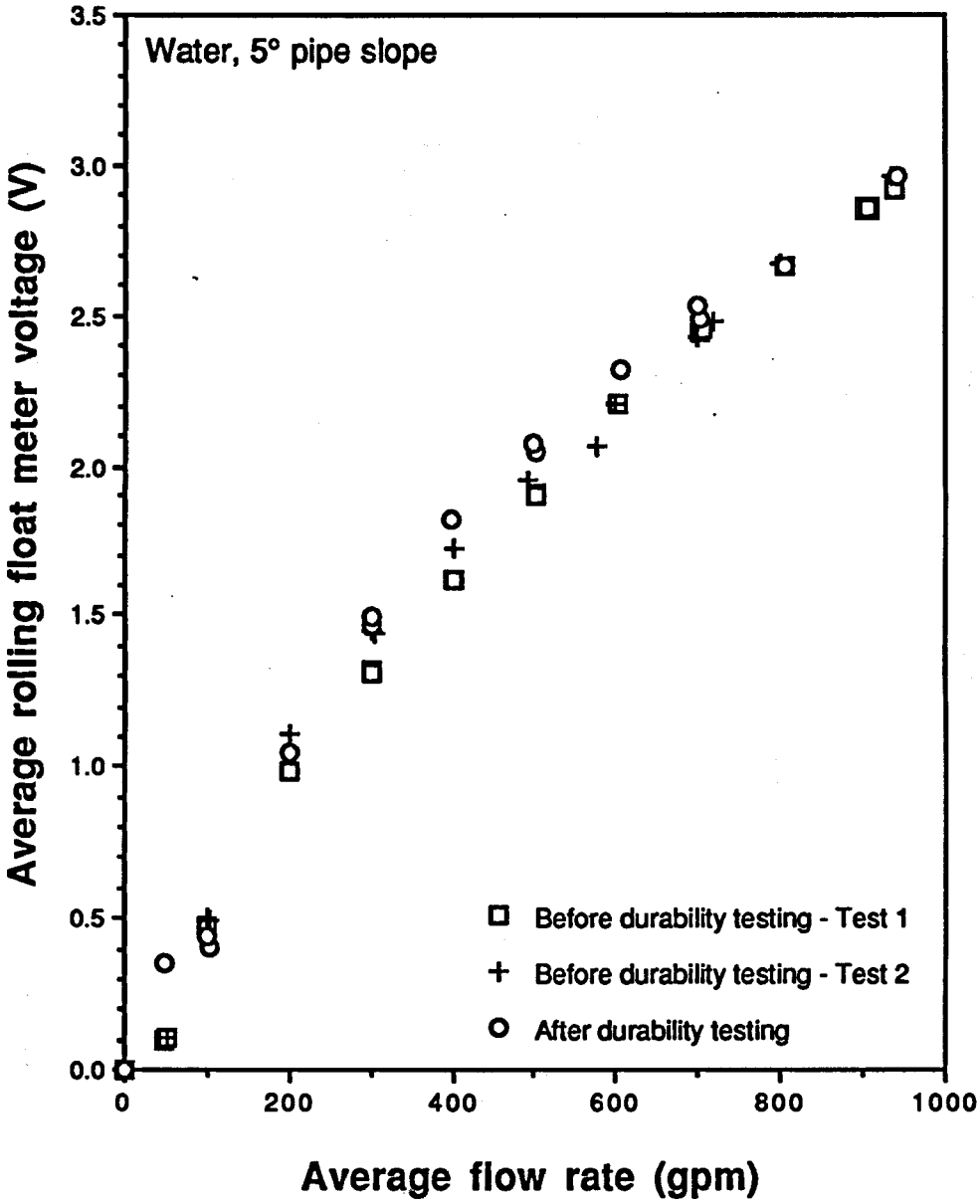

Figure 74 - Rolling float meter readings as a function of flow rate in the WHFF before and after high-temperature testing of the bearing assembly.

Appendix A

THEORETICAL PIPE FLOW ANALYSIS

In developing a prototype flowmeter that would measure the fluid level and velocity in a partially full, or "open channel," return line, a mathematical model of the fluid flow in the return pipe was needed to predict the range of fluid levels and velocities that would be encountered in a drilling rig return line. A mathematical model of the drilling fluid return line was developed using traditional mathematical equations for open-channel flow [9-12]. More detailed derivation of equations and discussion of open-channel flow can be found in Refs. 9-12, the analysis and corresponding mathematical equations are summarized here for convenience.

The following assumptions were made:

1) Steady flow,

2) Incompressible flow,

3) Uniform velocity profile at each cross-section,

4) Hydrostatic pressure distribution,

5) Pipe slope is small, $\theta \approx \sin\theta \approx \tan\theta = S_b$ and $\cos\theta \approx 1$,

6) In the accelerating flow regime, the local energy loss at a section is the same as that for non-accelerating flow with equal velocity and hydraulic radius.

A schematic of the fluid flow in the open channel return line is shown in Figure A1. The drilling fluid enters the return line at a critical height, y_c, which corresponds to the minimum specific energy for the given flow rate and pipe size. After entering the return line, the fluid speed in the direction of flow increases and the height decreases as the fluid is accelerated by gravity. The acceleration continues until the force due to gravitation is balanced by the friction force at the pipe wall. An equilibrium is established and the fluid height and velocity remain constant. This flow regime is called uniform flow.

The specific energy (or specific head) of the fluid at any location in an open channel flow is defined by:

$$E = \frac{V^2}{2g} + y, \tag{2}$$

where V is the average fluid velocity, V = Q/A, and y is the fluid height. From the entrance, the flow will lose energy due to change in pipe elevation and friction at the pipe walls. Therefore, if conditions at the entrance to the pipe are such that the specific energy is minimized, the energy of the flow at every location will be minimized. Thus, the height of the fluid at the entrance to the pipe is the height associated with the minimum specific energy of the flow. This is called the critical height (y_c). The minimum specific energy is found by differentiating Eq. 2 with respect to y and setting the resulting equation equal to zero. This yields:

$$\frac{dE}{dy} = -\frac{Q^2}{g A^3}\frac{dA}{dy} + 1 = 0 . \tag{3}$$

Given that dA = B(y) dy (where A, the flow area, and B, the flow width, are defined in Figure A2), then dA/dy = B(y). Stating both the area and flow width in terms of angle, α, and simplifying yields:

$$\frac{Q^2}{g} = \frac{A^3}{B(y)} = \frac{\{[\alpha - \sin\alpha]\frac{D^2}{8}\}^3}{D\sin[\pi - \alpha/2]}, \tag{4}$$

where D, the pipe diameter, and α are defined in Figure A2. The equation must be solved iteratively for α. The height of the fluid in the pipe is related geometrically to the angle, α, by:

$$y = \frac{D}{2}[\cos(\pi - \alpha/2) + 1]. \tag{5}$$

The height (y_c) and velocity of the fluid at the entrance to the return line pipe can thus be calculated.

In the uniform flow regime where the fluid is at a constant velocity and height, the only force in the direction of motion is the gravity component, which must be resisted by the wall shear stress (τ) acting over the area PL, where P is the wetted perimeter of the section of length L. This yields:

$$\tau P L = \rho g \sin(\theta) A L, \tag{6}$$

which, upon simplification, yields:

$$\tau = \rho g \frac{A}{P} S_b = \rho g R_h S_b, \tag{7}$$

where R_h is the hydraulic radius (A/P) and S_b is the pipe slope ($\sin\theta$). As in full-pipe flow, the wall shear stress can be empirically related to the fluid velocity by the Darcy friction factor, f, by:

$$\tau = \frac{f}{4}\rho\frac{V^2}{2}. \tag{8}$$

Typically, open channel flows occur in large, fairly rough pipes at high flow rates, and, as such, the friction factor is a function of surface roughness only and is independent of fluid properties and velocity. This is analogous to flow in the fully rough regime for turbulent pipe flow. Instead of the Darcy friction factor, wall shear stress in open channel flows is typically calculated in terms of the Manning coefficient, n, which is a roughness coefficient having different values for different types of boundary roughness. The coefficient, n, is treated as dimensionless, however, the coefficient has units of $L^{-1/3}t$. Values of n are typically given in SI units ($m^{-1/3}s$). The Manning coefficient is related to the Darcy friction factor by:

$$\left(\frac{8g}{f}\right)^{1/2} = \frac{R_h^{1/6}}{n}. \tag{9}$$

The equation for uniform flow is then:

$$\tau = \frac{n^2 g \rho V^2}{R_h^{1/3}} = \rho g R_h S_b. \tag{10}$$

Simplifying and solving for flow rate, Q, the equation becomes:

$$Q = AV = \frac{R_h^{2/3} S_b^{1/2}}{n} A, \tag{11}$$

for calculations in SI units. In English units the numerator of this equation must be multiplied by $(0.3048 \text{ m/ft})^{-1/3} \approx 1.49$ for the same values of n. Therefore, in English units the equation is:

$$Q = AV = \frac{1.49 R_h^{2/3} S_b^{1/2}}{n} A. \tag{12}$$

The equation (SI) in terms of α is given as:

$$\frac{Q n}{S_b^{1/2}} = \left\{ \frac{D}{4} \left[1 - \left(\frac{\sin\alpha_u}{\alpha_u} \right) \right] \right\}^{2/3} \left[(\alpha_u - \sin\alpha_u) \frac{D^2}{8} \right], \tag{13}$$

and must be solved iteratively for α_u, and the uniform depth calculated as in Eq. 5.

Applying the energy equation to a control volume of fluid in the accelerating flow region results in the following (assuming the pipe slope is small, $\cos\theta \approx 1$):

$$\frac{V^2}{2g} + y + z = \frac{V^2}{2g} + d\left[\frac{V^2}{2g}\right] + y + dy + z + dz + dh_l, \tag{14}$$

where the pipe elevation, dz, can be written in terms of the pipe slope, $dz = -S_b\, dx$, and the head loss, h_l, can be written in terms of the energy grade line, $dh_l = S\, dx$. The differential equation can then be written as:

$$\frac{d}{dx}\left[\frac{V^2}{2g}\right] + \frac{dy}{dx} = S_b - S \tag{15}$$

Again, V and y can be written in terms of α, and Eq. 15 can be solved numerically in a marching procedure from $x = 0$ at $y = y_c$. To determine S, it is assumed that the local energy loss is equal to that for a flow at uniform depth with the same velocity and hydraulic radius. For flow at uniform depth, local energy loss, S, is equal to S_b. Then from Eq. 11 for uniform flow:

$$V = \frac{R_h^{2/3} S^{1/2}}{n}, \tag{16}$$

and it follows that:

$$S = \frac{n^2 V^2}{R_h^{4/3}}. \tag{17}$$

The local energy loss, S, is based on mean properties between two points.

At step n+1, S is calculated initially assuming the values of V_n and R_{hn}, V_{n+1} and R_{hn+1} are calculated, and the procedure is repeated using average values for the new calculation of S. This is repeated until there is no change in the calculated values at n+1. In this manner, the fluid level and average velocity can be calculated at discrete locations along the length of the pipe until the point where uniform flow conditions exist.

To avoid error, the step size, Δx, must be small so there are no large variations in properties between any two adjacent points. Typically, the prediction was performed with a step size, Δx, of 1 inch; a sensitivity analysis showed that Δx from 0.5 to 6 inches yielded the same results for 10 and 12-inch diameter pipes.

The final mathematical equations used to model the system are independent of fluid properties. This is a result of: 1) the assumption that the flow in the pipe would be fully turbulent and, therefore, the friction factor would be independent of the fluid viscosity; and 2) the assumption that the shear stress, τ, is empirically related to ρV^2 by a friction factor (Eq. 8).

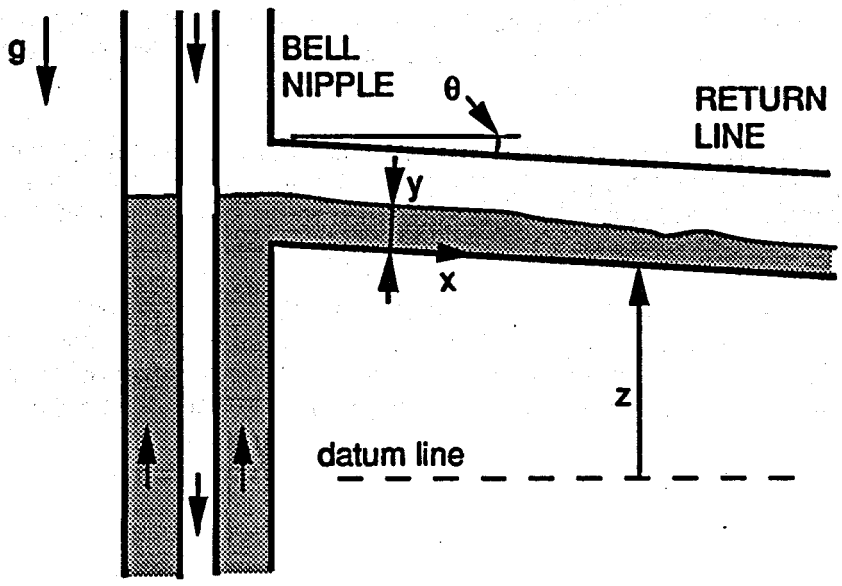

Figure A1 - Schematic of the drilling fluid return line.

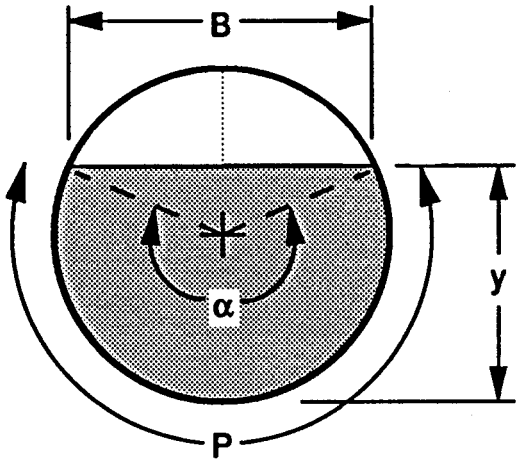

A = Flow area
B = Flow width
D = Pipe diameter
P = Wetted perimeter
y = Flow height

$$y = \frac{D}{2}[\cos(\pi - \alpha/2) + 1]$$

$$B = D \sin(\pi - \alpha/2)$$

$$A = \frac{D^2}{8}(\alpha - \sin\alpha)$$

Figure A2. Pipe flow nomenclature.

Appendix B

ROLLING FLOAT METER DRAWINGS

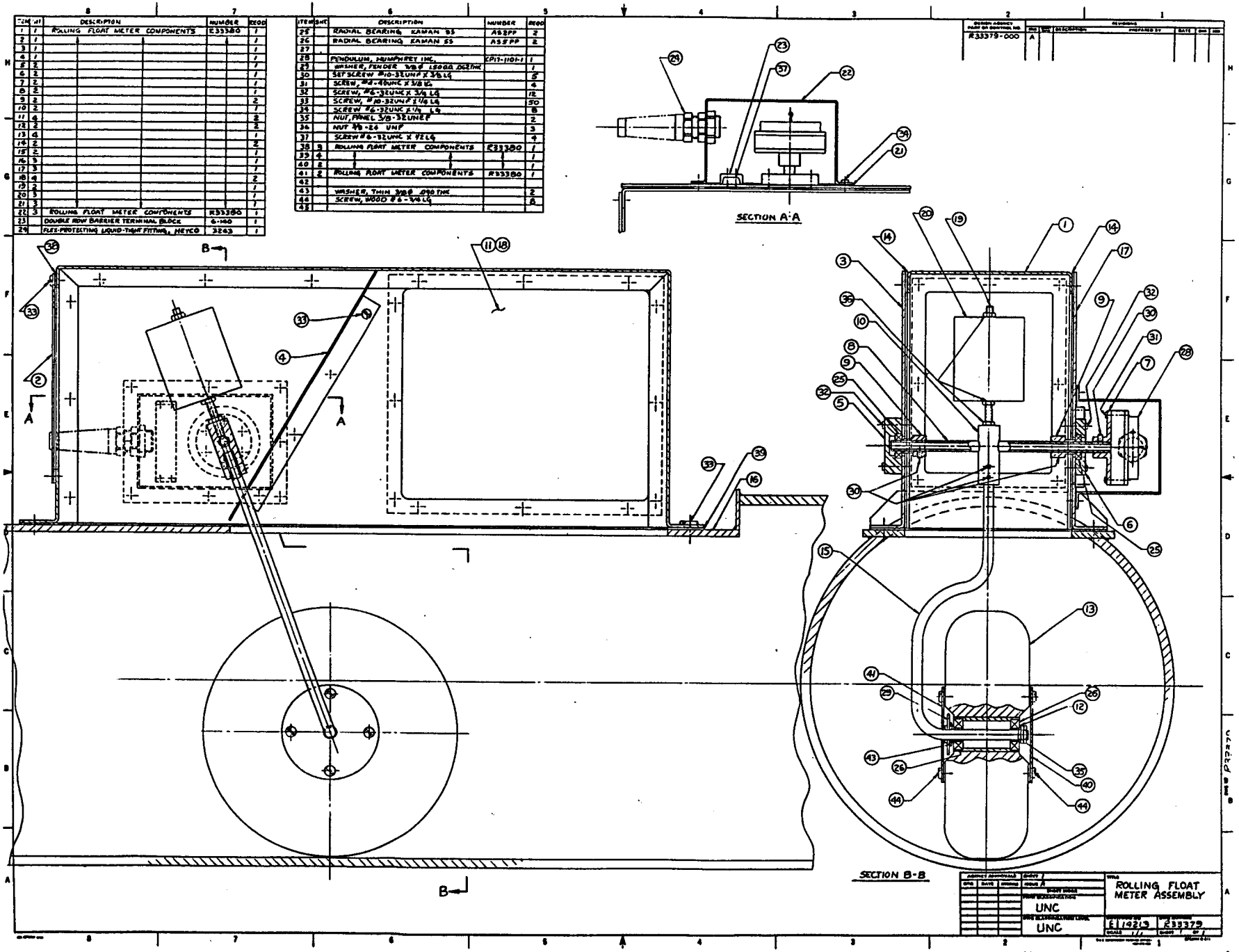

ITEM	QTY	DESCRIPTION	NUMBER	REQD
1	1	ROLLING FLOAT METER COMPONENTS	R33380	1
2	1			1
3	1			1
4	1			1
5	2			1
6	2			1
7	2			1
8	2			1
9	2			2
10	2			1
11	4			2
12	2			2
13	4			1
14	2			2
15	2			1
16	5			1
17	3			1
18	4			2
19	2			1
20	3			1
21	3			1
22	3	ROLLING FLOAT METER COMPONENTS	R33380	1
23		DOUBLE ROW BARRIER TERMINAL BLOCK	6-140	1
24		FLEX-PROTECTING LIQUID-TIGHT FITTING, HEYCO	3263	1

ITEM	QTY	DESCRIPTION	NUMBER	REQD
25		RADIAL BEARING, KAMAN 95	A95PP	2
26		RADIAL BEARING, KAMAN 55	A55PP	2
27				
28		PENDULUM, HUMPHREY INC.	EP17-1101-1	1
29		WASHER, FENDER 3/8" I.D. .090 THK		1
30		SET SCREW #10-32UNF X 3/8 LG		5
31		SCREW, #2-56UNC X 3/8 LG.		4
32		SCREW, #6-32UNC X 3/4 LG		12
33		SCREW, #10-32UNF X 1/8 LG		50
34		SCREW #6-32UNC X 1/4 LG		8
35		NUT, PANEL 3/8-32UNEF		2
36		NUT #8-32 UNF		3
37		SCREW #6-32UNC X 9/16 LG		4
38	3	ROLLING FLOAT METER COMPONENTS	R33380	1
39	4			1
40	2			1
41	2	ROLLING FLOAT METER COMPONENTS	R33380	1
42				
43		WASHER, THIN 3/8Ø .030 THK		2
44		SCREW, WOOD #6-3/8 LG		6
45				

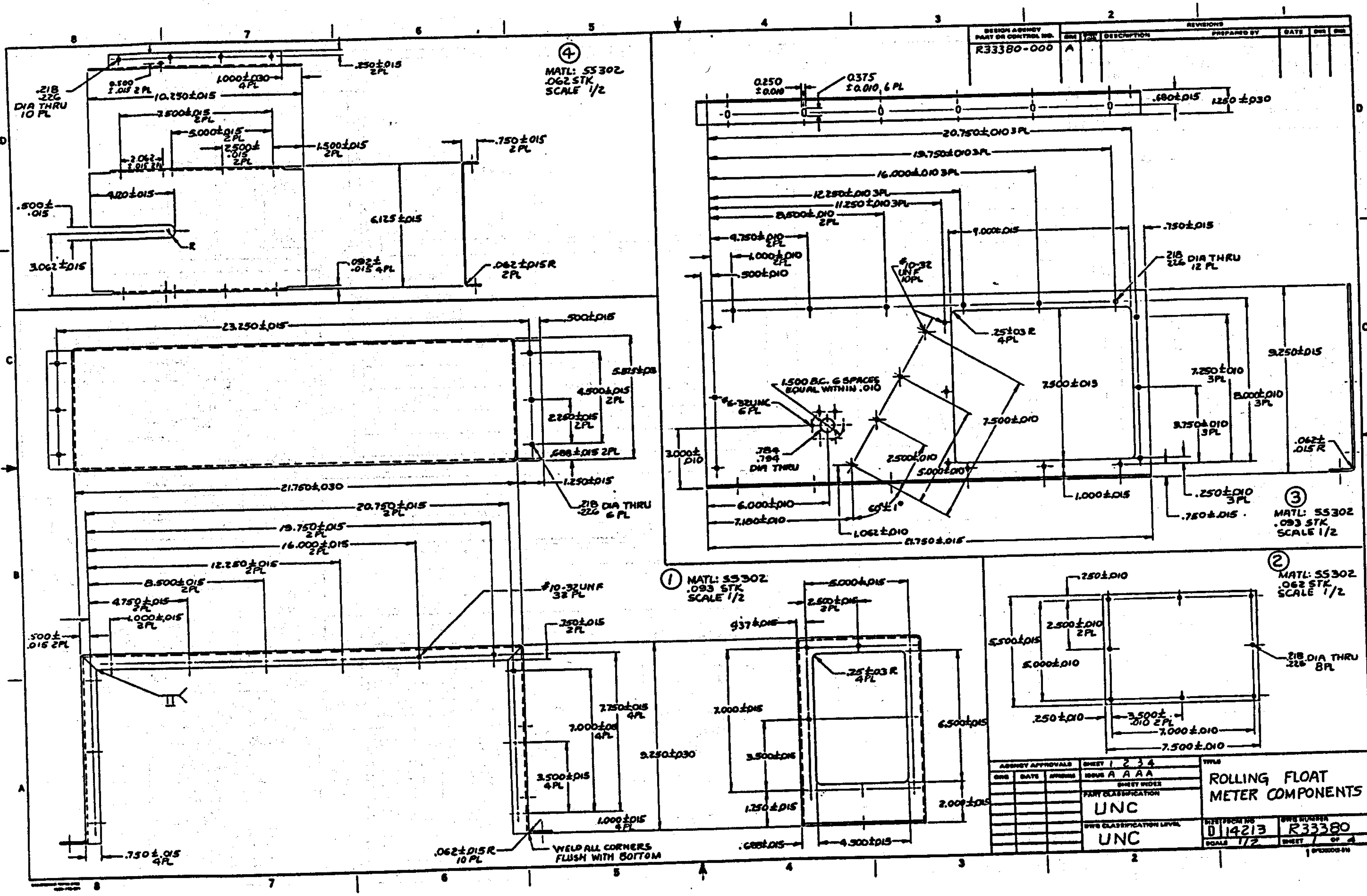
ROLLING FLOAT
METER COMPONENTS
R33380
R33380-000
UNC
UNC
D 14213
SCALE 1/2
AGENCY APPROVALS
PART CLASSIFICATION
DWG CLASSIFICATION LEVEL
REVISIONS
① MATL: SS302
.093 STK
SCALE 1/2
② MATL: SS302
.062 STK
SCALE 1/2
③ MATL: SS302
.093 STK
SCALE 1/2
④ MATL: SS302
.062 STK
SCALE 1/2
WELD ALL CORNERS
FLUSH WITH BOTTOM
#10-32 UNF
32 PL
.218
.226 DIA THRU
6 PL
.218
.226 DIA THRU
12 PL
.218
.226 DIA THRU
8 PL
.218
.226 DIA THRU
10 PL
1.500 B.C. 6 SPACES
EQUAL WITHIN .010
.784
.794 DIA THRU
#6-32UNC
6 PL
.25±.03 R
4 PL
23.250±.015
21.760±.030
20.750±.015
9.250±.030
9.250±.015
7.500±.010
7.000±.010
6.125±.015
5.000±.015
4.300±.015
10.250±.015
20.750±.010 3PL
19.750±.010 3PL
16.000±.010 3PL
21.750±.015

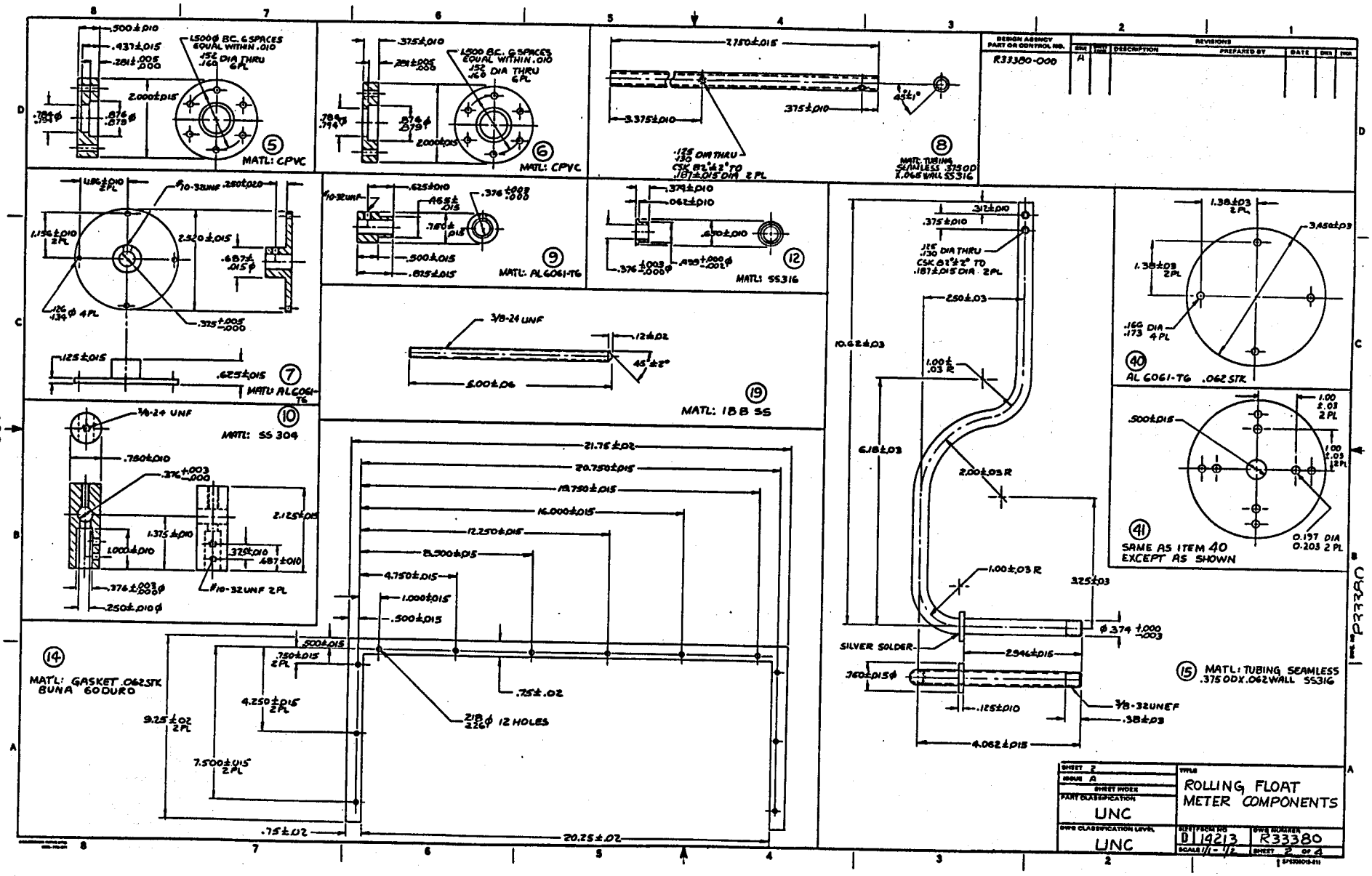
DESIGN AGENCY PART OR CONTROL NO.
R33380-000
REVISIONS
DESCRIPTION
PREPARED BY
DATE
5 MATL: CPVC
6 MATL: CPVC
8 MATL: TUBING SEAMLESS 316 SS .375 OD 1.065 WALL
7 MATL AL6061-T6
9 MATL: AL6061-T6
12 MATL: SS316
19 MATL: 18 8 SS
10 MATL: SS 304
40 AL 6061-T6 .062 STK
41 SAME AS ITEM 40 EXCEPT AS SHOWN
14 MATL: GASKET .062 STK BUNA 60 DURO
15 MATL: TUBING SEAMLESS .375 ODX.062 WALL SS316
SILVER SOLDER
ROLLING FLOAT METER COMPONENTS
PART CLASSIFICATION
UNC
DWG CLASSIFICATION LEVEL
UNC
DWG NUMBER
R33380
SHEET 2 OF 4

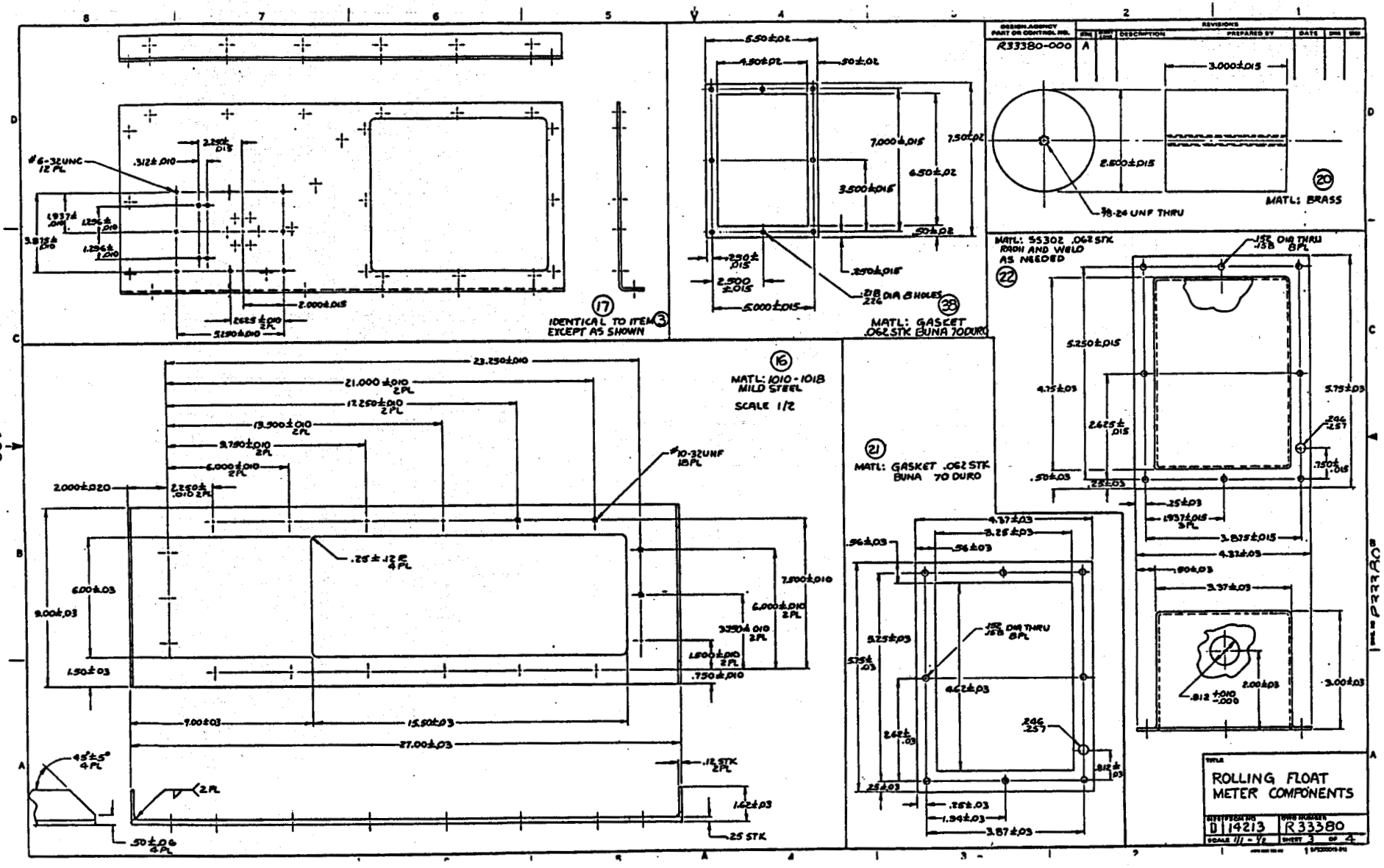
#6-32UNC 12 PL
.312±.010
2.250±.015
1.937±.010
1.296±.010
3.875±.010
1.296±.010
2.000±.015
5.250±.010
IDENTICAL TO ITEM (3) EXCEPT AS SHOWN
(17)
5.50±.02
4.50±.02
.90±.02
7.000±.015
7.50±.02
6.50±.02
3.500±.015
.50±.02
.290±.015
2.500±.015
5.000±.015
.098 DIA 8 HOLES
(18)
MATL: GASKET .062 STK BUNA 70DURO
DESIGN AGENCY PART OR CONTROL NO.
R33380-000
REVISIONS
ZONE | LTR | DESCRIPTION | PREPARED BY | DATE
A
3.000±.015
2.500±.015
3/8-24 UNF THRU
(20)
MATL: BRASS
MATL: 55302 .062 STK RHOH AND WELD AS NEEDED
(22)
.136 DIA THRU .338 CBORE 8PL
5.250±.015
4.75±.03
5.75±.03
2.625±.015
.244 .257
.750±.015
.50±.03
.25±.03
.25±.03
1.937±.015 3PL
3.875±.015
4.32±.03
.904±.03
3.37±.03
.812 +.010 -.000
2.00±.03
3.00±.03
23.250±.010
21.000±.010 2PL
17.250±.010 2PL
13.500±.010 2PL
9.750±.010 2PL
6.000±.010 2PL
2.000±.020
2.250±.010 2PL
#10-32UNF 18PL
.25±.12 4PL
6.00±.03
9.00±.03
1.50±.03
7.500±.010
6.000±.010 2PL
3.250±.010 2PL
1.500±.010 2PL
.750±.010
7.00±.03
15.50±.03
27.00±.03
45°±5° 4PL
2PL
.12 STK 2PL
1.62±.03
.25 STK
.50±.06 4PL
(16)
MATL: 1010 - 1018 MILD STEEL
SCALE 1/2
(21)
MATL: GASKET .062 STK BUNA 70 DURO
4.37±.03
3.25±.03
.96±.03
.96±.03
.136 DIA THRU .338 CBORE 8PL
5.25±.03
5.25±.03
4.62±.03
2.62±.03
.244 .257
.812±.03
.25±.03
.25±.03
1.94±.03
3.87±.03
TITLE
ROLLING FLOAT METER COMPONENTS
SPECIFICATION NO. D114213
DWG NUMBER R33380
SCALE 1/1 - 1/2
SHEET 3 OF 4

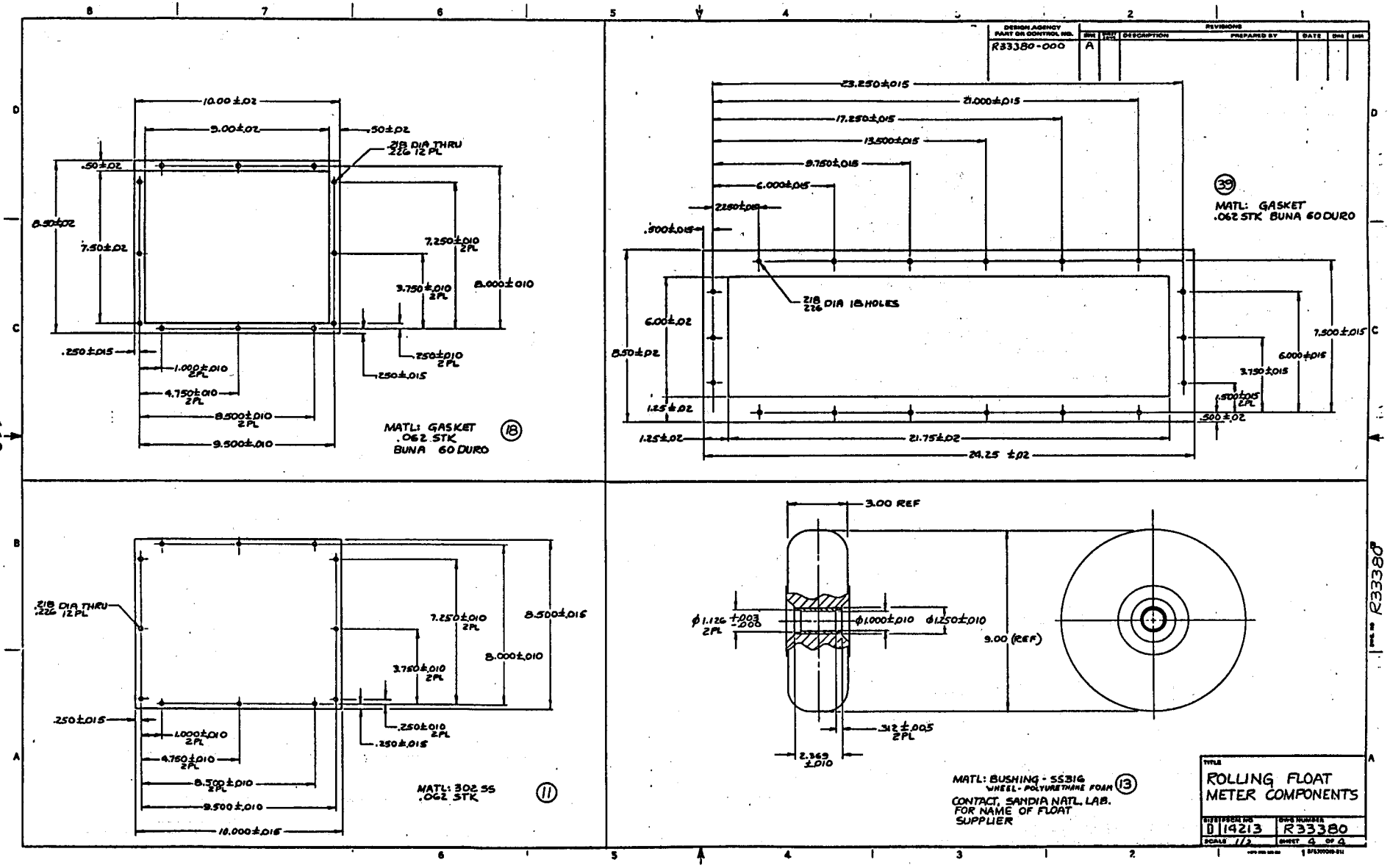
10.00 ±.02
9.00±.02
.50±.02
.218 DIA THRU .226 12 PL
.50±.02
8.50±.02
7.50±.02
7.250±.010 2PL
3.750±.010 2PL
8.000±.010
.250±.015
1.000±.010 2PL
4.750±.010 2PL
8.500±.010 2PL
9.500±.010
.250±.010 2PL
.250±.015
MATL: GASKET .062 STK BUNA 60 DURO
18
23.250±.015
21.000±.015
17.250±.015
13.500±.015
9.750±.015
6.000±.015
2.250±.015
.500±.015
.218 DIA 18 HOLES .226
6.00±.02
8.50±.02
1.25±.02
1.25±.02
21.75±.02
24.25 ±.02
7.500±.015
6.000±.015
3.750±.015
1.500±.015 2PL
.500±.02
39
MATL: GASKET .062 STK BUNA 60 DURO
.218 DIA THRU .226 12 PL
7.250±.010 2PL
8.500±.015
8.000±.010
3.750±.010 2PL
.250±.015
1.000±.010 2PL
4.750±.010 2PL
8.500±.010 2PL
9.500±.010
.250±.010 2PL
.250±.015
18.000±.015
MATL: 302 SS .062 STK
11
3.00 REF
ϕ1.126 +.003 -.002 2PL
ϕ1.000±.010
ϕ1.250±.010
9.00 (REF)
.312±.005 2PL
2.369 ±.010
MATL: BUSHING - SS316
WHEEL - POLYURETHANE FOAM
CONTACT, SANDIA NATL. LAB. FOR NAME OF FLOAT SUPPLIER
13
DESIGN AGENCY PART OR CONTROL NO.
R33380-000
REVISIONS
SYM A
DESCRIPTION
PREPARED BY
DATE
TITLE
ROLLING FLOAT METER COMPONENTS
SIZE D
FSCM NO 14213
DWG NUMBER R33380
SCALE 1/2
SHEET 4 OF 4
R33380

BEARING AND SPLASH GUARD DETAILS

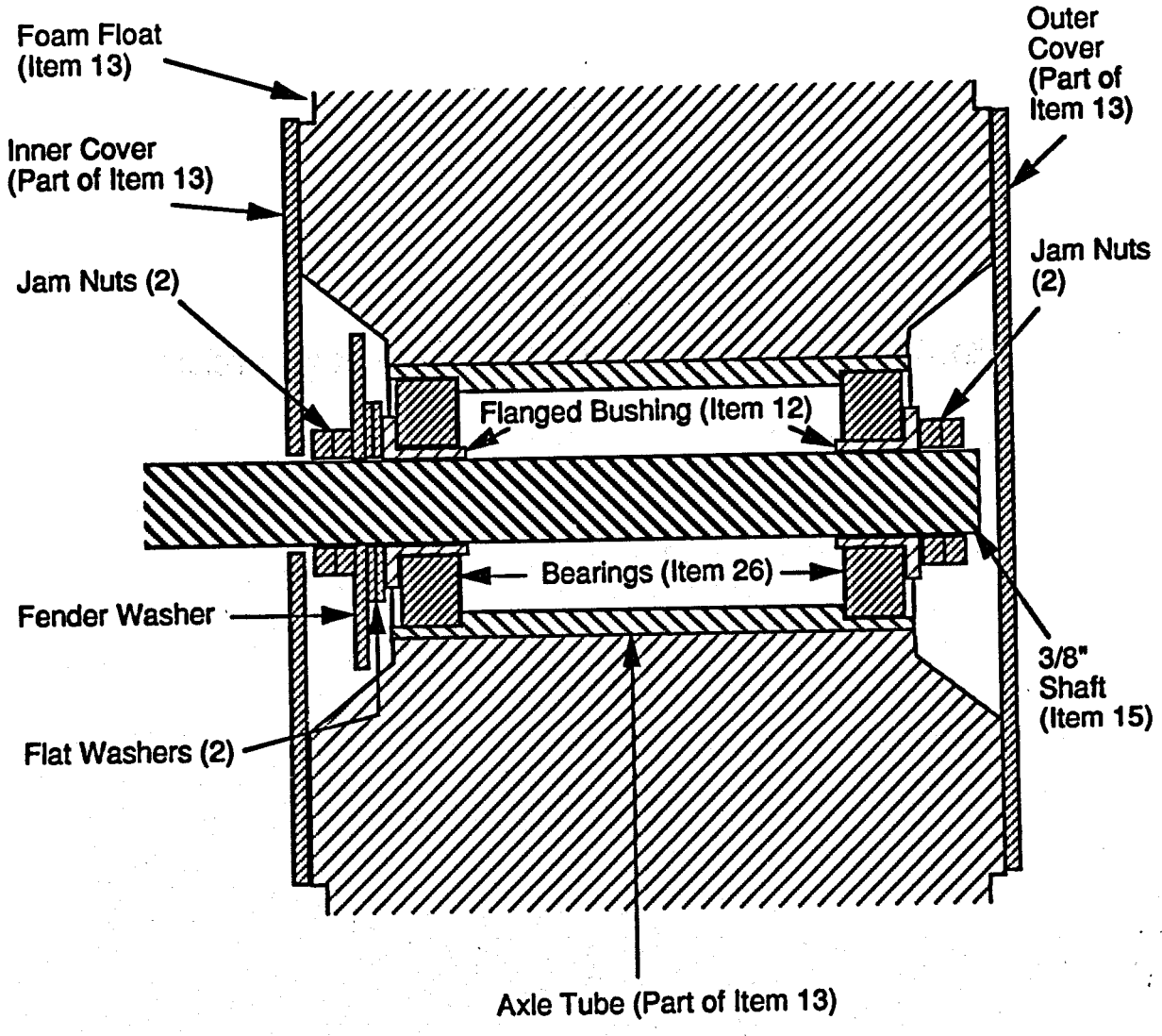

Appendix C

MODELS AND MANUFACTURERS OF TESTED FLOWMETERS

Acoustic Level Meter

Model 1011 ultrasonic flowmeter, 110 VAC input power, 4-20 mA output (for measuring fluid height in 12-inch diameter pipe).

Manufacturer
Marsh-McBirney, Inc.
4539 Metropolitan Court
Frederick, MA 21701
(800) 368-2723

Doppler Ultrasonic Flowmeter

Polysonics Model MST-P, portable Doppler ultrasonic flowmeter for clean liquids.

Manufacturer
Polysonics
10335 Landsbury, Suite 300
Houston, Texas 77099
(713) 530-0885

Magnetic Flowmeter

YEMAG model YM325G-AA1-LSA*A with 10-inch ANSI 150 flanges, PFA Teflon liner, and 316 SS electrodes and earth rings. Included YMA11-A1A*A Flow Converter and YMO11-1-030F*A-30 feet of interconnecting cable.

Manufacturer
Yokogawa Electric Corporation
American Headquarters
2 Dart Road
Shenandoah Industrial Park
Newnan, Georgia 30265-1094
(404) 253-7000

Paddlemeter

Mud flow sensor for 10-inch pipe (laboratory testing), MD P/N MFTX4A-1
Mud flow sensor for 12-inch pipe (field testing), MD P/N MFTX4A-2

Manufacturer
Martin Decker - Totco
3011 Antonio Avenue
Bakersfield, CA 93308
(713) 987-9855

Pump Rotary Speed Transducer

Model No. RPGC Rotary Pulse Generator, 60 PPR (pulse per revolution), Part Number RPGC-00-51/A

Manufacturer
Red Lion Controls
International Headquarters
20 Willow Springs Circle
York, Pennsylvania, 17402
(717) 767-6511

DISTRIBUTION

Keith A. Womer
Martin-Decker Totco
1200 Cypress Creek Road
Cedar Park, Texas 78613-3614

Tom Gayhart
Martin-Decker Totco
1200 Cypress Creek Road
Cedar Park, Texas 78613-3614

Michael R. Taylor, P. Geol.
EXLOG, Inc.
P.O. Box 40265
Houston, Texas 77240-0265

Trevor Burgess
Schlumberger-Anadrill
200 Macco Boulevard
Sugar Land, Texas 77478

David White
Schlumberger-Sedco Forex
P.O. Box 599
92542 Montrouge Cedex, France

François Julien
Schlumberger-Sedco Forex
P.O. Box 599
92542 Montrouge Cedex, France

Richard Mundell
Shell Oil Company
Export Materials Services
P.O. Box 4319
Houston, TX 77210-4319

Frank Shepard
EXLOG, Inc.
7101 Hollister Street
Houston, Texas 77040

James B. Combs
Geohills Associates
27790 Edgerton Rd.
Los Altos, CA 94022

Neal Davis
Chevron Service Co.
Drilling Technology Center
P.O. Box 4450
Houston, TX 77210

Robert Deputy
ARCO Oil & Gas Co.
2300 W. Plano Parkway
Plano, TX 75075
Charles George
Halliburton Services
Drawer 1431
Duncan, OK 73536-0408

Barry Harding
Ocean Drilling Program
Texas A&M University
1000 Discovery Dr.
College Station, TX 77840

A. P. S. Howells
Atlas Wireline Services
10011 Meadowglen
P.O. Box 1407
Houston, TX 77251

James Langford
Security Division
Dresser Industries, Inc.
P.O. Box 210600
Dallas, TX 75211-0600

Bill Lyons
New Mexico Tech.
Socorro, NM 87801

George McClaren
Tonto Drilling Services
P.O. Box 25128
2200 South 4000 West
Salt Lake City, UT 84125-0128

Nic Nickels
Eastman Christensen
3636 Airway Drive
Santa Rosa, CA 95403

Steve Pye
Unocal Geothermal
1201 West 5th St.
P.O. Box 7600
Los Angeles, CA 90017

Tommy Warren
Amoco Production Center
P.O. Box 3385
Tulsa, OK 74102

Dr. George A. Cooper
Dept. of Materials Science & Mineral
Engineering
University of California
Berkeley, CA 94720

Glen Loeppke
1421 San Rafael N.E.
Albuquerque, NM 87122

Marcus Wernig (2)
309 D. 1st Street
College Station, TX 77840

U.S. Department of Energy (3)
Geothermal Division
Attn: Ted Mock
Lew Pratsch
Dave Lombard
Forrestal Bldg., C-122
1000 Independence Avenue S.W.
Washington, D.C. 20585

6100 Paul J. Hommert (actg.)
6111 James C. Dunn
6112 David A. Northrop
6113 James K. Linn
6114 Marion W. Scott
6115 Paul J. Hommert (actg.)
6116 Marianne C. Walck
6117 Wolfgang R. Wawersik
6118 Marianne C. Walck (actg.)
6119 Elaine D. Gorham
6121 Joe R. Tillerson
6111 Diane M. Schafer (25)
6111 David A. Glowka (25)
6111 Douglas D. Scott
6111 Elton K. Wright

8523-2 Central Technical Files
3141 S. A. Landenberger
3913-2 Document Processing
for DOE/OSTI
3151 G. C. Claycomb